UNIVERSIDAD AUTÓNOMA DE MADRID

Advanced Kernel Methods for Multi-Task Learning

by

Carlos Ruiz Pastor

A thesis submitted in partial fulfillment for the degree of Doctor of Philosophy

in the

Escuela Politécnica Superior

Computer Science Department

under the supervision of José R. Dorronsoro Ibero

September 2022

What is the essence of life? To serve others and to do good.

Aristotle.

Abstract

.

Resumen

Small.

Acknowledgements

.

Contents

Abbreviations

ADF	**A**ssumed **D**ensity **F**iltering
AF	**A**cquisition **F**unction
BO	**B**ayesian **O**ptimization
DGP	**D**eep **G**aussian **P**rocess
EI	**E**xpected **I**mprovement
EP	**E**xpectation **P**ropagation
GP	**G**aussian **P**rocess
KL	**K**ullback **L**iebler
MCMC	**M**arkov **C**hain **M**onte **C**arlo
PPESMOC	**P**arallel **P**redictive **E**ntropy **S**earch for **M**ultiobjective **O**ptimization with **C**onstraints
PES	**P**redictive **E**ntropy **S**earch
PESMOC	**P**redictive **E**ntropy **S**earch for **M**ultiobjective **O**ptimization with **C**onstraints
RS	**R**andom **S**earch
UCB	**U**pper **C**onfidence **B**ound

To my family

Chapter 1

Introduction

We begin this manuscript...

1.1 Introduction

1.2 Publications

This section presents, in chronological order, the work published during the doctoral period in which this thesis was written. We also include other research work related to this thesis, but not directly included on it. Finally, this document includes content that has not been published yet and is under revision.

Related Work

Work In Progress

1.3 Summary by Chapters

In this section...

Chapter 2 provides an introduction to GPs and the expectation propagation algorithm. Both are necessary concepts for the BO methods that we will describe in the following chapters. This chapter reviews the fundamentals of GPs and why they are so interesting for BO. More concretely, we review the most popular kernels, the analysis of the posterior and predictive distribution and how to tune the hyper-parameters of GPs: whether by maximizing the marginal likelihood or by generating samples from the hyper-parameter posterior distribution. Other alternative probabilistic surrogate models are also described briefly. Some of the proposed approaches of this thesis are extensions of an acquisition function called predictive entropy search, that is based on the expectation propagation approximate inference technique. That is why we provide in this chapter an explanation of the expectation propagation algorithm.

Chapter 3 introduces the basics of BO and information theory. BO works with probabilistic models such as GPs and with acquisition functions such as predictive entropy search, that uses information theory. Having studied GPs in Chapter 2, BO can be now understood and it is described in detail. This chapter will also

describe the most popular acquisition functions, how information theory can be applied in BO and why BO is useful for the hyper-parameter tuning of machine learning algorithms.

Chapter 4 describes an information-theoretical mechanism that generalizes BO to simultaneously optimize multiple objectives under the presence of several constraints. This algorithm is called predictive entropy search for multi-objective BO with constraints (PESMOC) and it is an extension of the predictive entropy search acquisition function that is described in Chapter 3. The chapter compares the empirical performance of PESMOC with respect to a state-of-the-art approach to constrained multi-objective optimization based on the expected improvement acquisition function. It is also compared with a random search through a set of synthetic, benchmark and real experiments.

Chapter 5 addresses the problem that faces BO when not only one but multiple input points can be evaluated in parallel that has been described in Section **??**. This chapter introduces an extension of PESMOC called parallel PESMOC (PPESMOC) that adapts to the parallel scenario. PPESMOC builds an acquisition function that assigns a value for each batch of points of the input space. The maximum of this acquisition function corresponds to the set of points that maximizes the expected reduction in the entropy of the Pareto set in each evaluation. Naive adaptations of PESMOC and the method based on expected improvement for the parallel scenario are used as a baseline to compare their performance with PPESMOC. Synthetic, benchmark and real experiments show how PPESMOC obtains an advantage in most of the considered scenarios. All the mentioned approaches are described in detail in this chapter.

Chapter ?? addresses a transformation that enables standard GPs to deliver better results in problems that contain integer-valued and categorical variables. We can apply BO to problems where we need to optimize functions that contain integer-valued and categorical variables with more guarantees of obtaining a solution with low regret. A critical advantage of this transformation, with respect to other approaches, is that it is compatible with any acquisition function. This transformation makes the uncertainty given by the GPs in certain areas of the space flat. As a consequence, the acquisition function can also be flat in these zones. This phenomenom raises an issue with the optimization of the acquisition function, that must consider the flatness of these areas. We use a one exchange neighbourhood approach to optimize the resultant acquisition function. We test our approach in synthetic and real problems, where we add empirical evidence of the performance of our proposed transformation.

Chapter ?? shows a real problem where BO has been applied with success. In this problem, BO has been used to obtain the optimal parameters of a hybrid Grouping Genetic Algorithm for attribute selection. This genetic algorithm is combined with an Extreme Learning Machine (GGA-ELM) approach for prediction of ocean wave features. Concretely, the significant wave height and the wave energy flux at a goal marine structure facility on the Western Coast of the USA is predicted. This chapter illustrates the experiments where it is shown that BO improves the performance of the GGA-ELM approach. Most importantly, it also outperforms a random search of the hyper-parameter space and the human expert criterion.

Chapter ?? provides a summary of the work done in this thesis. We include the conclusions retrieved by the multiple research lines covered in the chapters. We also illustrate lines for future research.

1.4 Definitions and Notation

Chapter 2

Foundations and Concepts

This chapter presents...

2.1 Introduction

2.2 Kernels

2.2.1 Motivation and Definition

2.2.2 Reproducing Kernel Hilbert Spaces

2.2.3 Examples and Properties

2.3 Risk Functions and Regularization

2.3.1 Empirical and Expected Risk

2.3.2 Regularized Risk Functional

2.3.3 Representer Theorem

2.4 Optimization

2.4.1 Convex Optimization

2.4.2 Unconstrained Problems

2.4.3 Constrained Problems

2.5 Statistical Learning

2.5.1 Uniform Convergence and Consistency

2.5.2 VC dimension and Structural Learning

2.6 Support Vector Machines

2.6.1 Linearly Separable Case

2.6.2 Non-Linearly Separable Case

2.6.3 Kernel Extension

2.6.4 SVM properties

2.6.5 Connection with Structural Learning

2.6.6 SVM Variants

2.7 Conclusions

In this chapter, we covered...

Chapter 3

Multi-Task Learning

This chapter presents...

3.1 Introduction

3.2 Why does Multi-Task Learning work?

3.2.1 Multi-Task Learning and Learning to Learn

Typically in Machine Learning the goal is to find the best hypothesis $h(x, \alpha_0)$ from a space of hypotheses $\mathcal{H} = \{h(x, \alpha), \alpha \in A\}$, where A is any set of parameters. This best candidate can be selected according to different inductive principles, which define a method of approximating a global function $f(x)$ from a training set: $z := \{(x_i, y_i),\ i = 1, \ldots, n\}$ where (x_i, y_i) are sampled from a distribution F. In the classical statistics we find the Maximum Likelihood approach, where the goal is to estimate the density $f(x) = P(y \mid x)$ and the hypotheses space is parametric, i.e. $\mathcal{H} = \{h(x, \alpha), \alpha \in A \subset \mathbb{R}^m\}$. The learner select the parameter α that maximizes the probability of the data given the hypothesis. Another more direct inductive principle is Empirical Risk Minimization, which is the most common one. In ERM the densities are ignored and an empirical error $\hat{R}_z(h(\cdot, \alpha))$ is minimized with the hope of minimizing the true expected error $R_F(h(\cdot, \alpha))$, which would result in a good generalization. Several models use the ERM principle to generalize from data such as Neural Networks or Support Vector Machines. These methods are designed to find a good hypothesis $h(x, \alpha)$ from a given space $\mathcal{H}$. The definition of such space $\mathcal{H}$ define the bias for these problems and its selection is crucial. If $\mathcal{H}$ does not contain any good hypothesis, the learner will not be able to learn. Also, if the hypotheses space is too large, the learning process is more difficult. The best hypotheses space we can provide is the one containing only the optimal hypothesis, but this is equivalent the original problem. When we only want to estimate a single function $f(x)$, a single-task scenario, there is no difference between learning the optimal hypotheses space (bias learning), that is, choosing $\mathcal{H} = \{h^*\}$, and ordinary learning of the optimal hypothesis function. That is, we can consider the family of hypotheses $\mathbb{H} = \{\{h(\cdot, \alpha)\}, h(\cdot, \alpha) \in \mathcal{H}\}$ and selecting the best single-element hypotheses space is equivalent to ordinary learning. Instead, we focus on the situation where we want to solve multiple related tasks, that is, estimating multiple functions $f_1(x), \ldots, f_T(x)$. In that case, we need a good space $\mathcal{H}$ that contains good solutions for the different tasks. In Baxter (2000) an effort is made to define the concepts needed to construct the theory about inductive bias learning or Learning to

Learn, which can be seen as a generalization of strict Multi-Task Learning. This is done by defining an environment of tasks and extending the work of Vapnik (2000), which defines the capacity of space of hypothesis; in its work, Baxter defines the capacity of a family of spaces of hypothesis.

Before presenting the concepts defined for Bias Learning, and to establish an analogy to those of ordinary learning, we briefly review some statistical learning concepts.

Ordinary Learning

In the ordinary statistical learning, some theoretical concepts are used:

- an *input space* $\mathcal{X}$ and an *output space* $\mathcal{Y}$,
- a *probability distribution* F, which is unknown, defined over $\mathcal{X} \times \mathcal{Y}$,
- a *loss function* $\ell(\cdot, \cdot) : \mathcal{Y} \times \mathcal{Y} \to \mathbb{R}$, and
- a *hypotheses space* $\mathcal{H} = \{h(x, \alpha), \alpha \in A \subset \mathbb{R}^m\}$ with hypothesis $h(\cdot, \alpha) : \mathcal{X} \to \mathcal{Y}$.

The goal for the learner is to select a hypothesis $h(x, \alpha) \in \mathcal{H}$, or equivalently $\alpha \in A$, that minimizes the expected risk

$$R_F(h(\cdot, \alpha)) = \int_{\mathcal{X} \times \mathcal{Y}} \ell(h(x, \alpha), y)\, dF(x, y).$$

The distribution F is unknown, but we have a training set $z = \{(x_1, y_1), \ldots, (x_n, y_n)\}$ of samples drawn from F. The approach is then is to apply the ERM inductive principle, that is to minimize the empirical risk

$$\hat{R}_z(h(\cdot, \alpha)) = \frac{1}{n} \sum_{i=1}^{n} l(h(x_i), y_i).$$

Thus, a learner $\mathcal{A}$ maps the set of training samples to a set of hypotheses:

$$\mathcal{A} : \bigcup (\mathcal{X} \times \mathcal{Y})^n \to \mathcal{H}.$$

Although $\hat{R}_z(h(\cdot, \alpha))$ is an unbiased estimator of $R_F(h(\cdot, \alpha))$, it has been shown Vapnik (2000) that this approach, despite being the most evident one, is not the best principle that can be followed. This has relation with two facts: the first one is that the unbiased property is an asymptotical one, the second one has to do with overfitting. Vapnik answers to the question of what can be said about R_F when $h(\cdot, \alpha^*)$ minimizes $\hat{R}_z(h(\cdot, \alpha))$, and, moreover, his results are valid also for small number of training samples n. More specifically, Vapnik sets the sufficient and necessary conditions for the consistency of an inductive learning process, i.e. for $\hat{R}_z(h(\cdot, \alpha)) \xrightarrow{P} R_F(h(\cdot, \alpha))$ uniformly. Vapnik also defines the capacity of a hypotheses space and use it to derive bounds on the rate of this convergence for any $\alpha \in A$ and, more importantly, bounds on the difference $\inf_{\alpha \in A} \hat{R}_z(h(\cdot, \alpha)) - \inf_{\alpha \in A} R_F(h(\cdot, \alpha))$. Under some general conditions, he proves that

$$\inf_{\alpha \in A} \hat{R}_z(h(\cdot, \alpha)) - \inf_{\alpha \in A} R_F(h(\cdot, \alpha)) \leq B(n/\mathrm{VCdim}(\mathcal{H})) \tag{3.1}$$

where B is some non-decreasing function and $\mathrm{VCdim}(\mathcal{H})$ is the capacity of the space $\mathcal{H}$, also named the VC-dimension $\mathcal{H}$. This means that the generalization ability of a learning process can be controlled in terms of two factors:

- The number of training samples n. A greater number of training samples assures a better generalization of the learning process.This looks intuitive and could be already inferred from the asymptotical properties.
- The VC-dimension VCdim $(\mathcal{H})$ of the hypotheses space $\mathcal{H}$, which is desirable to be small. This term is not intuitive and is the most important term in Vapnik theory.

The VC-dimension measures the capacity of a set of hypotheses $\mathcal{H}$. If the capacity of the set $\mathcal{H}$ is too large, we may find a hypothesis $h\left(x, \alpha^*\right)$ that minimizes $\hat{R}_z$ but does not generalize well and therefore, does not minimize R_F. This is the overfitting problem. On the other side, if we use a simple $\mathcal{H}$, with low capacity, we could be in a situation where there is not a good hypothesis $h\left(x, \alpha\right) \in \mathcal{H}$, so the empirical risk $\inf_{\alpha \in A} R_F$ is too large. This is the underfitting problem.

Bias Learning: Concept and Components

In Baxter (2000) the goal is not to learn the optimal hypothesis $h\left(\cdot, \alpha^*\right)$ from a fixed space $\mathcal{H}$ but to learn a good space $\mathcal{H}$ from which we can obtain an optimal hypothesis in different situations. Two main concepts are defined: the *family of hypotheses spaces* and an *environment* of related tasks. For simplicity we write $h(x)$ instead of $h(x, \alpha)$ and h instead of $h(\cdot, \alpha)$. Using these concepts, the bias learning problem has the following components:

- an *input space* $\mathcal{X}$ and an *output space* $\mathcal{Y}$,
- an *environment* $(\mathcal{P}, Q)$ where $\mathcal{P}$ is a set of distributions P defined over $\mathcal{X} \times \mathcal{Y}$, and we can sample from $\mathcal{P}$ according to a distribution Q,
- a *loss function* $\ell\left(\cdot, \cdot\right) : \mathcal{Y} \times \mathcal{Y} \rightarrow \mathbb{R}$, and
- a *family of hypotheses spaces* $\mathbb{H} = \{\mathcal{H}_\beta, \beta \in B\}$, where each element $\mathcal{H}_\beta$ is a set of hypotheses.

Analogous to ordinary learning, the goal is to minimize the expected risk, defined as

$$R_Q(\mathcal{H}_\beta) = \int_{\mathcal{P}} \inf_{h \in \mathcal{H}_\beta} R_P(h) dQ(P) = \int_{\mathcal{P}} \inf_{h \in \mathcal{H}_\beta} \int_{\mathcal{X} \times Y} l(h(x), y) dP(x, y) dQ(P). \tag{3.2}$$

Observe that this risk is not a function of a specific hypothesis but it depends on the selection of a whole hypotheses space $\mathcal{H}_\beta$. Again, we do not know $\mathcal{P}$ nor Q, but we have a training set samples from the environment $(\mathcal{P}, Q)$ obtained in the following way:

1. Sample T times from Q obtaining $P_1, \ldots, P_T \in \mathcal{P}$
2. For $r = 1, \ldots, T$ sample m pairs $z_r = \{(x_1^r, y_1^r), \ldots, (x_m^r, y_m^r)\}$ according to P_r where $(x_i^r, y_i^r) \in X \times Y$.

We obtain a sample $z = \{(x_i^r, y_i^r), r = 1,\ i = 1, \ldots,\ m = 1, \ldots, T\}$, with m examples from T different learning tasks, and

$$\boldsymbol{z} := \begin{matrix} (x_1^1, y_1^1) & \ldots & (x_m^1, y_m^1) \\ \vdots & \ddots & \vdots \\ (x_1^T, y_1^T) & \ldots & (x_m^T, y_m^T) \end{matrix}$$

is named as a (T, m)-sample. Using $\boldsymbol{z}$ we can define the empirical loss as

$$\hat{R}_{\boldsymbol{z}}(\mathcal{H}_\beta) = \sum_{r=1}^{T} \inf_{h \in \mathcal{H}_\beta} \hat{R}_{z_r}(h) = \sum_{r=1}^{T} \inf_{h \in \mathcal{H}_\beta} \sum_{i=1}^{m} l(h(x_i^r), y_i^r), \tag{3.3}$$

which is an average of the empirical losses of each task. Note, however, that in the case of the bias learner this estimate is biased, since $R_{P_r}(h)$ does not coincide with $\hat{R}_{z_r}(h)$. Putting all together, a bias learner $\mathcal{A}$ maps the set of all (T, m)-samples to a family of hypotheses spaces:

$$\mathcal{A} : \bigcup (\mathcal{X} \times \mathcal{Y})^{(T,m)} \to \mathbb{H}.$$

To follow an analogous path to that of ordinary learning, the milestones in bias learning theory should include:

- Checking the consistency of the Bias Learning methods, i.e. proving that $\hat{R}_{\boldsymbol{z}}(\mathcal{H}_\beta)$ converges uniformly in probability to $R_Q(\mathcal{H}_\beta)$.
- Defining a notion of capacity of hypotheses space families $\mathbb{H}$.
- Finding a bound of $\hat{R}_{\boldsymbol{z}}(\mathcal{H}_\beta) - R_Q(\mathcal{H}_\beta)$ for any β using the capacity of the hypotheses space family. If possible, finding also a bound for $\inf_{\beta \in B} \hat{R}_{\boldsymbol{z}}(\mathcal{H}_\beta) - \inf_{\beta \in B} R_Q(\mathcal{H}_\beta)$.

To try to achieve these goals some previous definitions are needed. From this point, since any $\mathcal{H}$ is defined by a $\beta \in B$, we omit β and write just $\mathcal{H}$ for simplicity.

Bias Learning: Capacities and Uniform Convergence

In first place, a *sample-driven* pseudo-metric of $(T, 1)$-empirical risks is defined. Consider a sequence of T probabilities $\boldsymbol{P} = (P_1, \ldots, P_T)$ sampled from $\mathcal{P}$ according the distribution Q.

Definition 3.1 (*sample-driven* pseudometric)**.** Given a $(T, 1)$-sample

$$\left\{(x_1^1, y_1^1), (x_2^2, y_2^2), \ldots, (x_T^T, y_T^T)\right\},$$

consider the set of sequences of T hypothesis

$$\mathcal{H}^T := \{\boldsymbol{h} = (h_1, \ldots, h_T), h_1, \ldots, h_T \in \mathcal{H}\}.$$

We can define then the set of $(T, 1)$-empirical risks, with one sample per task, as

$$\mathcal{H}_\ell^T := \left\{ \boldsymbol{h}_\ell(x_1, y_1, \ldots, x_T, y_T) = \sum_{r=1}^{T} \ell(h(x_i), y_i), h_1, \ldots, h_T \in \mathcal{H} \right\}$$

The family of the set of $(T, 1)$-risks of hypothesis is then $\mathbb{H}^T = \bigcup_{\mathcal{H} \in \mathbb{H}} \mathcal{H}^T$. Now we can define

$$d_{\boldsymbol{P}}(\boldsymbol{h}_\ell, \boldsymbol{h}'_\ell) = \int_{(\mathcal{X} \times \mathcal{Y})^T} \left| \boldsymbol{h}_\ell(x_1, y_1, \ldots, x_T, y_T) - \boldsymbol{h}'_\ell(x_1, y_1, \ldots, x_T, y_T) \right| dP_1(x_1, y_1) \ldots dP_T(x_T, y_T)$$

for $\boldsymbol{h}_\ell, \boldsymbol{h}'_\ell \in \mathcal{H}_\ell, \mathcal{H}'_\ell$ as a pseudo-metric in $\mathbb{H}^T$.

Then, a *distribution-driven* pseudo-metric is defined.

Definition 3.2 (*distribution-driven* pseudo-metric)**.** Given a distribution P on $\mathcal{X} \times \mathcal{Y}$. Consider the set of infimum expected risk for each $\mathcal{H}$:

$$\mathcal{H}^* := \inf_{h \in \mathcal{H}} R_P(h).$$

The family of such sets is defined as $\mathbb{H}^* = \{\mathcal{H}^*, \mathcal{H} \in \mathbb{H}\}$. The pseudo-metric in this space is given by d_Q:

$$d_Q(\mathcal{H}_1^*, \mathcal{H}_2^*) = \int_{\mathcal{P}} |\mathcal{H}_1^* - \mathcal{H}_2^*| \, dQ$$

for $\mathcal{H}_1^*, \mathcal{H}_2^* \in \mathbb{H}^*$. With these two pseudo-metrics, two capacities for families of hypotheses spaces are defined. For that the definition of ϵ-cover is needed.

Definition 3.3 (ϵ-cover)**.** Given a pseudo-metric d_S in a space $\mathcal{S}$, a set of l elements $s_1, \ldots, s_l \in \mathcal{S}$ is an ϵ-cover of $\mathcal{S}$ if $\forall s \in S \; d_S(s, s_i) \leq \epsilon$ for some $i = 1, \ldots, l$. Let $\mathcal{N}(\epsilon, \mathcal{S}, d_S)$ denote the size of the smallest ϵ-cover.

Then, we can define the following capacities of a family space $\mathbb{H}$:

- The *sample-driven capacity* $C\left(\epsilon, \mathbb{H}^T\right) := \sup_{\boldsymbol{P}} \mathcal{N}(\epsilon, \mathbb{H}^T, d_{\boldsymbol{P}})$.
- The *distribution-driven capacity* $C\left(\epsilon, \mathbb{H}^*\right) := \sup_Q \mathcal{N}(\epsilon, \mathbb{H}^*, d_Q)$.

Using these capacities, the convergence (uniformly over all $\mathcal{H} \in \mathbb{H}$) of bias learners can be proved (Baxter, 2000, Theorem 2). Moreover, the bias expected risk is bounded

$$\hat{R}_{\boldsymbol{z}}(\mathcal{H}) \leq R_Q(\mathcal{H}) + \epsilon$$

with probability $1 - \eta$, given sufficiently large T and m,

$$T \geq \max\left(\frac{256}{T\epsilon^2} \log \frac{8C\left(\frac{\epsilon}{32}, \mathbb{H}^*\right)}{\eta}, \frac{64}{\epsilon^2}\right), \; m \geq \max\left(\frac{256}{T\epsilon^2} \log \frac{8C\left(\frac{\epsilon}{32}, \mathbb{H}^T\right)}{\eta}, \frac{64}{\epsilon^2}\right).$$

It should be noted that the bound for m is inversely proportional to T, that is, the more tasks we have, the less samples we need for each task.

Multi-Task Learning

The previous result is a result for pure Bias Learning, where we have an $(\mathcal{P}, Q)$-environment of tasks. In Multi-Task Learning, we have a fixed number of tasks T and a fixed sequence of distributions $\boldsymbol{P} = (P_1, \ldots, P_T)$, where P_i is a distribution over $(\mathcal{X} \times \mathcal{Y})^m$. The goal is not learning a hypotheses space $\mathcal{H}$ but a sequence of hypothesis $\boldsymbol{h} = (h_1, \ldots, h_T), h_1, \ldots, h_T \in \mathcal{H}$. Thus, the Multi-Task expected risk is

$$R_{\boldsymbol{P}}(\boldsymbol{h}) = \sum_{r=1}^{T} R_{P_r}(h_r) = \sum_{r=1}^{T} \int_{\mathcal{X} \times Y} l(h_r(x), y) dP_r(x, y), \tag{3.4}$$

and the empirical risk is defined as

$$\hat{R}_{\boldsymbol{z}}(\boldsymbol{h}) = \sum_{r=1}^{T} \hat{R}_{z_r}(h_r) = \sum_{r=1}^{T} \sum_{i=1}^{m} l(h_r(x_i^r), y_i^r). \tag{3.5}$$

A similar result to that of Bias Learning is given for Multi-Task Learning (Baxter, 2000, Theorem 4):

$$\hat{R}_{\boldsymbol{z}}(\boldsymbol{h}) \leq R_{\boldsymbol{P}}(\boldsymbol{h}) + \epsilon,$$

with probability $1 - \eta$ given that the number of samples per task

$$m \geq \max\left(\frac{64}{T\epsilon^2}\log\frac{4C\left(\frac{\epsilon}{16}, \mathbb{H}^T\right)}{\eta}, \frac{16}{\epsilon^2}\right).$$

Observe that we do not need the *distribution-driven* capacity in this case, just the *sample-driven* capacity.

Feature Learning

Feature Learning is a common way to encode bias. The most popular example are Neural Networks, where all the hidden layers can be seen as a Feature Learning engine that learns a mapping from the original space to a space with "strong" features. In general, a set of "strong" feature maps is defined as $\mathcal{F} = \{f, f : \mathcal{X} \to \mathcal{V}\}$. Using these features, functions $g \in \mathcal{G}$ (which are tipically simple) are built: $\mathcal{X} \to_f \mathcal{V} \to_g \mathcal{Y}$. Thus, for each map f, the hypotheses space can be expressed as $\mathcal{H}_f = \{h = \mathcal{G} \circ f, g \in \mathcal{G}\}$, and the family of hypotheses spaces is $\mathbb{H} = \{\mathcal{H}_f, f \in \mathcal{F}\}$. Now, the Bias Learning problem is the problem of finding a good mapping f. It is proved (Baxter, 2000, Theorem 6) that in the Feature Learning case the capacities of $\mathbb{H}$ can be bounded by the capacities of $\mathcal{F}$ and $\mathcal{G}$ as

$$\begin{aligned} C\left(\epsilon, \mathbb{H}^T\right) &\leq C\left(\epsilon_1, \mathcal{G}\right)^T C_{\mathcal{G}_\ell}(\epsilon_2, \mathcal{F}), \\ C\left(\epsilon, \mathbb{H}^*\right) &\leq C_{\mathcal{G}_\ell}(\epsilon, \mathcal{F}) \end{aligned}$$

with $\epsilon = \epsilon_1 + \epsilon_2$. Here, $C_{\mathcal{G}_\ell}(\epsilon, \mathcal{F})$ is defined as $C_{\mathcal{G}_\ell}(\epsilon, \mathcal{F}) := \sup_P \mathcal{N}(\epsilon, \mathcal{F}, d_{[P,\mathcal{G}_\ell]})$, where

$$d_{[P,\mathcal{G}_\ell]}(f, f') = \int_{\mathcal{X}\times\mathcal{Y}} sup_{g\in\mathcal{G}} \left|\ell\left(g \circ f(x), y\right) - \ell\left(g \circ f'(x), y\right)\right| dP(x, y)$$

is a pseudo-metric. Using these results alongside those presented for Bias Learning is useful to establish bounds for Feature Learning models like Neural Networks.

Generalized VC-Dimension for Multi-Task Learning

The concepts presented until now rely on the concepts of two capacities of a family of hypotheses spaces $\mathbb{H}$ to establish bounds in the difference $\hat{R}_{\boldsymbol{z}}(\boldsymbol{h}) - R_Q(\boldsymbol{h})$, that is, the probability of deviations between the empirical and expected risks for a given hypothesis sequence. However, it would be more useful to find some result concerning the empirical error and the *best expected error*. To achieve this, a generalized VC-dimension is developed in Baxter (2000) for Multi-Task Learning with Boolean hypothesis.

Definition 3.4. Let $\mathcal{H}$ be a space of boolean functions and $\mathbb{H}$ a boolean hypotheses space family. Denote the set of $T \times m$ matrices in $\mathcal{X}$ as $\mathcal{X}^{T\times m}$ For each $X \in \mathcal{X}^{T\times m}$ and each $\mathcal{H} \in \mathbb{H}$ define the set of binary $T \times m$ matrices

$$\mathcal{H}_{|X} := \left\{ \begin{pmatrix} h\left(x_1^1\right) & \dots & h\left(x_m^1\right) \\ \vdots & \ddots & \vdots \\ h\left(x_1^T\right) & \dots & h\left(x_m^T\right) \end{pmatrix}, h \in \mathcal{H} \right\},$$

and the corresponding family of such sets as

$$\mathbb{H}_{|X} = \bigcup_{\mathcal{H}\in\mathbb{H}} \mathcal{H}_{|X}.$$

For each $T, m \geq 0$ define the number of binary matrices obtainable with $\mathbb{H}$ as

$$\Pi_{\mathbb{H}}(T, m) := \max_{X\in\mathcal{X}^{T\times m}} \left|\mathbb{H}_{|X}\right|.$$

Note that $\Pi_{\mathbb{H}}(T, m) \leq 2^{Tm}$ and if $\Pi_{\mathbb{H}}(T, m) = 2^{Tm}$ we say that $\mathbb{H}$ shatters $\mathcal{X}^{T\times m}$. For each $T > 0$ define

$$d_{\mathbb{H}}(T) := \max_{m:\Pi_{\mathbb{H}}(T,m)=2^{Tm}} m,$$

Here, $d_{\mathbb{H}}(T)$ is the generalized VC-dimension. Also define

$$\overline{d}(\mathbb{H}) := \text{VCdim}\left(\mathbb{H}^1\right) = \text{VCdim}\left(\bigcup_{\mathcal{H}\in\mathbb{H}} \mathcal{H}\right),$$
$$\underline{d}(\mathbb{H}) := \max_{\mathcal{H}\in\mathbb{H}} \text{VCdim}\left(\mathcal{H}\right).$$

$$d_{\mathbb{H}}(T) \geq \max\left(\left\lfloor \frac{\overline{d}(\mathbb{H})}{T} \right\rfloor, \underline{d}(\mathbb{H})\right).$$

where it can be observed that

$$\overline{d}(\mathbb{H}) \geq d_{\mathbb{H}}(T) \geq \underline{d}(\mathbb{H}). \tag{3.6}$$

Now we can present the relevant result expressed in (Baxter, 2000, Corollary 13).

Theorem 3.5. *Given a sequence* $\boldsymbol{P} = (P_1, \ldots, P_T)$ *on* $(\mathcal{X} \times \{0, 1\})^T$*, and a sample* $\boldsymbol{z}$ *from this distribution. Consider also a sequence* $\boldsymbol{h} = (h_1, \ldots, h_T)$ *of boolean hypothesis* $h_i \in \mathcal{H}$*, then for every* $\epsilon > 0$

$$\left|R_{\boldsymbol{P}}(\boldsymbol{h}) - \hat{R}_{\boldsymbol{z}}(\boldsymbol{h})\right| \leq \epsilon,$$

with probability $1 - \eta$ *given that the number of samples per task*

$$m \geq \frac{88}{\epsilon^2}\left[2d_{\mathbb{H}}(T)\log\frac{22}{\epsilon} + \frac{1}{T}\log\frac{4}{\eta}\right]. \tag{3.7}$$

Here, since $d_{\mathbb{H}}(T) \geq d_{\mathbb{H}}(T+1)$, it is easy to see that as the number of task T increases, the number of examples needed per task can decrease. Moreover, as shown in (Baxter, 2000, Theorem 14), if this bound on m is not fulfilled, then we can always find a sequence of distributions $\boldsymbol{P}$ such that

$$\inf_{h\in\mathcal{H}} \hat{R}_{\boldsymbol{z}}(\boldsymbol{h}) > \inf_{h\in\mathcal{H}} R_{\boldsymbol{P}}(\boldsymbol{h}) + \epsilon.$$

With this results we can see that the condition (3.7) has some important properties:

- It is a computable bound, given that we know how to compute $d_{\mathbb{H}}(T)$.

- It provides a sufficient condition for the uniform convergence (in probability) of the empirical risk to the expected risk.
- It provides a necessary condition for the consistency of Multi-Task Learners, i.e. uniform convergence of the best empirical risk to the best expected risk.

3.2.2 Learning with Related Tasks

Using the work of Baxter (2000) as the foundation, several important notions and results are presented in Ben-David and Borbely (2008) for boolean hypothesis functions defined over $\mathcal{X} \times \{0,1\}$. One of the main contributions of this work is a notion of task relatedness. In Baxter (2000) the tasks are related by sharing a common inductive bias that can be learned. In Ben-David and Borbely (2008) a precise mathematical definition for task relatedness is given. The other important contribution is the focus on the individual risk of each task. In Baxter (2000) all the results are given for the Multi-Task empirical and expected risks, which are an average of the risks of each task. However, bounding this average does not establish a sharp bound of the risk of each particular task. This is specially relevant if we are in a Transfer Learning scenario, where there is a target task that we want to solve and the remaining tasks can be seen as an aid to improve the performance in the target.

A Notion of Task Relatedness: $\mathcal{F}$-Related Tasks

The main concept for the theory developed in Ben-David and Borbely (2008) is a set of $\mathcal{F}$ of transformations $f : \mathcal{X} \to \mathcal{X}$. Given a probability distribution F over $\mathcal{X} \times \{0,1\}$, a set of tasks with distributions $P_1, \ldots, P_T$ are $\mathcal{F}$-related if, for each task there exists some $f_i \in \mathcal{F}$ such that $P_i = f_i(F)$.

Definition 3.6 ($\mathcal{F}$-related task)**.** Consider a measurable space $(\mathcal{X}, \mathcal{A})$ and the corresponding measurable product space $(\mathcal{X} \times \{0,1\}, \mathcal{A} \times \wp(\{0,1\}))$, where $\wp(\Omega)$ is the powerset of set Ω. Consider P a probability distribution over this product space and a function $f : \mathcal{X} \to \mathcal{X}$, then we define the distribution $f[P]$ such that for any $S \in \mathcal{A}$,

$$f[P](S) := P(\{(f(x), b), (x, b) \in S\}).$$

Let $\mathcal{F}$ be a set of transformations $f : \mathcal{X} \to \mathcal{X}$, and let P_1, P_2 be distributions over $(\mathcal{X} \times \{0,1\}, \mathcal{A} \times \wp(\{0,1\}))$, then the distributions P_1, P_2 are $\mathcal{F}$-related if $f[P_1] = P_2$ or $f[P_2] = P_1$ for some $f \in \mathcal{F}$.

This notion establishes a clear definition of related tasks but we are interested in how a learner can use this relatedness to improve the learning process. For that, considering that $\mathcal{F}$ is a group under function composition, we regard at the action of the group $\mathcal{F}$ over the set of hypotheses $\mathcal{H}$. This action defines the following equivalence relation in $\mathcal{H}$:

$$h_1 \sim_{\mathcal{F}} h_2 \iff \exists f \in \mathcal{F}, h_1 \circ f = h_2.$$

This equivalence relation defines equivalence classes $[h]$, that is let $h' \in \mathcal{H}$ be an hypothesis, then $h' \in [h]$ iff $h' \sim_{\mathcal{F}} h$. We consider the quotient space

$$\mathcal{H}_{\mathcal{F}} := \mathcal{H}/\sim_{\mathcal{F}} = \{[h], h \in \mathcal{H}\}.$$

It is important to observe that $\mathcal{H}_{\mathcal{F}} = \mathbb{H}'$ is a hypotheses space family, since it is a set of equivalence classes $[h] = \mathcal{H}'$, which are sets of hypotheses.

The Multi-Task Empirical Risk Minimization

This equivalence classes are useful to divide the learning process in two stages, this is called the *Multi-Task ERM*. Consider the samples $z_1, \dots, z_T$ from T different tasks, then

1. Select the best hypothesis class $[h^{\mathcal{F}}] \in \mathcal{H}_{\mathcal{F}}$:

$$[h^{\mathcal{F}}] := \min_{[h]\in\mathcal{H}_{\mathcal{F}}} \inf_{h_1,\dots,h_T\in[h]} \frac{1}{T}\sum_{r=1}^{T} \hat{R}_{z_i}(h_i),$$

2. Select the best hypothesis $h^{\diamond}$ for the target task (without loss of generality, consider the first one):

$$h^{\diamond} = \inf_{h\in[h^{\mathcal{F}}]} \hat{R}_{z_1}(h).$$

For example, consider the handwritten digits recognition problem, we might integrate T different datasets designed in different conditions. Each dataset have been created using certain conditions of light and some specific scanner for getting the images. Even different pens or pencils might be influential in the stroke of the numbers. All these conditions are the $\mathcal{F}$ transformations, and each $f \in \mathcal{F}$ generate a different bias for the dataset. However, there exists a probability for "pure" digits, e.g. the pixels of digit one have higher probability around a line in the middle of the picture than in the sides. This "pure" probability distribution P_0 and all the distributions $P_1, \dots, P_T$ from which our datasets have been sampled might be $\mathcal{F}$-related among them and with P_0. If we first determine the $\mathcal{F}$-equivalent class of hypothesis $[h]$ suited for digit recognition in the first stage, then it will be easier to select $h_1, \dots, h_T \in [h]$ for each dataset in the second one.

Bounds for $\mathcal{F}$-Related Tasks

The results of Theorem 3.5 can be applied to the hypothesis quotient space of equivalent classes $\mathcal{H}_{\mathcal{F}}$. However the following results is needed first. Let P_1, P_2 be $\mathcal{F}$-related distributions, then this statement can be proved (Ben-David and Borbely, 2008, Lemma 2):

$$\inf_{h\in\mathcal{H}} R_{P_1}(h) = \inf_{h\in\mathcal{H}} R_{P_2}(h). \tag{3.8}$$

This indicates that the the expected risk is invariant under transformations of $\mathcal{F}$. Now, one of the main results (Baxter, 2000, Theorem 2) can be given.

Theorem 3.7. *Let $\mathcal{F}$ be a set of transformations $f : \mathcal{X} \to \mathcal{X}$ that is a group under function composition. Let $\mathcal{H}$ be a hypotheses space so that $\mathcal{F}$ acts as a group over $\mathcal{H}$, and consider the quotient space $\mathcal{H}_{\mathcal{F}} = \{[h], h \in \mathcal{H}\}$. Consider $\boldsymbol{P} = (P_1, \dots, P_T)$ a sequence of $\mathcal{F}$-related distributions over $\mathcal{X} \times \{0, 1\}$, and $\boldsymbol{z} = (z_1, \dots, z_T)$ the corresponding sequence of samples where z_i is sampled using P_i, then for every $[h] \in \mathcal{H}_{\mathcal{F}}$ and $\epsilon > 0$*

$$\left| \inf_{h_1,\dots,h_T\in[h]} \frac{1}{T}\sum_{r=1}^{T} \hat{R}_{z_r}(h_r) - \inf_{h'\in[h]} R_{P_1}(h') \right| \leq \epsilon$$

with probability greater than η if the number of samples from each distribution satisfies

$$|z_i| \geq \frac{88}{\epsilon^2}\left[2d_{\mathcal{H}_{\mathcal{F}}}(T)\log\frac{22}{\epsilon} + \frac{1}{T}\log\frac{4}{\eta}\right]. \tag{3.9}$$

Note that, in contrast to Theorem 3.5, this result bounds the expected risk of a single task, not the average risk. This is the consequence of applying Theorem 3.5 and substituting the average empirical error using the result from (3.8). Also observe that here the hypotheses space family used is the quotient space $\mathcal{H}_{\mathcal{F}}$, and the VC-dimension of such family is used. Using this result, a bound for learners using the Multi-Task ERM principle is given (Ben-David and Borbely, 2008, Theorem 3)

Theorem 3.8. *Consider $\mathcal{F}$ and $\mathcal{H}$ as in the previous theorem. Consider also the previous sequences of distributions $(P_1, \dots, P_T)$ and corresponding samples $(z_1, \dots, z_T)$. Consider $\underline{d}(\mathcal{H}_{\mathcal{F}}) = \max_{h \in \mathcal{H}} VCdim([h])$. Let $h^{\diamond}$ be the hypothesis selected using the Multi-Task ERM principle, then for every $\epsilon_1, \epsilon_2 > 0$*

$$\hat{R}_{z_1}(h^{\diamond}) - \inf_{h' \in \mathcal{H}} R_{P_1}(h') \leq 2(\epsilon_1 + \epsilon_2)$$

with probability greater than η if

$$|z_1| \geq \frac{64}{\epsilon^2}\left[2\underline{d}(\mathcal{H}_{\mathcal{F}}) \log \frac{12}{\epsilon} + \frac{1}{T}\log\frac{8}{\eta}\right], \tag{3.10}$$

and for $i \neq 1$

$$|z_i| \geq \frac{88}{\epsilon^2}\left[2d_{\mathcal{H}_{\mathcal{F}}}(T) \log \frac{22}{\epsilon} + \frac{1}{T}\log\frac{8}{\eta}\right]. \tag{3.11}$$

The idea of the proof of this theorem helps to understand how using different tasks can help to improve the performance in the target task. Consider $h^* = \inf_{h \in \mathcal{H}} R_{P_1}(h)$ the best hypothesis for the P_1 distribution. According to Theorem 3.7, for $[h^*]$ we have that

$$\inf_{h_1, \dots, h_T \in [h^*]} \frac{1}{T}\sum_{r=1}^{T} \hat{R}_{z_r}(h_r) \leq \inf_{h' \in [h^*]} R_{P_1}(h') + \epsilon_1.$$

Also, in the first stage of Multi-Task ERM principle, we select the hypothesis class $[h^{\mathcal{F}}]$ that minimizes $\inf_{\boldsymbol{h} \in [h]} R_{\boldsymbol{P}}(\boldsymbol{h})$ where $\boldsymbol{h}$ is a sequence of hypothesis of $\mathcal{H}_{\mathcal{F}}$. According to Theorem 3.7, for $[h^{\mathcal{F}}]$ we have that

$$\inf_{h' \in [h^{\mathcal{F}}]} R_{P_1}(h') \leq \inf_{h_1, \dots, h_T \in [h^{\mathcal{F}}]} \frac{1}{T}\sum_{r=1}^{T} \hat{R}_{z_r}(h_r) + \epsilon_1.$$

Using these two inequalities we get

$$\inf_{h' \in [h^{\mathcal{F}}]} R_{P_1}(h') \leq \inf_{h' \in [h^*]} R_{P_1}(h') + 2\epsilon_1$$

under the condition (3.9). This bounds the risk of the hypotheses space given by the equivalence class of $h^{\mathcal{F}}$ and establishes the inequality (3.11).

Once we select $[h^{\mathcal{F}}]$, the second stage is just ERM using this hypotheses space. According to the Vapnik (1982),

$$\inf_{h \in \mathcal{H}} R_{z_1}(h) - \inf_{h \in \mathcal{H}} R_{P_1}(h) \leq \epsilon_2$$

if

$$|z_1| \geq \frac{64}{\epsilon^2}\left[2\mathrm{VCdim}\,(\mathcal{H}) \log \frac{12}{\epsilon} + \frac{1}{T}\log\frac{8}{\eta}\right].$$

Since the ERM will not use the whole space $\mathcal{H}$ but the subset $[h^{\mathcal{F}}] \subset \mathcal{H}$, and

$$\text{VCdim}\left([h^{\mathcal{F}}]\right) \leq \max_{[h]\in\mathcal{H}_{\mathcal{F}}} \text{VCdim}\left([h]\right) = \underline{d}(\mathcal{H}_{\mathcal{F}}).$$

then we can write the inequality (3.10) of the theorem. The advantage of using multiple tasks is then illustrated in this bound and it will be defined by the gap between $\text{VCdim}\left(\mathcal{H}\right)$ and $\underline{d}(\mathcal{H}_{\mathcal{F}})$. If $\underline{d}(\mathcal{H}_{\mathcal{F}})$ is smaller than $\text{VCdim}\left(\mathcal{H}\right)$, the number of samples needed to solve the target task will also be smaller. Also, the sample complexity of the rest of tasks is given by $d_{\mathcal{H}_{\mathcal{F}}}(T)$.

That is, Multi-Task Learning allows to select a subset of hypotheses from which a learner can use the ERM principle. In this stage, the sample complexity is controlled by the generalized VC-dimension of the set of equivalent classes of hypothesis. Once the best equivalent class has been selected, the VC-dimension of this subset, compared to the VC-dimension of the whole set of hypotheses, is what marks the difference between Single Task and Multi-Task Learning.

Analysis of generalized VC-dimension with $\mathcal{F}$-related tasks

As we have seen in Theorem 3.8, the VC-dimensions $\text{VCdim}\left(\mathcal{H}\right), \underline{d}(\mathcal{H}_{\mathcal{F}})$ and $d_{\mathcal{H}_{\mathcal{F}}}(T)$ are crucial for stating the advantage of Multi-Task over Single Task Learning. To understand better how these concepts interact, Ben-David et al. give some theoretical results. Recall that, given a hypotheses space $\mathcal{H}$, $\mathcal{H}_{\mathcal{F}}$ is a family of hypotheses spaces composed by the hypotheses spaces $[h], h \in \mathcal{H}$, then

$$\begin{aligned}
d_{\mathcal{H}_{\mathcal{F}}}(T) &= \max_{\left\{m, \Pi_{\mathcal{H}_{\mathcal{F}}}=2^{Tm}\right\}} m, \\
\underline{d}(\mathcal{H}_{\mathcal{F}}) &= max_{h\in\mathcal{H}}\text{VCdim}\left([h]\right), \\
\overline{d}(\mathcal{H}_{\mathcal{F}}) &= \text{VCdim}\left(\bigcup_{[h]\in\mathcal{H}_{\mathcal{F}}} [h]\right) = \text{VCdim}\left(\mathcal{H}\right).
\end{aligned}$$

Using the result from (3.6) we observe that

$$\underline{d}(\mathcal{H}_{\mathcal{F}}) \leq d_{\mathcal{H}_{\mathcal{F}}}(T) \leq \text{VCdim}\left(\mathcal{H}\right).$$

That is, the best we can hope when bounding the sample complexity in Theorem 3.8 is $\underline{d}(\mathcal{H}_{\mathcal{F}}) = d_{\mathcal{H}_{\mathcal{F}}}(T)$. Ben-David et al. give evidence that, with some restrictions on $\mathcal{H}$, this lower bound can be achieved (Ben-David and Borbely, 2008, Theorem 4).

Theorem 3.9. *If the support of h is bounded, i.e. $|\{x \in \mathcal{X}, h(x) = 1\}| < M$, for all $h \in \mathcal{H}$, then there exists T_0 such that for all $T > T_0$*

$$d_{\mathcal{H}_{\mathcal{F}}}(T) = \underline{d}(\mathcal{H}_{\mathcal{F}}).$$

Thus, a sufficient condition on the hypotheses space $\mathcal{H}$ to achieve the lowest $d_{\mathcal{H}_{\mathcal{F}}}(T)$ is a bounded support of any hypothesis. Although this condition may be too restricting, it can also be proved that the upper limit of $d_{\mathcal{H}_{\mathcal{F}}}(T)$, that is, $\text{VCdim}\left(\mathcal{H}\right)$, under some conditions on $\mathcal{F}$ is not achieved.

The following result (Ben-David and Borbely, 2008, Theorem 6) shows this.

Theorem 3.10. *If $\mathcal{F}$ is finite and $\frac{T}{\log(T)} \geq VCdim(\mathcal{H})$, then*

$$d_{\mathcal{H}_{\mathcal{F}}}(T) \leq 2\log(|\mathcal{F}|)$$

This inequality indicates that, given a finite set of transformation $\mathcal{F}$, there are scenarios when VCdim $(\mathcal{H})$ is arbitrarily large but $d_{\mathcal{H}_{\mathcal{F}}}(T)$ is bounded, and therefore, the right-hand side of inequality (3.11) is also bounded. That is, the Multi-Task bound, which substitutes VCdim $(\mathcal{H})$ by $d_{\mathcal{H}_{\mathcal{F}}}(T)$ is a better one in this cases.

3.2.3 Other bounds for Multi-Task Learning

The work of Baxter Baxter (2000) set the foundations for the theoretical analysis of MTL and LTL. In this work, an MTL extension to the VC-dimension is given, and it is used to develop some results bounding the difference between the Multi-Task empirical and expected risks

$$\left| R_{\boldsymbol{P}}(\boldsymbol{h}) - \hat{R}_{\boldsymbol{z}}(\boldsymbol{h}) \right|$$

for any sequence of hypothesis $\boldsymbol{h} \in \mathcal{H}^T$, see Theorem 3.5. This is a necessary condition for the consistency of Multi-Task Learners, but not a sufficient one. Then, Ben-David et al. Ben-David and Borbely (2008); Ben-David and Schuller (2003) defines a notion of task relatedness, see Definition 3.6. Using this notion and building an appropiate hypotheses space $\mathcal{H} = [h]$, they bound the *excess risk* of an Empirical Multi-Task Learner, that is, the difference between the best empirical risk, achieved by such Learner, and the best possible expected risk (Theorem 3.8)

$$\left| \inf_{\boldsymbol{h} \in \mathcal{H}^T} R_{\boldsymbol{P}}(\boldsymbol{h}) - \inf_{\boldsymbol{h} \in \mathcal{H}^T} \hat{R}_{\boldsymbol{z}}(\boldsymbol{h}) \right|.$$

Moreover, using this task relatedness definition not only the Multi-Task average excess risk is bounded, but the individual excess risk of each task (Theorem 3.10).

The works discussed until this point on the VC-dimension, and the corresponding extensions to the MTL framework expressed in Definition 3.4, to bound the differences between empirical and expected risks. However in Ando and Zhang (2005), the authors rely on another notion of complexity, the Rademacher Complexity Bartlett and Mendelson (2002), which measures how well a family of hypothesis can approximate random noise. The Rademacher complexity, unlike the VC-dimension, is distribution-dependent. That is the VC-dimension only uses properties of the hypotheses space $\mathcal{H}$, while the Rademacher complexity also depends on the data distribution F. Other theoretical works obtain bounds for linear feature extractors methods for MTL, such as Cavallanti et al. (2010); Maurer (2006a,b). In the more general case of LTL, some improved bounds are found for specific cases like the trace norm regularized MTL models Maurer et al. (2013). Then, in Maurer et al. (2016) bounds for a wide class of MTL models based on Multi-Task Representation Learning (MTRL) are given, in both an MTL and an LTL setting. This bounds are not dependent on the data dimensions, as other bounds for linear models, and use an approach based on empirical process theory instead of the generalized VC-dimension to derive these bounds.

3.2.4 Learning Under Privileged Information

Another important motivation for Multi-Task Learning can be found in the Learning Under Privileged Information paradigm of Vapnik and Izmailov (2015). The standard

machine learning paradigm tries to find the hypothesis h from a set of hypotheses $\mathcal{H}$ that minimizes the expected risk $\hat{R}_z$ given a set of training samples. Vapnik is one of the main contributors to the theory of statistical learning, see Vapnik (2000). In this theory several important results are provided: necessary and sufficient conditions for the consistency of learning processes and bounds for the rate of convergence, which uses the notion of VC-dimension. A new inductive principle, Structural Risk Minimization (SRM), and an algorithm, Support Vector Machine (SVM), that makes use of this notion to improve the learning process.

Nowadays learning approaches based on Deep Neural Networks, which are not focused on controlling the capacity of the set of hypotheses, outperform the SVM approaches in many problems. However, these popular Deep Learning approaches require large amounts of data to learn good hypothesis. It is commonly believed that machines need much more samples to learn than humans do. The authors in Vapnik and Izmailov (2015); Vapnik and Vashist (2009) reflects on this belief and states that humans typically learn under the supervision of an Intelligent Teacher. This Teacher shares important knowledge by providing metaphors, examples or clarifications that are helpful for the students.

LUPI Paradigm

The additional knowledge provided by the Teacher is the Privileged Information that is available only during the training stage. To incorporate the concept of Intelligent Teacher in the Machine Learning framework, Vapnik introduces the paradigm of Learning Under Privileged Information (LUPI). In the LUPI paradigm describes the following model. Given a set of i.i.d. triplets

$$z = \{(x_1, x_1^*, y_1), \ldots, (x_n, x_n^*, y_n)\}\,,\ x \in \mathcal{X}, x^* \in \mathcal{X}^*, y \in \mathcal{Y}$$

generated according to an unknown distribution $P(x, x^*, y)$, the goal is to find the hypothesis $h\left(x, \alpha^*\right)$ from a set of hypotheses $\mathcal{H} = \{h\left(x, \alpha\right), \alpha \in A\}$ that minimizes some expected risk

$$R_F = \int \ell\left(h\left(x, \alpha\right), y\right) dF(x, y).$$

Note that the goal is the same that in the standard paradigm, however with the LUPI approach we are provided additional information, which is available only during the training stage. This additional information is encoded in the elements x^* of a space $\mathcal{X}^*$, which is different from $\mathcal{X}$. The goal of the Teacher is, given a pair (x_i, y_i), to provide a useful information $x^* \in \mathcal{X}^*$ given some probability $P\left(x^* \mid x\right)$. That is, the "intelligence" of the Teacher is defined by the choice of the space $\mathcal{X}^*$ and the conditional probability $P\left(x^* \mid x\right)$. To understand better this paradigm consider the following example.

Example. Consider that the goal is to find a decision rule that classifies biopsy images into cancer or non-cancer. Here, $\mathcal{X}$ is the space of images, i.e. the matrix of pixels, for example $[0, 1]^{64\times 64}$. The label space is $\mathcal{Y} = \{0, 1\}$. An Intelligent Teacher might provide a student of medicine with commentaries about the images, for example: "There is an area of unusual concentration of cells of Type A." or "There is an aggresive proliferation of cells of Type B". These commentaries are the elements x^* of certain space X^* and the Teacher also chooses the probability $P\left(x^* \mid x\right)$, that is, when to express this additional information.

Analysis of convergence rates

To get a better insight of how the Privileged Information can help in the Learning process, Vapnik provides a theoretical analysis of its influence on the learning rates. In the standard learning paradigm, how well the expected risk R_F can be bounded is controlled by two factors: the empirical risk $\hat{R}_z$ and the VC-dimension of the set of hypotheses $\mathcal{H}$. In the case of classification, where $\mathcal{Y} = \{-1, 1\}$ and the loss $\ell(h(x, \alpha), y) = \mathbf{1}_{h(x,\alpha)y \leq 0}$, the risks can be expressed as

$$R_F(\alpha) = \int \mathbf{1}_{yh(x,\alpha)\leq 0} dF(x, y) = P(h(x, \alpha)\, y \leq 0),$$
$$\hat{R}_z(h(\cdot, \alpha)) = \sum_{i=1}^{n} \mathbf{1}_{y_i h(x_i,\alpha)\leq 0} = \nu(\alpha).$$

In (Vapnik, 1982, Theorem 6.8) the following bound for the rate of convergence is given with probability $1 - \eta$:

$$P(h(x, \alpha_n)\, y \leq 0) \leq \nu(\alpha_n) + O\left(\frac{d \log\left(\frac{2n}{d}\right) - \log \eta}{n} \sqrt{\nu(\alpha_n) \frac{n}{d \log\left(\frac{2n}{d}\right) - \log \eta}}\right).$$

That is, the bound is controlled by the ratio d/n, where d is the VCdim $(\mathcal{H})$. If this VC-dimension is finite, the bound goes to zero as n grows. However, two different cases can be considered.

Separable case: the training data can be classified in two groups without errors. That is, there exists $\alpha_n \in \eta$ such that $y_i h(x_i, \alpha_n) > 0$ for $i = 1, \ldots, n$, and thus $\nu(\alpha_n) = 0$. In this case, the following bound for the rate of converge holds

$$P(h(x, \alpha_n)\, y \leq 0) \leq O\left(\frac{d \log\left(\frac{2n}{d}\right) - \log \eta}{n}\right).$$

Non-Separable case: the training data cannot be classified in two groups without errors. That is, for all $\alpha_n \in A$, there exists $i = 1, \ldots, n$, such that $y_i h(x_i, \alpha_n) \leq 0$, and thus $\nu(\alpha_n) > 0$. In this case, the following bound for the rate of converge holds

$$P(h(x, \alpha_n)\, y \leq 0) \leq \nu(\alpha_n) + O\left(\sqrt{\frac{d \log\left(\frac{2n}{d}\right) - \log \eta}{n}}\right).$$

Note that there is an important difference here in the rate of convergence. The separable case has a convergence rate of d/n, while the non-separable case has a rate of $\sqrt{d/n}$. Vapnik tries to address the question of why there exists such difference.

Oracle SVM

Vapnik tries to answer these question by looking at Support Vector Machines. In the separable case, one has to minimize the functional

$$J(w) = \|w\|^2$$

subject to the constraints

$$y_i \left(w x_i + b \right) \geq 1.$$

However, in the non-separable case the functional to minimize is

$$J(w, \xi_1, \ldots, \xi_n) = \|w\|^2 + C \sum_{i=1}^{n} \xi_i$$

subject to the constraints

$$y_i \left(w x_i + b \right) \geq 1 - \xi_i.$$

That is, in the separable case d parameters (of w) have to be estimated using n examples, while in the non-separable case $d + n$ parameters (considering w and the slack variables $\xi_1, \ldots, \xi_n$) have to be estimated with n examples.

The authors wonder what would happen if the parameters $\xi_1, \ldots, \xi_n$ were known. In Vapnik and Izmailov (2015) an *Oracle* SVM is considered. Here, the learner (Student) is supplied with a set of triplets

$$(x_1, \xi_1^0, y_1), \ldots, (x_n, \xi_n^0, y_n)$$

where $\xi_1^0, \ldots, \xi_n^0$ are the slack variables for the best decision rule $h\left(x, \alpha_0\right) = \inf_{\alpha \in A} R_F(h\left(\cdot, \alpha\right))$:

$$\xi_i^0 = \max\left(0, 1 - h\left(x, \alpha_0\right)\right), \ \forall i = 1, \ldots, n.$$

An *Oracle* SVM has to minimize the functional

$$J(w) = \|w\|^2$$

subject to the constraints

$$y_i \left(w x_i + b \right) \geq 1 - \xi_i^0.$$

Since the slack variables ξ_i^0 are known in advance, it can be shown (Vapnik and Vashist, 2009) that for the *Oracle* SVM the following bound holds

$$P(h\left(x, \alpha_n\right) y \leq 0) \leq P(1 - \xi^0 \leq 0) + O\left(\frac{d \log\left(\frac{2n}{d}\right) - \log \eta}{n} \right),$$

where $P(1 - \xi^0 \leq 0)$ is the probability error of the hypothesis $h\left(x, \alpha_0\right)$. That is, we recover the rate d/n.

From Oracle to Intelligent Teacher

The *Oracle* SVM is a theoretical construct, but we can approximate it by modelling the slack variables with the information provided by the Teacher in the LUPI paradigm. That is, the Teacher defines a space $\mathcal{X}^*$ and a set of functions $\{f^*(x^*, \alpha^*), \alpha^* \in A^*\}$. Then model the slack variables as

$$\xi^* = f^*(x^*, \alpha^*).$$

From the pairs generated by some random generator in nature, the Teacher also defines the probability $P\left(x^* \mid x\right)$ to provide the triplets

$$(x_1, x_1^*, y_1), \ldots, (x_n, x_n^*, y_n).$$

Then, we can consider the problem where the goal is to minimize

$$J(\alpha, \alpha^*) = \sum_{i=1}^{n} \max(0, f^*(x_i^*, \alpha^*))$$

subject to the constraints

$$h\left(x_i, \alpha\right) \geq 1 - f^*(x_i^*, \alpha^*).$$

Let $f(x, \alpha_n), h(x.\alpha_n)$ that minimize this problem. Then, in (Vapnik and Vashist, 2009, Proposition 2) the following results for the bound of convergence is given

$$P(h\left(x, \alpha_n\right) y \leq 0) \leq P(1 - f^*(x^*, \alpha_n^*) \leq 0) + O\left(\frac{(d + d^*) \log\left(\frac{2n}{(d+d^*)}\right) - \log \eta}{n}\right),$$

where d^* is the VC-dimension of the space of hypothesis $\{f(x, \alpha^*) \in A^*\}$. This result shows that, to maintain the best convergence rate d/n, we need to estimate the $P(1 - f^*(x^*, \alpha_n^*) \leq 0)$. Although this probability is unknown, we can control it. Considering

$$\alpha_0^* = \inf_{\alpha^* \in A^*} \int_{\mathcal{X}^*} \max(0, f^*(x^*, \alpha^*) - 1) dP(x^*)$$

and

$$\alpha_n^* = \inf_{\alpha^* \in A^*} \sum_{i=1}^{n} \max(0, f^*(x_i^*, \alpha^*) - 1).$$

Consider $\{f^*(x^*, \alpha^*), \alpha^* \in A^*\}$ such that $f^*(x^*, \alpha^*) < B, \alpha^* \in A^*$, then

$$\{\max(0, f^*(x^*, \alpha^*) - 1), \alpha^* \in A^*\}$$

is a set of totally bounded non-negative functions, then we have the standard bound (Vapnik, 2000),

$$P(1 - f^*(x^*, \alpha_0^*) \leq 0) \leq P(1 - f^*(x^*, \alpha_n^*) \leq 0) + O\left(\sqrt{\frac{d^* \log\left(\frac{2n}{d^*}\right) - \log \eta}{n}}\right),$$

with probability $1 - 2\eta$. That is, to have a rate of d/n for α_n, we need to estimate α_n^*, which has a rate of $\sqrt{d^*/n}$. However, observe that $\mathcal{X}^*$ is the space suggested by the Teacher, which hopefully has a much lower capacity, and thus, the convergence will be faster in this space.

SVM+

Vapnik describes an extension of the SVM that embodies the LUPI paradigm Vapnik and Izmailov (2015); Vapnik and Vashist (2009). Given a set of triplets

$$(x_1, x_1^*, y_1), \ldots, (x_n, x_n^*, y_n),$$

the idea is to model the slack variables of the standard SVM using the elements $x^* \in \mathcal{X}^*$ as

$$\xi(x^*, y) = [y(w^* \phi^*(x^*) + b^*)]_+ = \max\left(y(w^* \phi^*(x^*) + b^*), 0\right).$$

The minimization problem is the following:

$$\begin{aligned} \underset{w,w^*,b,b^*}{\arg\min} \quad & C\sum_{i=1}^{n}\left[y_i(\langle w^*,\phi^*(x_i^*)\rangle + b^*)\right]_+ + \frac{1}{2}\langle w,w\rangle + \frac{\mu}{2}\langle w^*,w^*\rangle \\ \text{s.t.} \quad & y_i(\langle w,\phi(x_i)\rangle + b) \geq 1 - \left[y_i(\langle w^*,\phi^*(x_i^*)\rangle + b^*)\right]_+ . \end{aligned} \tag{3.12}$$

Here ϕ and ϕ^* are two transformations that can be different. However, note that problem (3.12) is not convex due to the positive part term in the objective function. Vapnik et al. propose a relaxation of this problem to obtain a convex one. The idea is to model the slack variables ξ as

$$\xi(x^*,y) = [y(w^*\phi^*(x^*) + b^*)] + \zeta(x^*,y),$$

where $\zeta(x^*,y) \geq 0$. The minimization problem is then

$$\begin{aligned} \underset{w,w^*,b,b^*,\zeta_i}{\arg\min} \quad & C\sum_{i=1}^{n}\left([y_i(\langle w^*,\phi^*(x_i^*)\rangle + b^*)] + \zeta_i\right) + C\Delta\sum_{i=1}^{n}\zeta_i \\ & \quad + \frac{1}{2}\langle w,w\rangle + \frac{\mu}{2}\langle w^*,w^*\rangle \\ \text{s.t.} \quad & y_i(\langle w,\phi(x_i)\rangle + b) \geq 1 - \left[y_i(\langle w^*,\phi^*(x_i^*)\rangle + b^*) + \zeta_i\right], \\ & y_i(\langle w^*,\phi^*(x_i^*)\rangle + b^*) + \zeta_i \geq 0, \\ & \zeta_i \geq 0, \\ \text{for} \quad & i = 1,\ldots,n. \end{aligned} \tag{3.13}$$

Problem (3.13) is convex and the corresponding dual problem is

$$\begin{aligned} \underset{\alpha_i,\delta_i}{\arg\min} \quad & \frac{1}{2}\sum_{i,j=1}^{n} y_iy_j\alpha_i\alpha_jk(x_i,x_j) + \frac{1}{2\mu}\sum_{i,j=1}^{n} y_iy_j(\alpha_i-\delta_i)(\alpha_j-\delta_i)k^*(x_i^*,x_j^*) - \sum_{i=1}^{n}\alpha_i \\ \text{s.t.} \quad & 0 \leq \delta_i \leq C \\ & 0 \leq \alpha_i \leq C + \delta_i, \\ & \sum_{i=1}^{n}\delta_iy_i = 0,\ \sum_{i=1}^{n}\alpha_iy_i = 0, \\ \text{for} \quad & i = 1,\ldots,n. \end{aligned} \tag{3.14}$$

where we use the kernel functions

$$k(x_i,x_j) = \langle\phi(x_i),\phi(x_j)\rangle\,,\ k^*(x_i^*,x_j^*) = \left\langle\phi^*(x_i^*),\phi^*(x_j^*)\right\rangle.$$

We can observe in Problem (3.14) that the LUPI paradigm exerts a similarity control, correcting the similarity in space $\mathcal{X}$ with the similarity in the privileged space $\mathcal{X}^*$. For that reason, $\mathcal{X}$ and $\mathcal{X}^*$ are named Decision Space and Correction Space, respectively.

Connection between SVM+ and MTLSVM

In Liang and Cherkassky (2008) the connection between SVM+ and Multi-Task Learning SVM (MTLSVM) is discussed. The MTLSVM proposed in Liang and Cherkassky (2008)

is a Multi-Task Learning model based on the SVM. It solves the primal problem

$$\begin{array}{lll} \underset{w,b,v_r,b_r,\xi_i^r}{\arg\min} & C\sum_{r=1}^{T}\sum_{i=1}^{m_r}\xi_i^r + \frac{1}{2}\langle w,w\rangle + \sum_{r=1}^{T}\frac{\mu}{2}\langle v_r,v_r\rangle & \\ \text{s.t.} & y_i^r(\langle w,\phi(x_i^r)\rangle + b + \langle v_r,\phi_r(x_i^r)\rangle + b_r) \geq 1-\xi_i^r, & (3.15) \\ & \xi_i^r \geq 0, & \\ \text{for} & r=1,\ldots,T;\ i=1,\ldots,m_r. & \end{array}$$

Here, a combination of a common model for all tasks

$$\langle w,\phi(x_i)\rangle + b$$

and a task-specific model

$$\langle v_r,\phi_r(x_i^r)\rangle + b_r$$

is used. Here, the common transformation ϕ and the task-independent ones ϕ_r can be different The dual problem corresponding to (3.15) is

$$\begin{array}{lll} \underset{\alpha_i}{\arg\min} & \frac{1}{2}\sum_{r,s=1}^{T}\sum_{i,j=1}^{m_r} y_i^r y_j^s \alpha_i^r \alpha_j^s k(x_i^r,x_j^s) + \frac{1}{2\mu}\sum_{r,s=1}^{T}\sum_{i,j=1}^{m_r} y_i^r y_j^s \alpha_i^r \alpha_j^s \delta_{rs} k_r(x_i^r,x_j^s) & \\ & \quad -\sum_{r=1}^{T}\sum_{i=1}^{m_r}\alpha_i^r & \\ \text{s.t.} & 0 \leq \alpha_i^r \leq C & (3.16) \\ & \sum_{i=1}^{m_r}\alpha_i^r y_i^r = 0, & \\ \text{for} & r=1,\ldots,T;\ i=1,\ldots,m_r. & \end{array}$$

In Liang and Cherkassky (2008) some similarities between MTLSVM and SVM+ are pointed out. Problem (3.15) can be regarded as an adaptation of (3.13) to solve MTL problems, where different tasks are incorporated and multiple correcting spaces are defined using the transformations ϕ_r. If we consider the problem (3.15) with a single task, it is a modification of the SVM+ problem (3.13) where the slack variables are modeled as

$$\xi(x,y) = y(w^*\phi^*(x) + b^*).$$

That is, it is a relaxation of the original problem (3.13), where the second constraint to model the positive part of the slack variables disappears. This relaxation gives place to some important differences between both models. Since the auxiliary primal variables ζ_i are no longer required, this is reflected in a simpler dual form (3.16), where only n dual variables have to be estimated, instead of the $2n$ dual variables of (3.14). The Multi-Task part in (3.16) resides in the δ_{rs} function, which makes the correction of similarity only possible between elements of the same task.

A major remark can be make about the differences between MTLSVM and SVM+. The results for the improved rate of convergence with an Intelligent Teacher may not be valid with MTLSVM, since we are not modelling the slack variables ξ adequately. It is still a work in progress to study the rate of convergence of MTLSVM and to establish more clear links with SVM+.

3.3 Kernels for Multi-Task Learning

The Multi-Task Learning paradigm can be seen as learning a vector-valued function $f : \mathcal{X} \to \mathbb{R}^T$, where each element of the vector corresponds to a different task.

3.3.1 Vector-Valued Reproducing Kernel Hilbert Spaces

Consider $\mathcal{Y}$ a Hilbert space with inner product $(.,.)$, then we can study the Hilbert spaces of functions with values in $\mathcal{Y}$. The kernels in such spaces are operator-valued functions $K : \mathcal{X} \times \mathcal{X} \to \mathcal{L}(\mathcal{Y})$. We look at these spaces from three different and equivalent perspectives: continuous evaluation functionals, positive-definite kernels and feature maps.

Continuous evaluation functionals. The first approach considered is that of continuous evaluation functionals. That is, given a Hilbert space with continuous evaluation functionals, we can find the reproducing kernel operator. Consider the vector-valued Hilbert space $\mathcal{H}$ of functions defined in $\mathcal{X}$ and values in $\mathcal{Y}$

$$\begin{aligned} \mathcal{H} &\to \mathcal{Y} &&\to \mathbb{R} \\ f &\to f(x) &&\to (y, f(x)) \end{aligned}$$

Consider the functionals $L_{x,y} f = (y, f(x))$, if this functionals are continuous, we can apply Riesz Representation theorem. That is, for every $x \in \mathcal{X}, y \in \mathcal{Y}$ we can find an unique $g_{x,y} \in \mathcal{H}$ such that for all $f \in \mathcal{H}$,

$$L_{x,y} f = (y, f(x)) = \langle g_{x,y}, f \rangle_{\mathcal{H}} . \tag{3.17}$$

We can now give the definition of vector-valued Hilbert space from the point of view of continuous functionals (Micchelli and Pontil, 2005, Definition 2.1)

Definition 3.11 (vector-valued RKHS)**.** We say that $\mathcal{H}$ is a vector-valued RKHS when for any $x \in \mathcal{X}$ and $y \in \mathcal{Y}$, the functional $L_{x,y} f = (y, f(x))$ is continuous.

Note that this is a definition similar to the scalar case but we use the inner product of $\mathcal{Y}$ to construct the scalar-valued functionals $L_{x,y}$. The price we pay is that it is necessary to express the Riesz representation as dependent of the elements $y \in \mathcal{Y}$. To get rid of this dependence for every $x \in \mathcal{X}$ we can define the linear operator

$$\begin{aligned} g_x : \mathcal{Y} &\to \mathcal{H} \\ y &\to g_x y = g_{x,y}. \end{aligned}$$

This operator is well defined because $g_{x,y}$ is unique for every $x \in \mathcal{X}, y \in \mathcal{Y}$ and its linearity is easy to check from the linearity of the inner product $(.,.)$.
Using this results can now define the operator

$$\begin{aligned} K(x, \hat{x}) : \mathcal{Y} &\to \mathcal{Y} \\ y &\to K(x, \hat{x}) y = (g_{\hat{x}} y)(x) \end{aligned} \tag{3.18}$$

for every $x, \hat{x} \in \mathcal{X}$. Observe that $K(x, \hat{x})$ is linear since g_x is linear. It is possible then to prove that $K(x, \hat{x})$ is a reproducing kernel in $\mathcal{H}$ as seen (Micchelli and Pontil, 2005, Propositon 2.1). To do that, first we have to define a vector-valued kernel and the corresponding reproducing property.

Definition 3.12 (operator-valued Kernel)**.** If $\mathcal{Y}$ is a finite-dimensional Hilbert space, an operator-valued kernel is a function

$$K : \mathcal{X} \times \mathcal{X} \to \mathcal{L}(\mathcal{Y})$$

which is symmetric and positive definite.

For the clarity of the text an operator-valued K will be referred just as kernel unless an explicit distinction is needed.

Definition 3.13 (Reproducing Property of operator-valued operators)**.** If $\mathcal{Y}$ is a Hilbert space, a function

$$K : \mathcal{X} \times \mathcal{X} \to \mathcal{L}(\mathcal{Y})$$

has the reproducing property if $\forall x \in \mathcal{X}, y \in \mathcal{Y}, \forall f \in \mathcal{H}$, $(y, f(x)) = \langle K(\cdot, x)y, f \rangle$.

A kernel with the reproducing property is also called a reproducing kernel. The next proposition shows how we can build a reproducing kernel for a space $\mathcal{H}$ in which the evaluation functionals are continuous.

Proposition 3.14. *If for every $x, \hat{x} \in \mathcal{X}$, the function $K(x, \hat{x})$ is defined as in Equation (3.18), then the function*

$$K : \mathcal{X} \times \mathcal{X} \to \mathcal{L}(\mathcal{Y})$$

is a reproducing kernel.

Proof. To prove that K is a reproducing kernel we need to see

1. $K(x, \hat{x})$ is bounded for every $x, \hat{x} \in \mathcal{X}$ so K is well defined.
2. K is symmetric: $K(x, \hat{x})^* = K(\hat{x}, x)$.
3. K is positive definite: given $n \in \mathbb{N}$, for any $x_1, \ldots, x_n \in \mathcal{X}, y_1, \ldots, y_n \in \mathcal{Y}$,

$$\sum_{i,j=1}^{n} (y_i, K(x_i, x_j)y_j) \geq 0.$$

4. It has the reproducing property: $\forall x \in \mathcal{X}, y \in \mathcal{Y}, \forall f \in \mathcal{H}$, $(y, f(x)) = \langle K(\cdot, x)y, f \rangle$.

To prove 1 and 2,observe that by applying (3.17) to $f = g_{\hat{x}}\hat{y}$, for every $x \in \mathcal{X}, y \in \mathcal{Y}$ there exists an unique $g_{x,y} = g_x y$ such that

$$(y, (g_{\hat{x}}\hat{y})(x)) = \langle g_x y, g_{\hat{x}}\hat{y} \rangle . \tag{3.19}$$

and combining this result with (3.18) we get

$$(y, K(x, \hat{x})\hat{y}) = (y, (g_{\hat{x}}\hat{y})(x)) = \langle g_x y, g_{\hat{x}}\hat{y} \rangle .$$

Also, using the definitions,

$$(K(\hat{x}, x)y, \hat{y}) = ((g_x y)(\hat{x}), \hat{y}) = (\hat{y}, (g_x y)(\hat{x})) = \langle g_{\hat{x}}\hat{y}, g_x y \rangle .$$

Since both operators $K(x, \hat{x}), K(\hat{x}, x)$ are linear, by the Uniform Boundness Principle Akhiezer and Glazman (1961), $K(x, \hat{x}), K(\hat{x}, x)$ are bounded (hence continuous) and

$K(x, \hat{x})^* = K(\hat{x}, x)$.
To prove 3 we write

$$\sum_{i,j=1}^{n} (y_i, K(x_i, x_j) y_j) = \sum_{i,j=1}^{n} \langle g_{x_i} y_i, g_{x_j} y_j \rangle = \left\| \sum_{i=1}^{n} g_{x_i} y_i \right\|^2 \geq 0$$

Finally, to prove 4 we use that $\forall x \in \mathcal{X}, y \in \mathcal{Y}, \forall f \in \mathcal{H}, \exists g_{x,y} \in \mathcal{H}$ such that

$$(y, f(x)) = \langle g_{x,y}, f \rangle = \langle g_x y, f \rangle = \langle K(\cdot, x) y, f \rangle .$$

□

Semi-positive definite kernels. The second approach changes the point of view. Given a kernel K, the Hilbert space from which K is the reproducing kernel is built. To do this, we use (Micchelli and Pontil, 2005, Theorem 2.1) which extends the Moore-Aronszanj's Theorem:

Theorem 3.15. *If $K : \mathcal{X} \times \mathcal{X} \to \mathcal{L}(\mathcal{Y})$ is a kernel, then there exists a unique (up to an isometry) RKHS which admits K as its reproducing kernel.*

The proof is similar to that of the Moore-Aronszanj's Theorem, considering the space of the completion of the span of $\{K_x = K(\cdot, x), x \in \mathcal{X}\}$.

Feature map. The last approach is based on feature maps, which provide a very simple way of generating kernels.

Lemma 3.16. *Any feature map $\Phi : \mathcal{X} \to \mathcal{L}(\mathcal{W}, \mathcal{Y})$ defines a kernel as*

$$K(x, \hat{x}) = \Phi(x)\Phi(\hat{x})^* : \mathcal{Y} \to \mathcal{Y}. \tag{3.20}$$

Proof. We need to prove that it is bounded, symmetric and positive definite:

1. Since $\Phi(x)$ is continuous, the adjoint is $\Phi(x)^*$ is continuous and the composition $\Phi(x) \circ \Phi(\hat{x})^*$ is also continuous.
2. It is symmetric since $(\Phi(x) \circ \Phi(\hat{x})^*)^* = ((\Phi(x)^*)^* \circ \Phi(\hat{x})^*) = (\Phi(x) \circ \Phi(\hat{x})^*)$.
3. Is positive definite since, given any $x_1, \ldots, x_n \in \mathcal{X}, y_1, \ldots, y_n \in \mathcal{Y}$

$$\begin{aligned} \sum_{i,j=1}^{n} (y_i, K(x_i, x_j) y_j) &= \sum_{i,j=1}^{n} (y_i, \Phi(x_i)\Phi(x_j)^* y_j) \\ &= \sum_{i,j=1}^{n} (\Phi(x_i)^* y_i, \Phi(x_j)^* y_j) = \left\| \sum_{i=1}^{n} \Phi(x_i)^* y_i \right\|^2 \geq 0. \end{aligned}$$

□

Since K as defined in (3.20) is a kernel, according to Theorem 3.15 we can find its corresponding vector-valued hilbert space $\mathcal{H}$.

Representer Theorem for Operator-Valued Kernels

The Representer Theorem is a crucial result in Optimization and Machine Learning. Given a regularized empirical risk, under some assumptions, the theorem gives a precise description of the minimizer f^* as a finite linear combination of functions $K(\cdot, x_i)$ where x_i are part of the empirical sample. This result is extended in (Micchelli and Pontil, 2005, Theorem 4.2) for operator-valued kernels.

Theorem 3.17. *Let $\mathcal{Y}$ be a Hilbert space and let $\mathcal{H}$ be the Hilbert space of $\mathcal{Y}$-valued functions with an operator-valued reproducing kernel K. Let $V : \mathcal{Y}^n \times \mathbb{R}_+ \to \mathbb{R}$ be a function strictly increasing in its second variable and consider the problem of minimizing the functional*

$$E(f) := V((f(x_1), \dots, f(x_n)), \|f\|^2) \tag{3.21}$$

in $\mathcal{H}$. If f_0 minimizes the E, then $f_0 = \sum_{j=1}^{n} K(\cdot, x_j)c_j$ where $c_j \in \mathcal{Y}$. In addition, if V is strictly convex, the minimizer is unique.

A useful bijection between kernels

The scalar-valued kernels are well known and studied but this is not the case for operator-valued kernels. However, as shown in Baldassarre et al. (2012); Hein et al. (2004) we can find a bijection between operator-valued kernels and scalar-valued ones.

Lemma 3.18. *Let $\mathcal{Y}$ be a finite-dimensional Hilbert space and $K : \mathcal{X} \times \mathcal{X} \to \mathcal{L}(\mathcal{Y})$ be an operator-valued kernel. Consider also the scalar-valued kernel $L : (\mathcal{X}, \mathcal{Y}) \times (\mathcal{X}, \mathcal{Y}) \to \mathbb{R}$ such that $L((x, z), (\hat{x}, \hat{z})) = (z, K(x, \hat{x})\hat{z})$, then the map $K \to L$ is a bijection.*

Moreover, if we focus on finite dimensional Hilbert spaces, that is, isomorphic to $\mathbb{R}^d$ given an operator-valued kernel K the corresponding scalar-valued kernel L is defined using the normal basis as

$$L((x, e_r), (\hat{x}, e_s)) = (e_r, K(x, \hat{x})e_s) = K(x, \hat{x})_{rs}.$$

That is, each pair $(x, \hat{x})$ defines a matrix which contains the information of how the different outputs, or tasks, are related.

3.3.2 Tensor Product of Reproducing Kernel Hilbert Spaces

Consider the space of the tensor product of two scalar-valued RKHS' $\mathcal{H}_1 \otimes \mathcal{H}_2$ with reproducing kernels K_1, K_2, where the functions $f \in \mathcal{H}_i$ are defined as $f : \mathcal{X}_i \to \mathcal{Y}_i$ for $i = 1, 2$. This tensor space is also a Hilbert space endowed with the inner product:

$$\begin{array}{lll} \langle , \rangle : (\mathcal{X}_1 \otimes \mathcal{X}_2) \times & (\mathcal{X}_1 \otimes \mathcal{X}_2) \to & \mathbb{R} \otimes \mathbb{R} \\ (f_1 \otimes f_2) & (\hat{f}_1 \otimes \hat{f}_2) \to & \left\langle f_1, \hat{f}_1 \right\rangle \left\langle f_2, \hat{f}_2 \right\rangle . \end{array} \tag{3.22}$$

It is easy to check that this inner product is symmetric because the inner products of both $\mathcal{H}_1$ and $\mathcal{H}_2$ are symmetric. It is linear because the inner products of both $\mathcal{H}_1$ and $\mathcal{H}_2$ are linear and the tensor product is linear. Finally, it is positive definite since $\langle f_1, f_1 \rangle \langle f_2, f_2 \rangle \geq 0$ and $\langle f_1, f_1 \rangle \langle f_2, f_2 \rangle = 0 \implies \langle f_i, f_i \rangle = 0$ for $i = 1$ or $i = 2$; taking $i = 1$ without loss of generality, then $f_1 = 0$, so $f_1 \otimes f_2 = 0$. To apply the Riesz Theorem in this Hilbert space it is necessary to check wether the evaluation functionals are continuous or, equivalently, bounded.

Proposition 3.19 (RKHS as tensor product of RKHS')**.** *The space $\mathcal{H} = \mathcal{H}_1 \otimes \mathcal{H}_2$ with the inner product defined in (3.22) have bounded evaluation functionals $L_{x_1 \otimes x_2}$ defined as $L_{x_1 \otimes x_2}(f_1 \otimes f_2) = L_{x_1}(f_1) \otimes L_{x_2}(f_2) = f_1(x_1) f_2(x_2)$ for $x_1 \otimes x_2 \in \mathcal{X}_1 \otimes \mathcal{X}_2$.*

Proof. It is necessary to ensure that the operators $L_{x_1 \otimes x_2}$ are bounded. Given any $f_1 \otimes f_2 \in \mathcal{H}_1 \otimes \mathcal{H}_2$,

$$\|L_{x_1 \otimes x_2}(f_1 \otimes f_2)\| := \|f_1(x_1) f_2(x_2)\| \leq \|f_1(x_1)\| \, \|f_2(x_2)\| \leq M_{x_1} \|f_1\|_{\mathcal{H}_1} M_{x_2} \|f_2\|_{\mathcal{H}_2} .$$

□

We also need to define the kernel function for this tensor product space.

Proposition 3.20. *The kernel function*

$$\begin{array}{rrcl} K_1 \otimes K_2 : & (\mathcal{H}_1 \otimes \mathcal{H}_2) \times & (\mathcal{H}_1 \otimes \mathcal{H}_2) \to & \mathbb{R} \\ & (x_1 \otimes x_2) & (\hat{x}_1 \otimes \hat{x}_2) \to & K_1(x_1, x_2) K_2(x_1, x_2) \end{array}$$

is a reproducing kernel for the Hilbert space $\mathcal{H}_1 \otimes \mathcal{H}_2$.

Proof. First, $K_1 \otimes K_2$ is a kernel, that is, it is symmetric and positive-definite. The proof is very similar to the symmetry and positive definitiness proof of the inner product (3.22). To observe that $K_1 \otimes K_2$ has the reproducing property, we write

$$\langle K_1 \otimes K_2(\cdot, x_1 \otimes x_2), f_1 \otimes f_2 \rangle := \langle K_1(\cdot, x_1), f_1 \rangle \, \langle K_2(\cdot, f_2), x_2 \rangle = f_1(x_1) f_2(x_2).$$

□

Another useful bijection between kernels

To understand the connection between tensor product RKHS' and vector-valued RKHS' we study a special case of operator-valued kernels. A standard assumption is that the relation among the different outputs is independent of the pair $(x, \hat{x})$:

$$K(x, \hat{x}) = k(x, \hat{x}) M$$

where k is a scalar-valued kernel and M is some fixed operator $M \in \mathcal{L}(\mathcal{Y})$. That is, the operator $K(x, \hat{x})$ decouples in two parts: the similarity between x and $\hat{x}$ measured by $k(\cdot, \cdot)$ and the interaction between the different outputs expressed by M. In those cases it is easier to express the operator-valued kernel as the tensor product of two spaces. The following lemma shows how we can express such tensor product kernel.

Lemma 3.21. *Let $\mathcal{Y}$ be a finite-dimensional Hilbert space and $K : \mathcal{X} \times \mathcal{X} \to \mathcal{L}(\mathcal{Y})$ be a separable operator-valued kernel, that is $K(x, \hat{x}) = k(x, \hat{x}) M$ with $M \in \mathcal{L}^+(\mathcal{Y})$. Consider the kernel $K_{\mathcal{X}} \otimes K_{\mathcal{Y}} : (\mathcal{X} \otimes \mathcal{Y}) \times (\mathcal{X} \otimes \mathcal{Y}) \to \mathbb{R}$ such that $K_{\mathcal{X}} \otimes K_{\mathcal{Y}}((x \otimes z), (\hat{x} \otimes \hat{z})) = K_{\mathcal{X}}(x, \hat{x}) K_{\mathcal{Y}}(z, \hat{z})$, with $K_{\mathcal{Y}}(z, \hat{z}) = (z, M\hat{z})$ then the map $K \to K_{\mathcal{X}} \otimes K_{\mathcal{Y}}$ is a bijection.*

Proof. First, observe that $K_{\mathcal{Y}}$ is the reproducing kernel of $\mathcal{Y}$ with the inner product induced by the operator $M^{-1} \in \mathcal{L}^+(\mathcal{Y})$. By the Lemma 3.18 there exists a bijection between K and L where $L((x, z), (\hat{x}, \hat{z})) = (z, K(x, \hat{x})\hat{z})$. When $K(x, \hat{x}) = k(x, \hat{x}) M$, we define

$$K_{\mathcal{X}} \otimes K_{\mathcal{Y}}(x \otimes z, \hat{x} \otimes \hat{z}) = K_{\mathcal{X}}(x, \hat{x}) K_{\mathcal{Y}}(z, \hat{z}) = K_{\mathcal{X}}(x, \hat{x}) \, (z, M\hat{z}) = L((x, z), (\hat{x}, \hat{z})),$$

and the bijection is trivial by definition.

Moreover, observe that using this kernel with a basis of $\mathcal{Y}$, $z = e_r, \hat{z} = e_s$,

$$K_{\mathcal{X}} \otimes K_{\mathcal{Y}}((x \otimes e_r), (\hat{x} \otimes e_s)) = K_{\mathcal{X}}(x, \hat{x})(M)_{rs}.$$

□

This kind of kernels are called separable kernels Álvarez et al. (2012); Kadri et al. (2016), however their connection with operator-valued kernels is not very clear. This subsection tries to explain the construction of separable kernels and how they relate to operator-valued kernels.

3.3.3 Using Kernels in Multi-Task Learning

There exists a plethora of work about Single-Task Learning within regularization theory, some general formulation is

$$\sum_{i=1}^{n} \ell(y_i, \langle w, \phi(x_i) \rangle) + \lambda \langle w, w \rangle . \tag{3.23}$$

Here, ℓ is the loss function and ϕ is a transformation to include non-linearity. Popular models such as Ridge Regression or SVMs are particular cases of this formulation for different choices of ℓ. One crucial result for problems using this formulation is the *Representer Theorem*, which states that the any minimizer of problem (3.23) has the form

$$w = \sum_{i=1}^{n} c_j \phi(x_j). \tag{3.24}$$

Given w represented as in (3.24), we write

$$\langle w, \phi(\hat{x}) \rangle = \sum_{i=1}^{n} c_j \langle \phi(x_j), \phi(\hat{x}) \rangle .$$

This is very useful because we can apply the kernel trick and use the transformations ϕ only implicitly. In this subsection it is shown how a broad class of Multi-Task problems can be expressed as regularized Single-Task problems.

Linear MTL Models

Building upon the ideas discussed in Evgeniou and Pontil (2004), two useful results are presented in Evgeniou et al. (2005), which show how we can apply Single-Task Learning methods to Multi-Task Learning problems. The first result (Evgeniou et al., 2005, Proposition 1) is defined for linear models and illustrates under which conditions we can adapt these results for MTL. Consider the linear MTL problem where we want to estimate the task parameters $u_r : r = 1, \ldots, T$, so we define $\boldsymbol{u}^\intercal = (u_1^\intercal, \ldots, u_T^\intercal) \in \mathbb{R}^{Td}$. Then we want to minimize

$$R(\boldsymbol{u}) = \sum_{r=1}^{T} \sum_{i=1}^{m} \ell(y_i^r, \langle u_r, x_i^r \rangle) + \mu J(\boldsymbol{u}), \tag{3.25}$$

where $J(\boldsymbol{u}) = \boldsymbol{u}^\intercal E \boldsymbol{u}$ is the regularizer where different choices of $J(\boldsymbol{u})$, i.e. choices of the matrix E, we can encode different beliefs about the task structure. For example, if $J(\boldsymbol{u}) = \sum_{r=1}^{T} \|u_r\|^2$ the problem decouples and we get independent task learning, so there is no relation among tasks; if $J(\boldsymbol{u}) = \sum_{r,s=1}^{T} \|u_r - u_s\|^2$ we are enforcing the parameters from different tasks to be close, so we expect all tasks to be similar.

Then, Evgeniou et al. propose to consider a vector $\boldsymbol{w} \in \mathbb{R}^p$ with $p \geq Td$ such that we can express $\langle u_r, x \rangle$ as $\langle B_r^\intercal \boldsymbol{w}, x \rangle$, where B_r is a $p \times d$ matrix yet to be specified. One condition for B_r is to be full rank so we can find such $\boldsymbol{w}$. Note that we can also interpret B_r as a feature map $f : \mathbb{R}^d \to \mathbb{R}^p$ such that $\langle u_r, x \rangle = \langle \boldsymbol{w}, B_r x \rangle$. Observe that using the matrices B_r we have the following MTL kernel

$$\hat{k}(x^r, y^s) = \hat{k}((x, r), (y, s)) = x^\intercal B_r^\intercal B_s y.$$

Using these feature maps we would like to write the MTL problem as a Single-Task problem

$$S(\boldsymbol{w}) = \sum_{r=1}^{T} \sum_{i=1}^{m} \ell(y_i^r, \langle \boldsymbol{w}, B_r x_i^r \rangle) + \mu \langle \boldsymbol{w}, \boldsymbol{w} \rangle, \tag{3.26}$$

We also define the feature matrix B as the concatenation $B = (B_r : r = 1, \ldots, T) \in \mathbb{R}^{p \times Td}$, then we present the first result of Evgeniou et al. (2005).

Proposition 3.22. *If the feature matrix B is full rank and we define the matrix E in equation (3.25) as to be $E = (B^\intercal B)^{-1}$ then we have that*

$$S(\boldsymbol{w}) = R(B^\intercal \boldsymbol{w}).$$

and therefore $\boldsymbol{u}^* = B^\intercal \boldsymbol{w}^*$.

One important consequence of this result is that since we can solve the MTL problem (3.25) as the STL problem (3.23), then we can apply the *Representer Theorem*. That is, the solution $\boldsymbol{w}^*$ of problem (3.23) has the form

$$\boldsymbol{w} = \sum_{r=1}^{T} \sum_{i=1}^{m} c_i B_r x_i^r,$$

and the prediction can be expressed as

$$\langle \boldsymbol{w}, \hat{x}^s \rangle = \sum_{r=1}^{T} \sum_{i=1}^{m} \alpha_i^r (x_i^r)^\intercal B_r^\intercal B_s \hat{x}^s = \sum_{r=1}^{T} \sum_{i=1}^{m} c_i \hat{k}(x_i^r, \hat{x}^s).$$

Kernel Extension of MTL Models

Evgeniou et al. also extend this results to kernelized models. In the following lemma (Evgeniou et al., 2005, Lemma 2) the give the conditions under which the extension is possible.

Lemma 3.23. *If G is a kernel on $\mathcal{T} \times \mathcal{T}$ and, for every $r = 1, \ldots, T$ there are prescribed mappings $z_r : \mathcal{X} \to \mathcal{T}$ such that*

$$K((x, r), (y, s)) = G(z_r(x), z_s(t)), \ x, t \in \mathcal{X}, \ r, s \in [T] \tag{3.27}$$

then K is a multi-task kernel.

That defines K as a semi-positive functional over the product space $\mathcal{X} \times \mathcal{T}$, which is named multi-task kernel. The mappings described in Evgeniou et al. (2005) are

$$z_r(x) = B_r x$$

where B_r are the $p \times d$ matrices previously defined. Then, two examples of multi-task kernels using this lemma are given. The polynomial kernel is defined as

$$K((x,r),(y,s)) = (x^\intercal B_r^\intercal B_s y)$$

and the multi-task Gaussian kernel is defined as

$$K((x,r),(y,s)) = \exp\left(-\gamma \left\|B_r x - B_s y\right\|^2\right).$$

That is, using the result of Proposition 3.22, when the matrix E has a block structure, we can incorporate the task-regularizer information into the Gaussian kernel using that

$$\begin{aligned}\left\|B_r x - B_s y\right\|^2 &= x^\intercal B_r^\intercal B_r x + y^\intercal B_s^\intercal B_s y - 2x_r^\intercal B_r^\intercal B_s y_s \\ &= x^\intercal E_{rr}^{-1} x + y^\intercal E_{ss}^{-1} y - 2x_r^\intercal E_{rs}^{-1} y_s.\end{aligned}$$

That is, we use the task information in the original space and then apply the non-linear transformation.

Alternative Kernel Extension of MTL Models

The kernel extension presented in Evgeniou et al. (2005) proposes to use a mapping in the original finite space to incorporate the task information and then applying the kernel trick over this new mapped features. However, these results do not permit to perform the, possibly infinite dimensional, mapping corresponding to a kernel and then incorporate the task information in the new space. Here we show another approach which makes it is possible to replicate the results for the infinite-dimensional case by using tensor products. Consider a general Hilbert space $\mathcal{H}$ and the functional

$$R(u_1,\ldots,u_T) = \sum_{r=1}^{T}\sum_{i=1}^{m} \ell(y_i^r, \langle u_r, \phi(x_i^r)\rangle) + \mu \sum_r \sum_s E_{rs} \langle u_r, u_s\rangle, \tag{3.28}$$

where $u_1,\ldots,u_T \in \mathcal{H}$ and E is a $T \times T$ matrix. The following lemma illustrates how to solve this problem as a single task problem.

Lemma 3.24. *The predictions $\langle u_r^*, \phi(x)\rangle$ of the solutions $u_1^*,\ldots,u_T^*$ from the Multi-Task optimization problem (3.28) can be obtained solving the problem*

$$S(\boldsymbol{w}) = \sum_{r=1}^{T}\sum_{i=1}^{m} \ell(y_i^r, \langle \boldsymbol{w}, (B_r \otimes \phi(x_i^r))\rangle) + \mu \boldsymbol{w}^\intercal \boldsymbol{w}, \tag{3.29}$$

where $\boldsymbol{w} \in \mathbb{R}^p \otimes \mathcal{H}$ with $p \geq T$ and B_r are the columns of a full rank matrix $B \in \mathbb{R}^{p\times T}$ such that $E^{-1} = B^\intercal B$.

Proof. Replicating the idea of Evgeniou et al. (2005), we can write

$$\boldsymbol{u} = \sum_{t=1}^{T} e_r \otimes u_r,$$

such that $\boldsymbol{u} \in \mathbb{R}^T \otimes \mathcal{H}$. Then, we can reformulate (3.28) as

$$R(\boldsymbol{u}) = \sum_{r=1}^{T}\sum_{i=1}^{m} \ell(y_i^r, \langle \boldsymbol{u}, e_r \otimes \phi(x_i^r)\rangle) + \mu\left(\boldsymbol{u}^\intercal (E \otimes I)\boldsymbol{u}\right), \tag{3.30}$$

Since $E \in \mathbb{R}^{T\times T}$ is positive definite, we can find $B \in \mathbb{R}^{p\times T}, p \geq T$ and $\operatorname{rank} B = T$ such that $E^{-1} = B^\intercal B$, using for example the SVD. Using the properties of the tensor product of linear maps,

$$E^{-1} \otimes I = (B^\intercal B) \otimes I = (B^\intercal \otimes I)(B \otimes I),$$

Consider the change of variable $\boldsymbol{u} = (B^\intercal \otimes I)\boldsymbol{w}$, where $\boldsymbol{w} \in \mathbb{R}^p \otimes \mathcal{H}$. Observe that this can always be done because B is full rank. Rewriting (3.30) using $\boldsymbol{w}$,

$$\begin{aligned} R((B^\intercal \otimes I)\boldsymbol{w}) &= \sum_{r=1}^{T}\sum_{i=1}^{m} \ell(y_i^r, \langle (B^\intercal \otimes I)\boldsymbol{w}, (e_r \otimes \phi(x_i^r))\rangle) + \mu \boldsymbol{w}^\intercal (B^\intercal \otimes I)^\intercal (E \otimes I)(B^\intercal \otimes I)\boldsymbol{w} \\ &= \sum_{r=1}^{T}\sum_{i=1}^{m} \ell(y_i^r, \langle \boldsymbol{w}, (B \otimes I)(e_r \otimes \phi(x_i^r))\rangle) + \mu \boldsymbol{w}^\intercal \boldsymbol{w}, \end{aligned}$$

which is equivalent to

$$S(\boldsymbol{w}) = \sum_{r=1}^{T}\sum_{i=1}^{m} \ell(y_i^r, \langle \boldsymbol{w}, (B_r \otimes \phi(x_i^r))\rangle) + \mu \boldsymbol{w}^\intercal \boldsymbol{w}.$$

We are thus considering a regularized functional $S(\boldsymbol{w})$ where we seek the minimum over functions w in the Hilbert space $\mathbb{R}^p \otimes \mathcal{H}$. Note that in this space the inner product is:

$$\begin{aligned} \langle , \rangle : (\mathbb{R}^p \otimes \mathcal{H}) \times \quad & (\mathbb{R}^p \otimes \mathcal{H}) \to && \mathbb{R} \\ (z_1, \phi(x_1)), \quad & (z_2, \phi(x_2)) \to && \langle z_1, z_2\rangle\, k(x_1, x_2) \end{aligned}$$

Where $k(\cdot,\cdot)$ is the reproducing kernel of the space of functions $\phi(\cdot)$. However we are only interested in those cases where $z = Be_r = B_r$ for some $r = 1, \ldots, T$, then $\langle B_r, B_s\rangle = E^{-1}_{rs}$. Since the regularizer is clearly increasing in $\|w\|^2$, we can apply the Representer theorem, which states that the minimizer of $S(\boldsymbol{w})$ has the form

$$\boldsymbol{w}^* = \sum_{r=1}^{T}\sum_{i=1}^{m} \alpha_i^r (B_r \otimes \phi(x_i^r)),$$

Using the correspondence between $\boldsymbol{u}^*$ and $\boldsymbol{w}^*$,

$$\boldsymbol{u}^* = B^\intercal \boldsymbol{w}^* = \sum_{r=1}^{T}\sum_{i=1}^{m} \alpha_i^r (\operatorname{vect}\left(\left(\langle B_1, B_r\rangle, \ldots, \langle B_T, B_r\rangle\right)\right) \otimes \phi(x_i^r)).$$

Then, we can recover the predictions corresponding to the solutions u_r^* as

$$\begin{aligned}
\langle u_r, \phi(\hat{x}^s)\rangle &= \langle \boldsymbol{u}, e_s \otimes \phi(\hat{x}^s)\rangle \\
&= \left\langle \sum_{s=1}^{T}\sum_{i=1}^{m} \alpha_i^r (\text{vect}\left(\left(\langle B_1, B_r\rangle, \ldots, \langle B_T, B_r\rangle\right)\right) \otimes \phi(x_i^r)), e_s \otimes \phi(\hat{x}^s) \right\rangle \\
&= \sum_{s=1}^{T}\sum_{i=1}^{m} \alpha_i^r \langle B_s, B_r\rangle \langle \phi(x_i^r), \phi(x_s)\rangle \\
&= \sum_{s=1}^{T}\sum_{i=1}^{m} \alpha_i^r (E^{-1})_{rs} k(x_i^r, \hat{x}^s).
\end{aligned}$$

□

Observe that, applying the corresponding feature map $B \otimes I$, the predictions can be obtained equivalently using the common $\boldsymbol{w}$ as

$$\begin{aligned}
\langle \boldsymbol{w}, (B \otimes I)(e_s \otimes \phi(\hat{x}^s))\rangle &= \langle \boldsymbol{w}, (B_s \otimes \phi(\hat{x}^s))\rangle \\
&= \sum_{r=1}^{T}\sum_{i=1}^{m} \alpha_i^r \langle B_r \otimes \phi(x_i^r), B_s \otimes \phi(\hat{x}^s)\rangle \\
&= \sum_{r=1}^{T}\sum_{i=1}^{m} \alpha_i^r \langle B_r, B_s\rangle \langle \phi(x_i^r), \phi(\hat{x}^s)\rangle \\
&= \sum_{r=1}^{T}\sum_{i=1}^{m} \alpha_i^r (E^{-1})_{rs} k(x_i^r, \hat{x}^s).
\end{aligned}$$

That is, we have expressed the Multi-Task problem as a Single-Task problem with the Multi-Task kernel is

$$\hat{k}(x_i^r, x_j^s) = (E^{-1})_{rs} k(x_i^r, x_j^s).$$

Note that the kernels obtained in this way, unlike those obtained using Lemma 3.27, split the inter-task relations and the similarity between data points. That is, we can implicitly send our data into another, a possibly infinite-dimensional, space and apply the task information after this transformation. This kind of kernels are usually called separable kernels Álvarez et al. (2012) but, to the best of knowledge, this is the first time the they are constructed using tensor products.

Examples of Multi-Task Kernels

Using the framework for Multi-Task learning with Kernel methods we can choose different regularizations, induced by the matrix E, which lead to different Multi-Task approaches.

Independent Tasks The trivial case when $E = I_T$ and therefore $B = I_T$, that is

$$B_r^\intercal = (\overbrace{0}^{1}, \ldots, \overbrace{1}^{r}, \overbrace{0}^{T}),$$

and the kernel is

$$\hat{k}(x_i^r, x_j^s) = \langle B_r, B_s\rangle k(x_i^r, x_j^s) = (\delta_{rs}) k(x_i^r, x_j^s).$$

This approach is not a proper MTL method because each task is learned separately, and no coupling is being enforced among tasks.

Independent Parts with Shared Common Model When the matrix B is selected such that its columns are

$$B_r^\intercal = (\overbrace{0}^{1}, \ldots, \overbrace{1}^{r}, \overbrace{0}^{T}, \overbrace{\frac{1}{\mu}}^{T+1}),$$

the corresponding multi-task kernel is:

$$\hat{k}(x_i^r, x_j^s) = \langle B_r, B_s \rangle \, k(x_i^r, x_j^s) = (\frac{1}{\mu} + \delta_{rs}) k(x_i^r, x_j^s)$$

This is equivalent to the approach presented in the work of Evgeniou and Pontil (2004) where it is named *regularized MTL*. The goal is to find a decision function for each task, each being defined by a vector

$$w_r = w + v_r,$$

where w is common to all tasks and v_r is task-specific. The primal problem of *regularized MTL* SVM, using the unified formulation, is

$$\begin{aligned} \underset{w,v_r,\xi_i^r}{\arg\min} \quad & C \sum_{r=1}^{T} \sum_{i=1}^{m_r} \xi_i^r + \frac{1}{2} \langle w, w \rangle + \sum_{r=1}^{T} \frac{\mu}{2} \langle v_r, v_r \rangle \\ \text{s.t.} \quad & y_i^r (\langle w, x_i^r \rangle + \langle v_r, x_i^r \rangle) \geq p_i^r - \xi_i^r, \\ & \xi_i^r \geq 0, \\ \text{for} \quad & r = 1, \ldots, T; \; i = 1, \ldots, m_r. \end{aligned} \tag{3.31}$$

Note that μ is a parameter that controls the tradeoff between the relevance of common and specific models. That is, when μ tends to infinite, the resulting model approaches a common-task standard SVM; when μ tends to zero, a independent task approach is taken, with one standard SVM problem for each task. This is also reflected in the corresponding dual problem

$$\begin{aligned} \underset{\alpha_i}{\arg\min} \quad & \frac{1}{2} \sum_{r,s=1}^{T} \sum_{i,j=1}^{m_r} y_i^r y_j^s \alpha_i^r \alpha_j^s \langle x_i^r, x_j^s \rangle + \frac{1}{2\mu} \sum_{r,s=1}^{T} \sum_{i,j=1}^{m_r} y_i^r y_j^s \alpha_i^r \alpha_j^s \delta_{rs} \langle x_i^r, x_j^s \rangle \\ & - \sum_{r=1}^{T} \sum_{i=1}^{m_r} p_i^r \alpha_i^r \\ \text{s.t.} \quad & 0 \leq \alpha_i^r \leq C \\ \text{for} \quad & r = 1, \ldots, T; \; i = 1, \ldots, m_r. \end{aligned} \tag{3.32}$$

In this dual form, as μ grows, the task-specific part goes to zero, and the most important term is the first one, corresponding to the common part. The opposite effect is obtained when μ shrinks. Moreover, in Evgeniou and Pontil (2004) it is shown that solving (3.31)

is equivalent to solving the problem

$$\begin{aligned}
\underset{ww_r,\xi_i^r}{\arg\min} \quad & C\sum_{r=1}^{T}\sum_{i=1}^{m_r}\xi_i^r + \frac{1}{2}\sum_{r=1}^{T}\|w_r\|^2 + \frac{\mu}{2}\sum_{r=1}^{T}\left\|w_r - \sum_{s=1}^{T} w_s\right\|^2 \\
\text{s.t.} \quad & y_i^r(\langle w_r, x_i^r\rangle) \geq p_i^r - \xi_i^r, \\
& \xi_i^r \geq 0, \\
\text{for} \quad & r = 1,\ldots,T;\ i = 1,\ldots,m_r.
\end{aligned}$$

Now, only the w_r variables are included, and it is clearer that μ penalizes the variance of the w_r vectors, so all models w_r will tend to a common model as μ grows.

This is a very interesting approach because, as it was pointed out in Liang and Cherkassky (2008), this approach has connections with the SVM+ approach from Vapnik and Izmailov (2015).

Graph Laplacian When the tasks are considered as nodes in a graph, and the weights of the edges of this graph portrait the relation between each pair of tasks, the matrix E can be seen as a Laplacian matrix $L = D - A$. Here A is the adjacency matrix indicating the weights of the edges between each pair of tasks, and D is the degree matrix, a diagonal matrix where each diagonal term is the sum of the corresponding row of A. Observe that using this matrix, the regularization term is

$$\begin{aligned}
\boldsymbol{u}^\intercal(L\otimes I)\boldsymbol{u} &= \sum_{r=1}^{T}\sum_{s=1}^{T} u_r^\intercal L_{rs} u_s \\
&= \sum_{r=1}^{T}\sum_{s=1}^{T} u_r^\intercal (D-A)_{rs} u_s \\
&= \sum_{r=1}^{T}\sum_{s=1}^{T} u_r^\intercal \left(\delta_{rs}\sum_q A_{rq}\right) u_s - \sum_{r=1}^{T}\sum_{s=1}^{T} u_r^\intercal A_{rs} u_s \\
&= \sum_{r=1}^{T} u_r^\intercal \sum_q A_{rq} u_r + \sum_{r=1}^{T} u_s^\intercal \sum_q A_{sq} u_s - \sum_{r=1}^{T}\sum_{s=1}^{T} u_r^\intercal A_{rs} u_s \\
&= \sum_{r=1}^{T}\sum_{s=1}^{T} u_r^\intercal A_{rs} u_s + u_s^\intercal A_{rs} u_s - u_r^\intercal A_{rs} u_s \\
&= \sum_{r=1}^{T}\sum_{s=1}^{T} A_{rs}\|u_r - u_s\|^2 \ .
\end{aligned}$$

That is, the distance between task models is penalized, weighted by the degree of similatiy between the tasks as indicated by the graph. Here, the multi-task kernel is defined as

$$\hat{k}(x_i^r, x_j^s) = \langle B_r, B_s\rangle\, k(x_i^r, x_j^s) = \left(L^+\right)_{rs} k(x_i^r, x_j^s).$$

Observe that the pseudoinverse is used because the Laplacian matrices are semipositive definite.

3.4 Multi-Task Learning Methods: An Overview

In this section a general overview of the MTL methods will be shown, categorizing some of the most relevant approaches. Recall that a Multi-Task Learning sample is

$$\{(x_i^r, y_i^r) \in \mathcal{X} \times \mathcal{Y}; i = 1, \dots, m_r; r = 1, \dots, T\},$$

where T is the number of tasks and m_r is the number of examples in task r. The goal is to find task-specialized hypotheses h_r such the regularized risk

$$\sum_{r=1}^{T} \sum_{i=1}^{m_r} \ell(h(x_i^r), y_i^r) + \Omega(h_1, \dots, h_T)$$

is minimized, where Ω is some regularizer of the hypotheses. To enforce the coupling between tasks, we can consider three main groups in this taxonomy: feature-based, Parameter-Based and Combination-Based strategies. The feature-based approaches define the hypotheses as the composition of a common feature-building function f and a task-specific function g_r, i.e. $h_r(x_i^r) = g_r \circ f(x_i^r)$, where f and g_r can be defined in multiple ways. The parameter-based approach is based on enforcing the coupling through the regularization of the parameters of linear models, which are built over some non-learnable features, i.e. $h_r(x_i^r) = w_r^\intercal \phi(x_i^r)$. Finally, the combination based approach uses the combination of a common part and task specific parts, i.e. $h_r(x_i^r) = g(x_i^r) + g_r(x_i^r)$, where g and g_r can be modeled in multiple ways. In this section we develop a subsection for each one of these approaches. Although most MTL strategies used in deep learning can be categorized as feature-based, and most kernel methods use parameter-based or combination-based strategies, given the relevance of these models, MTL with neural networks and MTL with kernel methods will be treated separately in their own subsections.

3.4.1 Feature-based MTL

The feature-based methods try to find a set of features that are useful for all tasks. To do that, a shared feature-building function f is considered, and the hypotheses are then $h_r(x_i^r) = g_r \circ f(x_i^r)$. Two main approaches are taken: feature learning, which tries to learn new features from the original ones, and feature-selection, which selects a subset of the original features.

Feature Learning approaches

In the feature learning approach, the feature-building function f can be modeled in different ways. When using neural networks, f can be modeled using shared layers of a neural network, while g_r is the linear model corresponding to the output layer, that is $h_r(x_i^r) = w_r^\intercal f(x_i^r, \Theta) + b_r$ where Θ are the parameters of the hidden layers and w_r, b_r are the parameters of the output layer. This is the idea behind the Multi-Task feedforward Neural Network first shown in Caruana (1997), which will be described in Subsection 3.4.4. With linear or kernel models both f and g_r are modeled as linear functions, for example if $f(x_i^r) = (u_1^\intercal \phi(x_i^r), \dots, u_k^\intercal \phi(x_i^r))$ for some $k \in \mathbb{N}^+$, where ϕ is the implicit transformation that is the identity for linear models. Then, $h_r(x_i^r) = a_r^\intercal (U^\intercal x_i^r)$, where $a_r \in \mathbb{R}^k$ are the parameters of the linear models g_r. Observe that in the linear case, we can describe this models as $h_r(x_i^r) = w_r^\intercal x_i^r$, with $w_r = U a_r$ where $U = (u_1, \dots, u_T)$. This idea, named Multi-Task Feature Learning, is presented in Argyriou et al. (2006),

where they consider the linear case with $k = d$, the original dimension of the data. Then, the matrix $W = (w_1, \dots, w_T)$ can be expressed as

$$\underset{d\times T}{W} = \underset{d\times d}{U}\,\underset{d\times T}{A}.$$

The authors impose also some restrictions to enforce that the features represented by $u_1, \dots, u_T$ capture different information and only a subset of them is necessary for each task. The minimization problem to obtain the optimal model parameters is

$$\underset{\substack{U\in\mathbb{R}^{d\times d}\\ A\in\mathbb{R}^{d\times T}}}{\arg\min} \sum_{r=1}^{T}\sum_{i=1}^{m_r} \ell(y_i^r, \langle Ua_r, x_i^r\rangle) + \lambda \|A\|_{2,1}^2 \text{ s.t. } U^\intercal U = I, \tag{3.33}$$

where the $L_{2,1}$ regularizer is used to impose row-sparsity across tasks, i.e. forcing some rows of A to be zero, which has the goal of using in all tasks a subset of the features represented by the columns of U ;while the matrix U is restricted to be orthonormal so that its columns do not contain overlapping information. Although problem (3.33) is not jointly convex in U and A, in Argyriou et al. (2006) and Argyriou et al. (2008) it is shown to be equivalent to the convex problem

$$\begin{aligned}&\underset{W\in\mathbb{R}^{d\times T}, D\in\mathbb{R}^{d\times d}}{\arg\min} \sum_{r=1}^{T}\sum_{i=1}^{m_r} \ell(y_i^r, \langle w_r, x_i^r\rangle) + \lambda \sum_{r=1}^{T} \left\langle w_r, D^{-1} w_r\right\rangle \\ &\text{s.t. } D \succeq 0,\ \operatorname{tr}(D) \le 1.\end{aligned} \tag{3.34}$$

If (A^*, U^*) is an optimal solution of (3.33), then

$$(W^*, D^*) = \left(U^*A^*, U^* \operatorname{diag}\left(\frac{\|a^1\|_2}{\|A\|_{2,1}}, \dots, \frac{\|a^d\|_2}{\|A\|_{2,1}}\right)(U^*)^\intercal\right),$$

where a^i are the rows of A, is an optimal solution of problem (3.34); conversely, given an optimal solution (W^*, D^*), if U^* has as columns an orthonormal basis of eigenvectors of D^* and $A^* = (U^*)^\intercal W^*$, (A^*, U^*) is an optimal solution of (3.33). To obtain an optimal solution (W^*, D^*) the authors, for a better stability, use a modified problem

$$\begin{aligned}&\underset{W\in\mathbb{R}^{d\times T}, D\in\mathbb{R}^{d\times d}}{\arg\min} \sum_{r=1}^{T}\sum_{i=1}^{m_r} \ell(y_i^r, \langle w_r, x_i^r\rangle) + \lambda \sum_{r=1}^{T} \left\langle w_r, D^{-1} w_r\right\rangle + \mu \operatorname{tr}\left(D^{-1}\right) \\ &\text{s.t. } D \succeq 0,\ \operatorname{tr}(D) \le 1.\end{aligned} \tag{3.35}$$

This problem is solved using an iterated two-step strategy. The optimization with respect to W decouples in each task and the standard Representer Theorem can be used to solve it, and the one with respect to D has a closed solution $D^* = (W^\intercal W + \mu I)^{\frac{1}{2}} / \operatorname{tr}\left((W^\intercal W + \mu I)^{\frac{1}{2}}\right)$,where the identity, which improves the stability, is consequence of the addition of the term $\operatorname{tr}\left(D^{-1}\right)$ in the objective function. It is interesting to observe that the regularizer of (3.34) can be expressed as $\operatorname{tr}(W^\intercal D^+ W)$ and by plugging D^* in this formula, when $\mu = 0$, we obtain the squared-trace norm regularizer for W:

$$\underset{W\in\mathbb{R}^{d\times T}}{\arg\min} \sum_{r=1}^{T}\sum_{i=1}^{m_r} \ell(y_i^r, \langle w_r, x_i^r\rangle) + \lambda \|W\|_*^2. \tag{3.36}$$

Here, $\|W\|_* = \operatorname{tr}\left((W^\intercal W)^{\frac{1}{2}}\right)$ denotes the trace norm (also known as nuclear norm), which can be seen as the continuous envelope of the rank since the nuclear norm is $\|W\|_* = \sum_{i=1}^{\min d,T} \lambda_i$ where λ_i are the eigenvalues of W, thus favouring low-rank solutions of W. That is, the initial problem (3.33) is equivalent to a problem where the trace norm regularization for matrix W is used.

In Argyriou et al. (2007) the idea of penalizing the eigenvalues is extended to any spectral funcion $F : \mathbb{S}^d_{++} \to \mathbb{S}^d_{++}$ where $\mathbb{S}^d_{++}$ is the set of matrices $A \in \mathbb{R}^{d\times d}$ symmetric and positive definite. The definition for the spectral function $F(A)$, for a diagonalizable matrix $A = V^\intercal \operatorname{diag}(\lambda_1, \ldots, \lambda_d)V$ is given in terms of a scalar function f that is applied over its eigenvalues:

$$F(A) = U^\intercal \operatorname{diag}(f(\lambda_1), \ldots, f(\lambda_d))U \ .$$

Then, a generalized regularizer for problem (3.34) can be expressed as

$$\sum_t \langle w_t, F(D)w_t\rangle = \operatorname{tr}\left(W^\intercal F(D)W\right) = \operatorname{tr}\left(F(D)WW^\intercal\right) .$$

It is easy to see that problem (3.34) is a particular case where $f(\lambda) = \lambda^{-1}$. In Maurer (2009) some bounds on the excess risks are given for this Multi-Task Feature Learning method.

Another relevant extension is shown in Agarwal et al. (2010), where instead of assuming that the task parameters w_r lie in a linear subspace, i.e. $w_r = Ua_r$, the authors generalize this idea by assuming the parameter w_r lies in a manifold $\mathcal{M}$. The resultant optimization problem to train the model is

$$\arg\min_{W,\mathcal{M},\boldsymbol{b}} \sum_{r=1}^{T}\sum_{i=1}^{m_r} \ell(y_i^r, \langle w_r, x_i^r\rangle + b_r) + \lambda \sum_{r=1}^{T} \mathcal{P}_{\mathcal{M}}(w_r), \tag{3.37}$$

where $\mathcal{P}_{\mathcal{M}}(w_r)$ represents the distance between w_r and its projection on the manifold $\mathcal{M}$. Observe that if we define w_r as $w_r = Ua_r$ as before, this distance is zero because $w_r \in \operatorname{span}(u_1, \ldots, u_T)$ for all $r = 1, \ldots, T$. Again, an approximation of (3.37) is used to obtain a convex problem, and it is solved using a two-step optimization algorithm.

Other distinct, relevant approach for Feature Learning is the one described in Maurer et al. (2013), where a sparse-coding method (Maurer and Pontil, 2010) is used for MTL. Maurer et al. present the problem

$$\arg\min_{D\in\mathcal{D}_k, A\in\mathbb{R}^{k\times T}} \sum_{r=1}^{T}\sum_{i=1}^{m_r} \ell(y_i^r, \langle Da_r, x_i^r\rangle) + \lambda \|D\|_{2,\infty} + \mu \|A\|_{1,\infty} . \tag{3.38}$$

Here, $\mathcal{D}_k$ is the set of k-dimensional dictionaries and every $D \in \mathcal{D}_k$ is a linear map $D : \mathbb{R}^k \to \mathcal{H}$; in the linear case, where $\mathcal{H} = \mathbb{R}^d$, the set $\mathcal{D}_k$ is the set of matrices $\mathbb{R}^{d\times k}$, such that

$$\underset{d\times T}{W} = \underset{d\times k}{D}\ \underset{k\times T}{A} .$$

Although (3.33) and (3.38) share a similar form, there are crucial differences. The matrix U in (3.33) is an orthogonal square matrix, while the matrix D of (3.38) is overcomplete with $k > d$ columns of bounded norm. Also, in problem (3.33) non-linear features can be used while problem (3.38) is linear. A problem very similar to (3.38) is presented in Kumar and III (2012) where the idea is the same but the regularizers are the $L_{2,2}$

(Frobenius) norm for D and the $L_{1,1}$ norm for A:

$$\underset{D\in\mathcal{D}_k, A\in\mathbb{R}^{k\times T}}{\arg\min} \sum_{r=1}^{T}\sum_{i=1}^{m_r} \ell(y_i^r, \langle Da_r, x_i^r\rangle) + \lambda \|D\|_{2,2} + \mu \|A\|_{1,1} . \tag{3.39}$$

Here, we can interpret this model as a linear sparse combination, encoded in A, of some features encoded in D: $w_r^\intercal \cdot x_i^r = \sum_{\kappa=1}^{k} a_r^\kappa \left(D_\kappa^\intercal \cdot x_i^r\right)$. Unlike the Multi-Task Feature Learning approach of Argyriou et al, this sparse coding formulation is only presented in the linear setting.

Feature Selection approaches

The feature selection approaches are also driven by learning a good set of features for all tasks; however they focus on subsets of the original features. Due to their nature, the works following this strategy are based on linear models. This is a more rigid approach than that of Feature Learning but is also more interpretable.

Most works on Multi-Task Feature Selection uses an $L_{p,q}$ regularization of the weights matrix W. The first work using this idea is Obozinski et al. (2006), where the authors solve the problem

$$\underset{W}{\arg\min} \sum_{r=1}^{T}\sum_{i=1}^{m_r} \ell(y_i^r, \langle w_r, x_i^r\rangle) + \lambda \|W\|_{2,1}^2 , \tag{3.40}$$

where the $L_{2,1}$ regularization enforces row sparsity and forces different tasks to share a subset of features w^i, which are the rows of W. In Liu et al. (2009) the $L_{\infty,1}$ regularization is used for the same goal. Then, in Gong et al. (2012a) this idea is generalized with a capped-$L_{p,1}$ penalty of W, which is defined as $\sum_{i=1}^{d} \min(\theta, \left\|w^i\right\|_p)$. That is, the parameter θ enables a more flexible regularization, with small values of θ the smallest rows are pushed towards zero since the rows with norms larger than θ will not dominate the sum. As θ grows this penalty will degenerate to the standard $L_{p,1}$ norm.

In Lozano and Swirszcz (2012) a multi-level lasso selection is presented where the main idea is to decompose each w_r^i, that is the i-th feature of the r-th task, as $w_r^i = \theta^i a_r^i$ and then, using the matrix $\Theta = \operatorname{diag}\left(\theta^1, \ldots, \theta^d\right)$, they define the problem

$$\underset{\Theta, a_1, \ldots, a_T}{\arg\min} \sum_{r=1}^{T}\sum_{i=1}^{m_r} \ell(y_i^r, \langle \Theta a_r, x_i^r\rangle) + \mu \operatorname{tr}\Theta + \nu \|A\|_{1,1} . \tag{3.41}$$

By doing this, the features i such that $\theta^i = 0$, are discarded for all tasks, but the rest may be shared among tasks or not depending on the values of a_r^i. Observe that this is similar to the sparse coding problem shown in (3.38) with D, the "feature building" matrix, being limited to diagonal matrices since it is acting here as a selection matrix:

$$w_r^\intercal \cdot x_i^r = \sum_{i=1}^{k} a_r^i \left(\theta_i \cdot x_i^r\right) .$$

The feature selection methods based on $L_{p,1}$ regularization are shown to be equivalent to a Bayesian approximation with a generalized Gaussian prior in Zhang et al. (2010). Moreover, this approach also allows to find the relationship among tasks and to identify outliers. In Hernández-Lobato and Hernández-Lobato (2013) a horseshoe prior is used

instead to learn feature covariance; and in Hernández-Lobato et al. (2015) this prior is also used to identify outlier tasks.

3.4.2 Parameter-based MTL

The parameter-based approaches, instead of trying to find a good shared feature space, enforce the coupling through the regularization of the parameters of linear models $h_r(x_i^r) = w_r^\intercal \phi(x_i^r)$, where ϕ is a fixed, non-learnable transformation. Since we have one vector w_r for each task, we can consider the matrix $W = (w_1 \dots w_T)$. Some approaches rely on the assumption that the Multi-Task weight matrix W has a low rank, others try to learn the pairwise task relations or to cluster the tasks. A different approach is the decomposition one, where the assumption is that the matrix W can be expressed as the summation of multiple matrices. We summarize each approach below.

Low-rank approaches

In the low-rank approaches the assumption is that task parameters w_r share a low-dimensional space, or, at least, are close to this subspace. This is similar to the Feature Learning approach, but it is not that rigid, since it allows for some flexibility. The idea in Ando and Zhang (2005) is that the task parameters can be decomposed as

$$w_r = u_r + \Theta^\intercal v_r,$$

where $\Theta \in \mathbb{R}^{k \times d}$ spans a shared low dimensional space, that is $\Theta\Theta^\intercal = I_k$ with $k < d$, and d is the dimension of the data. Under this consideration, to train the model it is necessary to solve the problem

$$\underset{\Theta \in \mathbb{R}^{k \times d}, \boldsymbol{u}, \boldsymbol{v}}{\arg\min} \sum_{r=1}^{T} \sum_{i=1}^{m_r} \ell(y_i^r, \langle u_r + \Theta^\intercal v_r, x_i^r \rangle) + \lambda \sum_{r=1}^{T} \|u_r\|^2 \text{ s.t. } \Theta\Theta^\intercal = I_k. \tag{3.42}$$

Observe that this problem shares some similarities with (3.33). However, this is a more flexible approach, since the vectors u_r allow for deviations of the task parameters from the shared subspace. Problem (3.42) can be reformulated as

$$\underset{\Theta \in \mathbb{R}^{k \times d}, \boldsymbol{w}, \boldsymbol{v}}{\arg\min} \sum_{r=1}^{T} \sum_{i=1}^{m_r} \ell(y_i^r, \langle w_r, x_i^r \rangle) + \lambda \sum_{r=1}^{T} \|w_r - \Theta^\intercal v_r\|^2 \text{ s.t. } \Theta\Theta^\intercal = I_k, \tag{3.43}$$

where the terms $\|w_r - \Theta^\intercal v_r\|^2$ enforces the similarity across tasks by bringing them closer to the shared subspace. Problem (3.43) is solved using a two-step optimization, iterating between minimizing in $\{\Theta, \boldsymbol{v}\}$ and minimizing in $\boldsymbol{u}$. In Chen et al. (2009) the following extension is proposed:

$$\underset{\Theta \in \mathbb{R}^{k \times d}, \boldsymbol{w}, \boldsymbol{v}}{\arg\min} \sum_{r=1}^{T} \sum_{i=1}^{m_r} \ell(y_i^r, \langle w_r, x_i^r \rangle) + \lambda \sum_{r=1}^{T} \|w_r - \Theta^\intercal v_r\|^2 + \mu \sum_{r=1}^{T} \|w_r\|^2 \text{ s.t. } \Theta\Theta^\intercal = I_k. \tag{3.44}$$

Moreover it is shown that (3.44), when relaxing the orthogonality constraint, can be expressed as a convex minimization problem.

A different approach relies on the use of the trace norm of the matrix W. This norm penalizes $\sum_{i=1}^{d} \lambda_i(W)^2$, where $\lambda_i(W)$ are the eigenvalues of W, and thus, forcing W to be low-rank. In the work of Pong et al. (2010) new formulations for problems with this

trace norm penalty and a primal-dual method for solving the problem is developed. A modification of the trace norm can be found in Han and Zhang (2016), where a capped-trace norm is defined as $\sum_{i=1}^{d} \min(\theta, \lambda_i(W)^2)$. This capped norm, like the capped-L_p norm, can enforce a lower rank matrix for small θ and also degenerates to the trace norm for large enough θ.

Task-Relation Learning approaches

In other approaches, like the feature learning approach or the low-rank approach, the assumption is that all task parameters share the same subspace, which may be detrimental when there exists a negative or neutral transfer. The Task-Relation Learning approach aims to find the pairwise dependencies among tasks and to possibly model positive, neutral and negative transfers between tasks.

One of the first works with the goal of explicitly modelling the pairwise task-relations is Bonilla et al. (2007), where a Multi-Task Gaussian Process (GP) formulation is presented. Assuming a Gaussian noise model $y_i^r \sim N\left(f_r(x_i^r), \sigma_r^2\right)$, Bonilla et al. place a GP prior over the latent functions f_r to induce correlation among tasks:

$$\boldsymbol{f} \sim N\left(\mathbf{0}_{dT}, K^f \otimes K_\theta^{\mathcal{X}}\right),$$

where $\boldsymbol{f} = (f_1, \ldots, f_T)$ and $A \otimes B$ is the Kronecker product of two matrices, so $\mathrm{Cov}(f_r(x), f_s(x')) = K_{rs}^f k_\theta^{\mathcal{X}}(x, x')$. That is, instead of assuming a block-diagonal covariance matrix for $\boldsymbol{f}$ as in previous works of Joint Learning (Lawrence and Platt, 2004), the authors in Bonilla et al. (2007) model the covariance as a product of inter-task covariance and inter-feature covariance. The inference of this model can be done using the standard GP inference for the mean and the variance of the prediction distribution. However, the interest resides in learning the task-covariance matrix K^f, but this leads to a non-convex problem. The authors propose a low-rank approximation of K^f, which weakens its expressive power. To overcome this disadvantage, in Zhang and Yeung (2010, 2013), using the idea of the Multi-Task GP, they consider linear models $f(x_i^r) = \langle w_r, x_i^r \rangle + b_r$ and the prior on matrix $W = (w_1 \ldots, w_T)$ is defined as

$$W \sim \left(\prod_{r=1}^{T} N\left(\mathbf{0}_d, \sigma_r^2 I_d\right)\right) MN\left(0_{d\times m}, I_d \otimes \Omega\right)$$

where $MN(M, A \otimes B)$ denotes the matrix-variate normal distribution with mean M, row covariance matrix A and column covariance matrix B. It is shown that the problem of selecting the maximum a posteriori estimation of W and the maximum likelihood estimations of Ω and $\boldsymbol{b}$ is a regularized minimization problem that, when relaxing the restrictions on Ω, can be expressed as

$$\begin{aligned} &\underset{\Omega\in\mathbb{R}^{d\times T}, W, \boldsymbol{b}}{\arg\min} \sum_{r=1}^{T}\sum_{i=1}^{m_r} \ell(y_i^r, \langle w_r, x_i^r\rangle + b_r) + \lambda \sum_{r=1}^{T} \|w_r\|^2 + \mu \sum_{r,s=1}^{T} \left(\Omega^{-1}\right)_{rs} \langle w_r, w_s\rangle \\ &\text{s.t. } \Omega \succeq 0, \operatorname{tr}\Omega = 1. \end{aligned} \tag{3.45}$$

Other approaches like Argyriou et al. (2013) reach a similar problem from other perspective. Argyriou et al. assume a representation of the structure of the tasks as a graph; then the graph Laplacian in the optimization problem can incorporate the

knowledge about the task structure as shown in Evgeniou et al. (2005):

$$\arg\min_{W,\boldsymbol{b}} \sum_{r=1}^{T}\sum_{i=1}^{m_r} \ell(y_i^r, \langle w_r, x_i^r\rangle + b_r) + \mu \sum_{r,s=1}^{T} (L)_{rs} \langle w_r, w_s\rangle , \tag{3.46}$$

where μ is a tuning parameter. Here the regularization can be also written using the adjacency matrix A as

$$\sum_{r,s=1}^{T} (L)_{rs} \langle w_r, w_s\rangle = \sum_{r,s=1}^{T} (A)_{rs} \|w_r - w_s\|^2 .$$

The goal of Argyriou et al. (2013) and Zhang and Yeung (2010) is to jointly learn the task parameters and the tasks relations. In both cases, they opt for a two-step optimization: one step to learn the task parameters and other to learn the task relations. In the first step, according to Evgeniou et al. (2005), the problem (3.46) can be solved in the dual space using a Multi-Task kernel

$$k_L(x_i^r, x_j^s) = (L + \lambda I)^{-1}_{rs} \, k(x_i^r, x_j^s).$$

In Zhang and Yeung (2010) the authors propose the use of the trace norm to enforce a low rank task-covariance matrix Θ, which leads to a closed solution. In Argyriou et al. (2013) they want to learn a matrix L that is a valid graph Laplacian, so they propose the following problem in the dual space:

$$\begin{aligned} &\arg\min_{\boldsymbol{\alpha},L} \boldsymbol{\alpha}^\intercal K_L \boldsymbol{\alpha} + \nu \boldsymbol{\alpha}^\intercal \boldsymbol{y} + \operatorname{tr}(L + \lambda I)^{-1} \\ &\text{s.t. } 0 \preceq (L + \lambda I)^{-1} \preceq \frac{1}{\lambda} I, \ (L + \lambda I)^{-1}_{\text{off}} \leq 0, \ (L + \lambda I)^{-1} \mathbf{1}_n = \frac{1}{\lambda} \mathbf{1}_n, \end{aligned} \tag{3.47}$$

where A_{off} denotes the off diagonal entries of A. The restrictions of problem (3.47) are to ensure that L is a valid graph Laplacian, and the trace term in the objective function is to force L to be low-rank so it is easier to find clusters of tasks. The objective function is not jointly convex but is convex in each $\boldsymbol{\alpha}$ and L when we fix the other. For the step to optimize the Laplacian matrix the authors develop an algorithm involving several projection steps using proximal operators. Another work focused on learning the task-relations is Dinuzzo (2013), where the approach the problem a learning problem in an RKHS of vector-valued functions $g : \mathcal{X} \to \mathbb{R}^T$, where the associated reproducing kernel is:

$$H(x_1, x_2) = K_{\mathcal{X}}(x_1, x_2) \cdot L$$

and L is a symmetric positive matrix called the *output* kernel. That is, the elements of such RKHS are not real-valued functions but vector-valued functions, where each element of the vector corresponds to a different task.

Task Clustering approaches

The Task Clustering approach tries to find C clusters or groups among the original set of T tasks. Usually, the goal is to learn jointly only the tasks in the same cluster, so no negative transfer takes place. The first clustering approach (Thrun and O'Sullivan, 1996) divides the optimization process in two separate steps: independently learning the task-parameters and jointly learning the clusters of tasks. Using models that involves

distances among points, e.g. kernel methods, they define for each task $r = 1, \dots, T$ the distance

$$\text{dist}_{\boldsymbol{\omega}_r}(x, x') = \sqrt{\sum_{i=1}^{d} \omega_r^i \, (x^i - x'^i)^2}.$$

That is, $\boldsymbol{\omega}_r$ parametrizes a distance with a different weight for each feature. Then, for each task an optimal weights vector $\boldsymbol{\omega}_r^*$ is computed minimizing the distance between examples of the same class and maximizing the distance among different classes:

$$A_r(\boldsymbol{\omega}_r) = \sum_{s=1}^{T} \delta_{r,s} \sum_{i=1}^{m_r} \sum_{j=1}^{m_s} (y_i^r y_j^s) \text{dist}_{\boldsymbol{\omega}_r}(x_i^r, x_j^r),$$

where δ_{rs} is 1 if $r = s$ and -1 otherwise. After the computation of the optimal parameters $\boldsymbol{\omega}_r^*$, the empirical loss on task r of a model fitted on data of task r using a distance parametrized by $\boldsymbol{\omega}_s^*$ is defined as e_{rs}. Then, the goal is to find clusters B_κ with $\kappa = 1, \dots, K$ minimizing

$$J(K) = \sum_{\kappa=1}^{C} \sum_{r \in B_\kappa} \frac{1}{|B_r|} \sum_{s \in B_\kappa} e_{r,s},$$

where the number of clusters C with minimum $J(C)$ is selected. That is, the clusters are selected using the results of independently trained tasks but using distances whose parameters are optimal for other tasks, then the transfer is done through the parameters $\boldsymbol{\omega}_r$.

Some proposals have also been made using regularization approaches. In Jacob et al. (2008), a problem based on Evgeniou and Pontil (2004) is proposed. Considering the $T \times T$ constant matrix $U = \frac{1}{T}\mathbf{1}\mathbf{1}^\intercal$, E the $T \times K$ cluster assignment binary matrix, and defining the adjacency matrix $M = E(E^\intercal E)^{-1}E^\intercal$, the problem is

$$\arg\min_{W} \sum_{r=1}^{T} \sum_{i=1}^{m_r} \ell(y_i^r, \langle w_r, x_i^r \rangle) + \lambda(\mu_\text{m}\Omega_\text{m}(W) + \mu_\text{b}\Omega_\text{b}(W) + \mu_\text{w}\Omega_\text{w}(W)), \tag{3.48}$$

where $\Omega_\text{m} = \text{tr}\,(WUW^\intercal)$ is the mean regularization, $\Omega_\text{b} = \text{tr}\,(W(M-U)W^\intercal)$ is the inter-cluster variance regularization and $\Omega_\text{w} = \text{tr}\,(W(I-M)W^\intercal)$ is the intra-cluster variance regularization. This problem cannot be solved using the results of Evgeniou et al. (2005) because the regularization used is not convex, so a convex relaxation is needed.

A similar approach is presented in Kang et al. (2011) where, using the results from Argyriou et al. (2008), they propose a trace norm regularizer of the matrices $W_\kappa = WQ_\kappa$, where Q_κ are $T \times T$ binary, diagonal matrices where the r-th element of the diagonal indicates whether task r corresponds to cluster κ. They consider the problem

$$\begin{aligned} \arg\min_{W, Q_1, \dots, Q_T, \boldsymbol{b}} \quad & \sum_{r=1}^{T} \sum_{i=1}^{m_r} \ell(y_i^r, \langle w_r, x_i^r \rangle + b_r) + \lambda \sum_{\kappa=1}^{C} \|WQ_\kappa\|_*^2 \\ \text{s.t.} \quad & \sum_{\kappa=1}^{C} Q_\kappa = I \text{ with } 0 \le Q_{\kappa t} \le 1. \end{aligned} \tag{3.49}$$

Here, the trace norm acts on each cluster, so it enforces that the matrices of vectors w_r in the same cluster have low-rank. This can be seen as a clusterized version of Multi-Task Feature Learning (Argyriou et al., 2006, 2008), that is, instead of assuming that all tasks share the same subspace, only the tasks in the same cluster do; however, the explicit learned features cannot be recovered. The optimization of matrices Q_κ on problem (3.49) is done by relaxing the binary nature of matrices Q_κ and reparametrizing them as

$$Q_\kappa[r,r] = \frac{\exp(\alpha_{\kappa r})}{\sum_{g=1}^{C} \exp(\alpha_{gr})},$$

then they perform gradient descent over the $\alpha_{\kappa r}$ of the regularizer $\|WQ_\kappa\|_*^2$.

Another approximation to clusterized MTL is provided in Crammer and Mansour (2012), where a two-step procedure is described as following. Considering that K initial clusters are fixed containing the T tasks, then two steps are repeated. First C single task models f_κ are fitted using the pooled data from tasks in cluster κ. Secondly each task r is assigned to the cluster κ whose function f_κ obtains the lowest error in task r. The proposal of Barzilai and Crammer (2015) takes the idea of the cluster assignation step from Crammer and Mansour (2012) and is also inspired by the sparse coding work of Kumar and III (2012). In this work the weights matrix is $W = DA$, where $D \in \mathbb{R}^{d\times C}$ contains as columns the hypotheses for each cluster and $G \in \mathbb{R}^{C\times T}$ is the task assignment matrix, that is, $g_r = G_r \in \{0,1\}$ and $\|g_r\|^2 = 1$. The corresponding optimization problem is

$$\begin{aligned} &\underset{D\in\mathbb{R}^{d\times C}, G\in\mathbb{R}^{C\times T}}{\arg\min} \sum_{r=1}^{T}\sum_{i=1}^{m_r} \ell(y_i^r, \langle Dg_r, x_i^r\rangle) + \lambda \|D\|_{2,1} \\ &\text{s.t. } g_r \in [0,1],\ \|g_r\|^2 = 1, \end{aligned} \tag{3.50}$$

where the constraints on g_r have been relaxed to be in the $[0,1]$ interval in order to make problem (3.50) convex. Observe that (3.50) is similar to (3.39) but different restrictions are used to ensure that G can be seen as a clustering assignment matrix.

Decomposition approaches

The Decomposition approach considers that the assumption that task parameters reside in the same subspace, or that the parameter matrix W, composed by each task parameters w_r as its columns, is low rank, is too restrictive for real world scenarios. The proposition is then to decompose the parameter matrix in the sum of two matrices, i.e. $W = U + V$ where usually U captures the shared properties of the tasks and V accounts for the information that cannot be shared among tasks. This models also receive the name of *dirty models* because they assume that the data is *dirty* and cannot be constrained to rigid subspaces. The optimization problem is

$$\underset{U,V\in\mathbb{R}^{d\times T}}{\arg\min} \sum_{r=1}^{T}\sum_{i=1}^{m_r} \ell(y_i^r, \langle u_r + v_r, x_i^r\rangle) + \lambda g(U) + \mu h(V), \tag{3.51}$$

where $g(U)$ and $h(V)$ are different regularizers for U and V, respectively. In Jalali et al. (2010) the authors use $g(U) = \|U\|_{1,\infty}$ to enforce block-sparsity and $h(V) = \|V\|_{1,1}$ to enforce element-sparsity. In Chen et al. (2010) $g(U) = \|U\|_*$ is used to enforce low-rank while maintaining $h(V) = \|V\|_{1,1}$. In Chen et al. (2011) both regularizers seek properties

shared among all tasks, $g(U) = \|U\|_*$ to enforce a low-rank and $h(V) = \|V\|_{1,2}$ for row-sparsity. In Gong et al. (2012b) they propose $g(U) = \|U\|_{1,2}$ to enforce row-sparsity, i.e. the tasks share a common subspace; and $h(V) = \|V^\intercal\|_{1,2}$ which penalizes the orthogonal parts to the common subspace of task-parameter; the authors state that it penalizes outlier tasks.

Other approaches generalize the decomposition method by assuming that the parameter matrix can be expressed as $W = \sum_{l=1}^{L} W_l$; then the problem to solve has the form

$$\underset{W_1,\dots,W_L \in \mathbb{R}^{d\times T}}{\arg\min} \sum_{r=1}^{T}\sum_{i=1}^{m_r} \ell(y_i^r, \left\langle \sum_{l=1}^{L} (W_l)_r, x_i^r \right\rangle) + \sum_{l=1}^{L} \lambda_l r(W_l). \tag{3.52}$$

In Zweig and Weinshall (2013) the regularizer used is $r(W_l) = \|W_l\|_{2,1} + \|W_l\|_{1,1}$ to enforce the row and element-sparsity. In Han and Zhang (2015) the regularizer is $r(W_l) = \sum_{r,s=1}^{T} \|(W_l)_r - (W_l)_s\|^2$ which, alongside some constraints, allows to build a tree of task groups, where the root contains all the tasks and the leafs only correspond to one task.

3.4.3 Combination-based

The combination-based methods use a combination of task-specific models and models that are common to all tasks. These two models are learned simultaneously with the goal of leveraging the common and specific information.

The first proposal, which uses the SVM as the base model, is found in Evgeniou and Pontil (2004). The goal is to find a decision function for each task, defined by a vector $w_r = w + v_r$ and a bias b_r. Here w is common to all tasks and v_r is task-specific. Instead of imposing some restrictions such as low-rank or inter-task regularization the idea is to impose the coupling by directly placing a model w that is common to all tasks. The v_r part is added so each model can be adapted to the specific task.

Multiple extensions of the work of Evgeniou and Pontil (2004) have been presented: in Li et al. (2015); Xu et al. (2014) the method is extended to the Proximal SVM (Fung and Mangasarian, 2001) and Least Squares SVM (Suykens and Vandewalle, 1999), respectively. Also, in Parameswaran and Weinberger (2010) the idea is adapted for the Large Margin Nearest Neighbor model (Weinberger and Saul, 2009). However, in this work we are interested mainly in two extensions: one is the work of Evgeniou et al. (2005) and the other is developed in Liang and Cherkassky (2008) and in Cai and Cherkassky (2009); both will be described in detail in Chapter 4. We can express the optimization problem as

$$\underset{w,V}{\arg\min} \sum_{r=1}^{T}\sum_{i=1}^{m_r} \ell(y_i^r, \langle w_r + v_r, x_i^r\rangle) + \mu_1 \|w\|^2 + \mu_2 \sum_{r=1}^{T} \|v_r\|^2, \tag{3.53}$$

where μ is a tradeoff parameter to leverage the common and task-specific information. When the dual problem of (3.53) is obtained, the result is a problem where the kernel encodes this combination of common and shared parts; that is, the kernel function has the form

$$k(x_i^r, x_j^s) = \mu_1 k(x_i^r, x_j^s) + \mu_2 \delta_{rs} k(x_i^r, x_j^s),$$

where μ_1, μ_2 are scalar parameters and δ_{rs} is 1 only if r and s are the same task, so it encodes the specific part of the model. In the linear case, this is equivalent to a feature

extension strategy, like the domain adaptation scheme proposed in III (2007) with only target and source domains, but that can be easily adapted to MTL.

3.4.4 Multi-Task Learning with Neural Networks

Deep learning has experimented an enormous development over the last decade, with multiple variants having great success in many fields and applications such as Convolutional Neural Networks for image recognition, Generative Adversarial Networks for generative models or Transformers for Natural Language Processing. The feature learning process natural to neural networks is usually the main idea behind multi-task learning strategies but not always. In this subsection we explore some of these strategies and their connection with other methods used in kernel or linear models.

As proposed in Ruder (2017) we can divide the Multi-Task approaches with neural networks in hard sharing and soft sharing. The hard sharing approach is the most common one, and it consists in sharing between all tasks the hidden layers of the network while keeping some task-specific layers at the end of the network. The first example dates back to Caruana (1997) where only the output layers are task-specific. The goal of this approach is to learn a set of features that is useful for all tasks simultaneously, so the transfer of information between tasks is done in this feature building process. Although this approach has some theoretical properties to improve learning (Baxter, 2000), it is a very rigid approach since it assumes that the learned features and the feature learning process must be the same for all tasks.

The soft sharing approach to Multi-Task learning tries to tackle these problems with different strategies. In Cavallanti et al. (2010) the authors propose to learn one perceptron for each task and the update of each perceptron is determined by an interaction matrix A. Given a pair (x_i^s, y_i^s), the update is

$$w_r(\tau + 1) = w_r(\tau) - \nu y_i^s A_{r,s}^{-1} x_i^s \tag{3.54}$$

where w_r are the parameters of the perceptron corresponding to task r. That is, the weights of task r are updated when a mistake is committed on task s and the update is scaled according to the position r, s of matrix A^{-1}. This approach only uses perceptrons, so its expressive power is quite limited. Also, the matrix A has to be defined a priori and is not learned from the data. In Long and Wang (2015) they propose a model to overcome these limitations. They use a multi-task architecture for computer vision with multiple shared layers and multiple task-specific layers. Moreover, they use a Bayesian approach to learn the task relationships. They place a tensor prior over the network parameters such that in each specific layer l, there are T matrices W_r^l for $r = 1, \ldots, T$, and if we denote as $\mathcal{W}^l$ the vector (tensor) of such matrices, then

$$p(\mathcal{W}^l) = TN\left(0, \Sigma_1, \Sigma_2, \Sigma_3\right),$$

where $TN\left(\right)$ is the tensorial normal distributions, and Σ_1, Σ_2 model the row-covariance and task-covariance in each matrix W_r^l and Σ_3 model the intertask covariance. The parameters $\mathcal{W}^l$ are learned automatically by using gradient descent and for the covariance matrices a Maximum Likelihood Estimator is used after each epoch. If we take a look at the update rule for the network parameters

$$W_r^l(\tau + 1) = W_r^l(\tau) - \nu \left(\frac{\partial \ell(f_r(x_i^r), y_i^r)}{\partial W_r^l} + \left[(\Sigma_1 \otimes \Sigma_2 \otimes \Sigma_3)^{-1} \text{vect} \left(\mathcal{W}^l \right)_{:,:,r} \right] \right),$$

where ℓ is the loss function, we can observe some similarities with the update (3.54), where the inverse of the Kronecker product of covariances models how each task affect the others. Although this approach learns the matrix relations, the architecture is still restrictive since it assumes that all tasks can share a number of hidden layers. In Misra et al. (2016) they propose a strategy named "Cross-stitch" networks which uses one network for each task, but these networks are connected using a linear combination of the outputs of every layer, including the hidden ones. Considering a case of multi-task learning with two tasks 1 and 2, if h_1^l, h_2^l are the output values of the l-th layers of the networks of tasks 1 and 2, respectively, then these outputs are combined as

$$\begin{bmatrix} \tilde{h}_1^l \\ \tilde{h}_2^l \end{bmatrix} = A^l \begin{bmatrix} h_1^l \\ h_2^l \end{bmatrix} = \begin{bmatrix} \alpha_{11}^l & \alpha_{12}^l \\ \alpha_{21}^l & \alpha_{22}^l \end{bmatrix} \begin{bmatrix} h_1^l \\ h_2^l \end{bmatrix}, \tag{3.55}$$

where the 2×2 matrix A^l is a "cross-stitch" unit and defines the linear combination to compute $\tilde{h}_1^l, \tilde{h}_2^l$ which will be the input values for the $(l+1)$-th layer. The network parameters and the "cross-stitch" values α can both be learned using backpropagation. If $A^l = I_{2\times 2}$ in all layers this is equivalent to two independent networks, one for each task, and using constant matrices as "cross-stitch" units results in two identical common networks. This strategy is extended in Ruder et al. (2017), where the authors include two modifications: network parameters of each network are divided in two spaces, each expecting to capture different properties of the data, and there are learnable skip-connections for each task. The first modification is using two spaces for each task, which implies that the number of parameters is doubled, that is, in each task-specific network and in each layer l there are 2 outputs for each task: $h_{r,a}^l, h_{r,b}^l$, each obtained with a different matrix of parameters $W_{r,a}^l, W_{r,b}^l$. Then, in the case of two tasks, as the combination shown in (3.55), A is a 4×4 matrix, because each $\alpha_{i,j}^l$ is a 2×2 matrix for $i, j \in \{1, 2\}$. The matrix A not only determines how the tasks are related but how each space of each task is related with the rest. To enforce that each space captures different properties they use the regularizers

$$\left\| (W_{r,a}^l)^\intercal W_{r,b}^l \right\|_{2,2}^2,$$

where the $L_{2,2}$ (Frobenius) norm is used, so the parameters matrices $W_{r,a}^l$ and $W_{r,b}^l$ span orthogonal spaces. Particular values of the matrices A^l can result in a combination-based approach where there is a shared common model and task-specific ones. The skip-connections are reflected in a final layer in each network that receives as input the linear combination of the activation values $h_{r,1}^l$ and $h_{r,2}^l$ for every layer l. This linear combination uses learnable parameters β_r for each task.

Other approaches consider tensor-based methods instead of the "cross-stitch" networks to learn the parameters of each task-oriented network and the degree of sharing between tasks from the data. In Yang and Hospedales (2017a) the authors propose a tensor-generative strategy to model the parameters of each layer. If W_r^l is the $d_1^l \times d_2^l$ parameter matrix for task r in layer l, in each layer we can consider the collection of such matrices as a $d_1^l \times d_2^l \times T$ tensor $\mathcal{W}^l$. We can build these tensors from other pieces in different ways, for example consider a latent basis matrices $d_1^l \times d_2^l \times K$ tensor $\mathcal{L}$, that is, a collection of

K matrices of dimension $d_1^l \times d_2^l$; and consider the $K \times T$ matrix S, then

$$W_r^l = \mathcal{W}_{:,:,r} = \sum_{\kappa=1}^{K} \mathcal{L}_{.,.,\kappa} S_{\kappa,r}.$$

That is, all task parameter matrices W_r^l are linear combinations of the latent-basis matrices defined in $\mathcal{L}$. Observe that this is a generalization of the sparse coding scheme presented in III (2009) and shown in equation (3.38). Since all the strategies to build $\mathcal{W}$ from other pieces is based on tensor products, the whole process is differentiable and all those pieces can be learned using gradient descent. The other tensor-based proposal is presented in Yang and Hospedales (2017b) where, instead of a tensor-building approach, they consider the tensors $\mathcal{W}^l$ as the collection of matrices W_r^l and use tensor-trace norms to enforce the coupling between different tasks. Since the tensor-trace norms is not differentiable, they use the subgradient for the backpropagation during training. This approach can be categorized as low-rank, that is, a parameter-based approach according to our taxonomy.

All the previous approaches consider the same architecture for each task. Although the skip-connections can alleviate this, the sharing of information is still made in a layer-wise manner, so the same architecture has to be considered for every network. In Sun et al. (2020) they propose a single network with L layers and with skip-connections between all layers, so each task can use a specific policy. That is, task 1 can use the first, third and fourth layer while task 2 might use the second and fourth only. In this example, the first and third are specific for task 1, the second layer is specific for task 2 while the fourth is a shared layer. In general, there is a binary $L \times T$ policies matrix U that determines which layers are used for each task. The problem is then a bi-level optimization

$$\min_{U} \min_{W_1,\ldots,W_L} \ell(U, W_1, \ldots, W_L).$$

The optimization with respect the network parameters is done using back-propagation, while the optimization with respect to U uses a specific algorithm.

3.4.5 Multi-Task Learning with Kernel Methods

Kernel Methods are also models that have been successful in a lot of areas. The principal appeal of these models is that the original features are implicitly transformed to a kernel space, possibly infinite-dimensional, where the problems of classification or regression for example are usually easier to solve.

Unlike deep learning models, the kernel features used are not learnable, but are implicitly defined a priori by the kernel function used like Gaussian, polynomial or Matérn kernels for example. This fact makes it more difficult to use a feature-based MTL approach with kernel models. Instead, other of the reviewed approaches can be taken.

One important approximation to MTL with kernel models is learning vector-valued functions, in which the target space is not scalar but a vector one. That is, the sample data X, Y are pairs $(x_i, \boldsymbol{y}_i)$ where $x_i \in \mathcal{X}$, e.g. $\mathcal{X} = \mathbb{R}^d$ and $y_i \in \mathcal{Y}^T$. This approach finds its motivation in multi-output learning, where multiple targets are learned are defined for each input. Using kernel models the multi-output regularized risk is

$$\sum_{i=1}^{n} \ell(W^\intercal \phi(\boldsymbol{x}_i) + \boldsymbol{b}, \boldsymbol{y}_i) + \mu\Omega(W), \tag{3.56}$$

where W is the matrix with T columns, one for each output and $\boldsymbol{b}$ is the vector of corresponding biases. A commonly used loss function ℓ is

$$\ell(W^\intercal \phi(\boldsymbol{x}_i) + \boldsymbol{b}, \boldsymbol{y}_i) = \|W^\intercal \phi(\boldsymbol{x}_i) + \boldsymbol{b} - \boldsymbol{y}_i\|_2^2$$

and Ω is a regularizer for matrix W that can enforce different behaviours, for example the trace norm regularizer is used for enforcing a low rank matrix. In Micchelli and Pontil (2004, 2005) the authors develop the theory for operator-valued kernels, that are the kernel functions corresponding to vector-valued functions. They show an extension of the representer theorem for operator-valued kernels when a Tikhonov regularization for vector-valued functions is used. Although these are interesting results, they do not provide explicit algorithms to learn such functions. Moreover, multi-task learning is not that well suited for this formulation, since for each data x_i^r there is a single scalar y_i^r. The multi-task regularized risk using this formulation is

$$\sum_{i=1}^{n} \ell(A \odot W^\intercal \phi(\boldsymbol{x}_i) + \boldsymbol{b}, \boldsymbol{y}_i) + \mu\Omega(W), \tag{3.57}$$

where A is a binary matrix with the same sparsity pattern that Y.

Other approach that seems better suited for kernel methods is combination-based one, first shown in Evgeniou and Pontil (2004), which can be seen in Eq. (3.53), and then extended in Cai and Cherkassky (2009, 2012). The kernelized optimization problem is

$$\arg\min_{w,V} \sum_{r=1}^{T} \sum_{i=1}^{m_r} \ell(y_i^r, \langle w, \phi(x_i^r)\rangle + \langle v_r, \phi_r(x_i^r)\rangle) + \lambda(\mu \|w\|^2 + \operatorname{tr}(V^\intercal V)). \tag{3.58}$$

Observe there are different kernel spaces because it is possible to use different implicit transformation for the common part ϕ and for each specific part ϕ_r. This can be done because the coupling between tasks is not made using some restrictions in some shared space, but using a common model for all tasks. Similary to the represnter theorem, it can be shown that

$$w = \sum_{s=1}^{T} \sum_{i=1}^{m_s} \alpha_i^s \phi(x_i^s), \; v_r = \sum_{i=1}^{m_r} \alpha_i^r \phi_r(x_i^r)$$

where the dual coefficients α_i^r are shared, so w is a combination of all inputs from all tasks while the specific parts v_r are only dependent on samples from the corresponding task. The fact that different spaces can be used for the common and specific parts make this formulation very flexible.

A feature-based strategy was also presented in Argyriou et al. (2008), the linear optimization problem is shown in (3.33), and the kernel extension is

$$\arg\min_{U \in \mathcal{L}(\mathcal{H}, \mathbb{R}^d), A \in \mathbb{R}^{d \times T}} \sum_{r=1}^{T} \sum_{i=1}^{m_r} \ell(y_i^r, \langle U a_r, \phi(x_i^r)\rangle) + \lambda \|A\|_{2,1}^2 \text{ s.t. } U^\intercal U = I_d, \tag{3.59}$$

where ϕ is the implicit transformation into the kernel space $\mathcal{H}$ and U is a linear operator between $\mathcal{H}$ and $\mathbb{R}^d$. To solve this they apply the same procedure than the one used in

the linear case, where they obtain a trace-norm regularized problem

$$\arg\min_{W\in\mathbb{R}^{d\times T}} \sum_{r=1}^{T}\sum_{i=1}^{m_r} \ell(y_i^r, \langle w_r, \phi(x_i^r)\rangle) + \lambda \|W\|_*^2, \tag{3.60}$$

and they propose a representer theorem for this problem, where

$$w_r = \sum_{s=1}^{T}\sum_{i=1}^{m_s} \alpha_i^s(r)\phi(x_i^s).$$

The authors also develop an algorithm to solve problem (3.60) using this result. A clusterized extension is presented in Kang et al. (2011) whose corresponding problem is shown in (3.49).

The task relation learning is also a common approach to MTL with kernel models. Using a Gaussian Process formulation, different strategies to learn the task-covariance matrix are shown in Bonilla et al. (2007); Lawrence and Platt (2004).

Finally, one important result for MTL with kernels is shown in Evgeniou et al. (2005), where a general MTL formulation with kernel methods is presented. Given a kernelized problem

$$\sum_{r=1}^{T}\sum_{i=1}^{m} \ell(y_i^r, \langle w_r, \phi(x_i^r)\rangle) + \mu(\operatorname{vec} W)^\intercal (E\otimes I)(\operatorname{vec} W),, \tag{3.61}$$

where E is a $T\times T$ matrix and we use $\operatorname{vec} W$ for the vectorized matrix W, then the solution can be expressed as

$$\operatorname{vec} W = \sum_{r=1}^{T}\sum_{i=1}^{m} \alpha_i^r B_r \phi(x_i^r),$$

with B_r being the columns of a matrix B such that $E = (B^\intercal B)^{-1}$. Then, as shown in Subsection 3.3.3, this is equivalent to using a kernel

$$\hat{k}(x_i^r, x_j^s) = (E^{-1})_{rs} k(x_i^r, x_j^s).$$

This result is used in latter works, such as Zhang and Yeung (2010) and Argyriou et al. (2013), where they propose using an inter-task regularization that penalize

$$\sum_{r,s=1}^{T} (\Theta)_{rs} \langle w_r, w_s\rangle = (\operatorname{vec} W)^\intercal (\Theta\otimes I)(\operatorname{vec} W).$$

where Θ is the inter-task relationship matrix and they propose different strategies to learn such matrix.

3.5 Multi-Task Problems

The concept of Multi-Task problem is not clear because different definitions have been considered in the literature. In this work only supervised problems will be considered, so we will refer to them just as problems.

Multiple kind of problems can be faced with a Multi-Task Learning approach. The most common definition of Multi-Task problem is a homogeneous setting, where all tasks

are sampled from the same space. That is, we have a space $\mathcal{X} \times \mathcal{Y}$ where $\mathcal{X}$ is the feature space and $\mathcal{Y}$ is the target space, which can be $\mathbb{R}$ in the regression case or $\{0, 1\}$ in the classification one, and each task has a possibly different distribution $P_r(x, y)$ over this shared space. In this type of problems, all the tasks have the same number of features and the same target space, that is, every task is either a regression or classification problem, there cannot be a mix of regression and classification tasks. There are other heterogeneous definitions where each task can be sampled from a different space $\mathcal{X}_r \times \mathcal{Y}_r$, and, therefore, a mix of regression or classification tasks can be considered. However, in this work we are only interested in the homogeneous case.

Within the homogeneous MTL problems we can consider the following cases, depending on the nature of each task and the task definition procedure:

- Pure Multi-Task Problems. These are problems where each task has been sampled from a possibly different distribution, so we have possibly different samples (X_r, Y_r).
  - MT single-reg: This is the case where each task is a regression problem with a single target, e.g. $\mathcal{Y} = \mathbb{R}$.
  - MT bin-clas: This is the case where each task is a binary classification problem , e.g. $\mathcal{Y} = \{0, 1\}$.
  - MT multi-reg: This is the case where each task is a regression problem with multiple targets, e.g. $\mathcal{Y} = \mathbb{R}^m$, where m is the number of targets.
  - MT multi-clas: This is the case where each task is a multi-class classification problem, e.g. $\mathcal{Y} = \{0, 1, \ldots, C\}$, where C is the number of classes.
- Artificial Multi-Task Problems: These are problems that can be seen as Multi-Task and be solved using MTL strategies, but it is not the only way to solve them. The main difference is that although the target samples might be different across tasks, the set of features sampled is shared by all tasks, i.e. $(X_r, Y_r) = (X, Y_r)$.
  - multi-reg: This is the case where a m-target regression problem is converted into a multi-task problem by replicating m times the features X and using one of the targets for each repetition, so we have m single target regression problems, each considered a different task.
  - multi-clas: This is the case where a multi-class classification problem with C classes is converted into a multi-task problem by replicating C times the features X and considering a one vs all scheme for each repetition with a different positive class in each one, so we have C binary classification problems, each considered a different task.

In Table 3.1 we show some of the most used multi-task learning problems, exposing its characteristics and the papers that use them.

Name	n	d	T	Nature	References
school	15362	27	139	MT single-reg	Evgeniou and Pontil (2004) Evgeniou et al. (2005) Argyriou et al. (2006, 2008, 2007) Bonilla et al. (2007) Zhang and Yeung (2010) Agarwal et al. (2010) Chen et al. (2011) Zhou et al. (2011) Gong et al. (2012b) Kumar and III (2012) Zhang and Yeung (2013) Han and Zhang (2016) Jeong and Jun (2018)
20-newsgroup	18000	t.v.	20	multi-clas	Ando and Zhang (2005) III (2009)
Reuters-RCV1	800000	t.v.	103	multi-clas	Yu et al. (2005) Ando and Zhang (2005)
computer	3600	13	180	MT single-reg	Argyriou et al. (2006, 2008, 2007) Evgeniou et al. (2005) Agarwal et al. (2010) Kumar and III (2012) Jeong and Jun (2018)
landmine	14820	10	29	MT bin-clas	Xue et al. (2007) Jebara (2011) III (2009) Jawanpuria and Nath (2012)
MHC-I	32302	184	47	MT bin-clas	Jacob et al. (2008) Jawanpuria and Nath (2012)
dermatology	366	33	6	multi-clas	Jebara (2004) Argyriou et al. (2008)
sentiment	2000	473856	4	MT bin-clas	III (2009) Zhang and Yeung (2010) Crammer and Mansour (2012) Zhang and Yeung (2013) Barzilai and Crammer (2015)
sarcos	44484	21	7	multi-reg	Zhang and Yeung (2010)

Continued on next page

Table 3.1 – continued from previous page

Name	n	d	T	Nature	References
					Chen et al. (2011) Zhou et al. (2011) Jawanpuria and Nath (2012) Zhang and Yeung (2013) Ciliberto et al. (2015)
isolet	7797	617	5	MT multi-clas	Parameswaran and Weinberger (2010) Gong et al. (2012a)
mnist	70000	400	10	multi-clas	Kang et al. (2011) Kumar and III (2012) Zweig and Weinshall (2013) Jeong and Jun (2018)
usps	9298	256	10	multi-clas	Kang et al. (2011) Kumar and III (2012) Zweig and Weinshall (2013) Jeong and Jun (2018)
adni	675	306	6	MT single-reg	Gong et al. (2012a) Gong et al. (2012b)
microarray	131	21	19	multi-reg	Lozano and Swirszcz (2012) Han and Zhang (2016)
cifar10	50000	1024	10	multi-clas	Zweig and Weinshall (2013) Han and Zhang (2016)
parkinson	5875	19	42	MT single-reg	Jawanpuria and Nath (2012) Jeong and Jun (2018)

TABLE 3.1: Multi-Task Learning Problems. The columns show the number of samples n, the dimension d, the number of tasks T and the nature of the problem.

3.6 Conclusions

In this chapter, we covered...

Chapter 4

A Convex Formulation for Multi-Task Learning

4.1 Introduction

As we have seen in Chapter 3, the MTL proposals can be categorized in feature-based, parameter-based and combination-based approaches. Feature-based proposals have the strategy of finding a shared representation of the original features that is benefitial for all tasks. Parameter-based strategies typically use multi-task regularization schemes that, using specific regularizers, push together the parameters of the task-specialized models. Finally, the combination-based strategies combine a common model and a task-specific one. In this chapter we will present a convex formulation for combination-based MTL. With this formulation, a general task-specialized model is defined as

$$h_r(\cdot) = \lambda_r g(\cdot) + (1 - \lambda_r) g_r(\cdot). \tag{4.1}$$

Here, we use the hyperparameters $\lambda_r \in [0, 1]$ to combine in a convex way the common part $g(\cdot)$ and specific parts $g_r(\cdot)$. This general formulation is very flexible, because we can use any family of functions to model $g(\cdot)$ or $g_r(\cdot)$. It is also easily interpretable, since $\lambda_r = 1$ for all $r = 1, \ldots, T$ results in a common model and $\lambda_r = 0$ in independent models for each task. All the values $\lambda_r \in (0, 1)$ correspond to pure MTL models, being more common when λ_r is close to 1 and more specific when λ_r is close to 0. Given an MTL sample

$$\boldsymbol{z} = \bigcup_{r=1}^{T} \{(x_1^r, y_1^r), \ldots, (x_m^r, y_m^r)\},$$

the MTL regularized risk functional that corresponds to this convex formulation is

$$R_{\boldsymbol{z}}(g, g_1, \ldots, g_T) := \sum_{r=1}^{T} \sum_{i=1}^{m_r} \ell(\lambda_r g(x_i^r) + (1 - \lambda_r) g_r(x_i^r), y_i^r) + \mu \left(\Omega(g) + \sum_{r=1}^{T} \Omega_r(g_r) \right), \tag{4.2}$$

where $\Omega(g)$ and $\Omega_r(g_r)$ are the regularizers for the common and r-th task parts, respectively. Observe that, since the regularization is made independently for each part, no multi-task specific regularization scheme is needed. The task coupling is made directly in the definition of the model, which combines common and specific part, and the risk $R_{\boldsymbol{z}}$ is optimized jointly in all parts. This has some advantages, like the preservation of

convexity in the risk minimization problem or an optimization procedure that requires only slight modifications to the standard one. In this chapter these characteristics will be presented in specific models using this convex MTL formulation. More specifically, it is shown how this formulation can be applied to two of the most popular model families: kernel methods, in Section 4.2, and neural networks, in Section 4.3. Then, in Section 4.4 a real-world application of the convex MTL to the prediction of renewable energy is presented.

4.2 Convex Multi-Task Learning with Kernel Methods

As explained in the previous chapters, kernel models offer many good properties such as an implicit transformation to a possibly infinite-dimensional space and the convexity of the problems that have to be solved for the training process. With these models a regularized risk problem is solved. A general formulation of a training problem for kernel models is

$$\hat{R}_z(w) := \sum_{i=1}^{n} \ell(w^\intercal \phi(\boldsymbol{x}_i) + b, y_i) + \mu\Omega(w), \tag{4.3}$$

where z is the sample $\{(x_1, y_1), \ldots, (x_n, y_n)\}$ and $\Omega(w)$ is a regularizer for w, typically the L_2 norm: $\|w\|^2$. Observe that b, the bias term, is not regularized since it does not affect the capacity of the hypothesis space. In (4.3) ϕ is a fixed transformation function such that there exists a "kernel trick", that is a kernel function k for which

$$\langle \phi(x), \phi(y) \rangle = k(x, y).$$

That is, ϕ is an element of RKHS, where k is the reproducing kernel. The Representer Theorem (Schölkopf et al., 2001) states that the optimal solution of problem (4.3) has the following form

$$w^* = \sum_{i=1}^{n} \alpha_i \phi(x_i)$$

where $\alpha_i \in \mathbb{R}$ are some coefficients. This means that our optimal solution w^* is also an element of the same RKHS. These models embrace the Structural Risk Minimization paradigm by limiting the capacity of the space of hypothesis, which is done by penalizing the L_2 norm of w. This is equivalent to limiting our space of candidates to vectors inside a ball of some fixed radius.

Multi-Task Learning with kernel models require imposing some kind of coupling between the models for each task in the learning process. The feature learning or feature sharing approach, which is usually adopted with neural networks, is not feasible when using kernel models, since the (implicit) transformation functions ϕ used are not learned but fixed, and determined by the choice of kernel function. Therefore, other strategies have to be developed. One approach to MTL with kernel models was developed in Evgeniou and Pontil (2004), and later extended in Cai and Cherkassky (2009, 2012), where the models for each task are defined as:

$$w_r = w + v_r,$$

where w is a common part, shared by all models, and v_r is a task-specific part. With this approximation, the transfer of information is performed by the common part w. The

regularized risk that is minimized is

$$R_{\boldsymbol{z}}(w, v_1, \ldots, v_T) := \sum_{r=1}^{T} \sum_{i=1}^{m_r} \ell(w^\intercal \phi(\boldsymbol{x}_i^r) + v_r^\intercal \phi_r(\boldsymbol{x}_i^r) + b_r, y_i^r) + \mu_c \|w\|^2 + \mu_s \sum_{r=1}^{T} \|v_r\|^2 , \quad (4.4)$$

where μ_c and μ_s are the hyperparameters to control the common and specific parts regularization, respectively. Here $\boldsymbol{z}$ is an MTL sample

$$\boldsymbol{z} = \bigcup_{r=1}^{T} \{(x_1^r, y_1^r), \ldots, (x_m^r, y_m^r)\}.$$

Observe also that in (4.4) different transformations are used: the transformation ϕ corresponds to common part of the model, while ϕ_r is task-specific. This is a joint learning approach that is developed for the L1-SVM, to which Evgeniou et al. give the name of *Regularized MTL*, but we will refer to it as additive MTL approach. Observe that as $\frac{\mu_c}{\mu_s} \to \infty$, we would have a common part w that tends to zero, which would results in independent models for each task, i.e. $w_r \approx v_r$. On the contrary, when $\frac{\mu_c}{\mu_s} \to 0$, the task-specific parts tend to zero and every model is the common part, i.e. $w_r \approx w$. There are two asymptotical behaviours: the first one tends to an ITL approach, while the second one tends to a CTL one. The MTL formulation is one strategy that lies between those two approaches, CTL and ITL, combining them to achieve a more flexible model.

The asymptotical properties of this approach offer an interpretation to understand the influence of each hyperparameter, but they are not easily applicable in practice. In Ruiz et al. (2019) we propose an alternative formulation for this joint learning approach. The models for each task are defined as a convex combination of the common and task specific parts:

$$w_r = \lambda w + (1 - \lambda) v_r,$$

where $\lambda \in [0, 1]$ is a hyperparameter. More specifically, and using the formulation of (4.1), we define the common part as $g(x) = w^\intercal \phi(x) + b$ and the task-specific parts as $g_r(x) = {v_r}^\intercal \phi_r(x) + b_r$, so the MTL models are

$$h_r(x_i^r) = \lambda \left\{ w^\intercal \phi(x_i^r) + b \right\} + (1 - \lambda) \left\{ v_r^\intercal \phi_r(x_i^r) + b_r \right\},$$

and the corresponding regularized risk is

$$R_{\boldsymbol{z}}(w, v_1, \ldots, v_T) := \sum_{r=1}^{T} \sum_{i=1}^{m_r} \ell(\lambda \left\{ w^\intercal \phi(x_i^r) + b \right\} + (1 - \lambda) \left\{ v_r^\intercal \phi_r(x_i^r) + b_r \right\}, y_i^r) + \mu_c \|w\|^2 + \mu_s \sum_{r=1}^{T} \|v_r\|^2 .$$

We will name this approach convex, in contrast to the additive approach of the original formulation. With this formulation, the interpretation of λ is straight-forward. The model with $\lambda = 1$ is equivalent to learning a single common model for all tasks, that is $w_r = w$. When $\lambda = 0$, the models for each task are completely independent: $w_r = v_r$. The convex formulation also define an MTL model that is between a CTL approach and an ITL one, but it presents an advantage over the additive one: the values of λ that recover the CTL and ITL approaches are known, and these values are attainable, it is not an asymptotical behaviour as in the additive formulation. Moreover, it is shown

in Ruiz et al. (2019) that the two formulations, the additive and convex, are equivalent with an L1-SVM setting.

4.2.1 L1-SVM and Equivalence Results

The L1-SVM Vapnik (2000) is the original and most popular variant of the SVMs and is also the basis of the MTL formulation in Evgeniou and Pontil (2004). I will present the development for the additive approach and the one for the convex using an L1-SVM setting. Then I will show the equivalence between the two approaches and discuss its differences.

Additive MTL L1-SVM.
The additive MTL primal problem formulation, presented in Evgeniou and Pontil (2004) and extended for task-specific biases in Cai and Cherkassky (2012), is

$$\begin{aligned} \underset{w,v_r,\xi}{\arg\min} \quad & J(w, v_r, \xi) = C \sum_{r=1}^{T} \sum_{i=1}^{m_r} \xi_i^r + \frac{1}{2} \sum_{r=1}^{T} \|v_r\|^2 + \frac{\mu}{2} \|w\|^2 \\ \text{s.t.} \quad & y_i^r (w \cdot \phi(x_i^r) + v_r \cdot \phi_r(x_i^r) + b_r) \geq p_i^r - \xi_i^r, \\ & \xi_i^r \geq 0;\ i = 1, \ldots, m_r,\ r = 1, \ldots, T. \end{aligned} \tag{4.5}$$

The prediction model is then

$$h_r(\boldsymbol{x}) = w \cdot \phi(x_i^r) + v_r \cdot \phi_r(x_i^r) + b_r$$

for regression and

$$h_r(\boldsymbol{x}) = \text{sign}\,(w \cdot \phi(x_i^r) + v_r \cdot \phi_r(x_i^r) + b_r)$$

for classification. Observe again that the transformation ϕ is used for the common part and is shared by all tasks, while the transformation ϕ_r is task-specific.

In (4.5) there are two kind of hyperparameters: C and μ, which, in combination, balance the different parts of the objective function. Hyperparameter C plays the same role than in the standard L1-SVM : it balances the tradeoff between the loss incurred by the model, represented by the hinge variables ξ_i^r and complexity of the models, represented by the norms $\|w\|$ and $\|v_r\|$. Large values of C highly penalize the loss, so the resulting models are more complex because they have to adapt to the training sample distribution, but these models generalize worse. Small values of C penalize more the norms of w and v_r so the resulting models are simpler but not so dependent on the training sample.

Hyperparameter μ, in combination with C, balances the specifity of our models. Large values of μ, penalize the common part, resulting in more specific models; while small values of μ, alongside large values of C, result in a vanishing regularization of the specific parts which leads to common models. We can find the following cases:

- Reduction to an ITL approach:

$$\mu \to \infty \implies h_r(\hat{x}) = v_r \cdot \phi_r(\hat{x}) + b_r.$$

  That is, the models are learned independently because the common part vanishes.

- Reduction to a CTL approach (with task-specific biases):

$$C \to 0, \mu \to 0 \implies h_r(\hat{x}) = w \cdot \phi(\hat{x}) + b_r.$$

  That is, the model for all tasks is common because the specific parts disappear.

- Pure MTL approach:

$$\mu_{\text{inf}} < \mu < \mu_{\text{sup}} \implies h_r(\hat{x}) = (w \cdot \phi(\hat{x})) + (v_r \cdot \phi_r(\hat{x})) + b_r.$$

  There is a range of μ, which is unknown, in which the models combine a common and task-specific part.

Observe that (4.5) is a convex problem. As in the standard case of the L1-SVM, the corresponding dual problem is solved. To obtain the dual problem, it is necessary to express the Lagrangian of problem (4.5),

$$\begin{aligned}
&\mathcal{L}(w, v_1, \ldots, v_T, d_1, \ldots, d_T, \boldsymbol{\xi}, \boldsymbol{\alpha}, \boldsymbol{\beta}) \\
&= C \sum_{r=1}^{T} \sum_{i=1}^{m_r} \xi_i^r + \frac{1}{2} \sum_{r=1}^{T} \|v_r\|^2 + \frac{\mu}{2} \|w\|^2 \\
&\quad - \sum_{r=1}^{T} \sum_{i=1}^{m_r} \alpha_i^r \left\{ y_i^r \left[w \cdot \phi(x_i^r) + v_r \cdot \phi_r(x_i^r) + b_r \right] - p_i^r + \xi_i^r \right\} \\
&\quad - \sum_{r=1}^{T} \sum_{i=1}^{m_r} \beta_i^r \xi_i^r,
\end{aligned} \tag{4.6}$$

where $\alpha_i^r, \beta_i^r \geq 0$ are the Lagrange multipliers. Here $\boldsymbol{\xi}$ represents the vector

$$(\xi_1^1, \ldots, \xi_{m_1}^1, \ldots, \xi_1^T, \ldots, \xi_{m_T}^T)^\intercal$$

and analogously we define $\boldsymbol{\alpha}$ and $\boldsymbol{\beta}$. Recall that the dual objective function is defined as

$$\begin{aligned}
\Theta(\boldsymbol{\alpha}, \boldsymbol{\beta}) &= \min_{w, v_1, \ldots, v_T, b, d_1, \ldots, d_T, \boldsymbol{\xi}} \mathcal{L}(w, v_1, \ldots, v_T, d_1, \ldots, d_T, \boldsymbol{\xi}, \boldsymbol{\alpha}, \boldsymbol{\beta}) \\
&= \mathcal{L}(w^*, {v_1}^*, \ldots, {v_T}^*, {d_1}^*, \ldots, {d_T}^*, \boldsymbol{\xi}^*, \boldsymbol{\alpha}, \boldsymbol{\beta})
\end{aligned}$$

Since $\mathcal{L}$ is convex with respect to the primal variables, it is just necessary to compute the corresponding gradients

$$\nabla_w \mathcal{L}|_{w^*, {v_1}^*, \ldots, {v_T}^*, b^*, {d_1}^*, \ldots, {d_T}^*, \boldsymbol{\xi}^*, \boldsymbol{\alpha}, \boldsymbol{\beta}} = 0 \implies \mu w^* - \sum_{r=1}^{T} \sum_{i=1}^{m_r} \alpha_i^r \left\{ y_i^r \phi(x_i^r) \right\} = 0, \tag{4.7}$$

$$\nabla_{v_r} \mathcal{L}|_{w^*, {v_1}^*, \ldots, {v_T}^*, b^*, {d_1}^*, \ldots, {d_T}^*, \boldsymbol{\xi}^*, \boldsymbol{\alpha}, \boldsymbol{\beta}} = 0 \implies {v_r}^* - \sum_{i=1}^{m_r} \alpha_i^r \left\{ y_i^r \phi_r(x_i^r) \right\} = 0, \tag{4.8}$$

$$\nabla_{b_r} \mathcal{L}|_{w^*, {v_1}^*, \ldots, {v_T}^*, b^*, {d_1}^*, \ldots, {d_T}^*, \boldsymbol{\xi}^*, \boldsymbol{\alpha}, \boldsymbol{\beta}} = 0 \implies \sum_{i=1}^{m_r} \alpha_i^r y_i^r = 0, \tag{4.9}$$

$$\nabla_{\xi_i^r} \mathcal{L}|_{w^*, {v_1}^*, \ldots, {v_T}^*, b^*, {d_1}^*, \ldots, {d_T}^*, \boldsymbol{\xi}^*, \boldsymbol{\alpha}, \boldsymbol{\beta}} = 0 \implies C - \alpha_i^r - \beta_i^r = 0 \tag{4.10}$$

Using these results and substituting back in the Lagrangian we obtain

$$
\begin{aligned}
&\mathcal{L}(w^*, {v_1}^*, \ldots, {v_T}^*, {d_1}^*, \ldots, {d_T}^*, \boldsymbol{\xi}^*, \boldsymbol{\alpha}, \boldsymbol{\beta}) = \\
&= \frac{1}{2}\sum_{r=1}^{T}\left\|\sum_{i=1}^{m_r}\alpha_i^r\left\{y_i^r\phi_r(\boldsymbol{x}_i^r)\right\}\right\|^2 + \frac{\mu}{2}\left\|\frac{1}{\mu}\sum_{r=1}^{T}\sum_{i=1}^{m_r}\alpha_i^r\left\{y_i^r\phi(\boldsymbol{x}_i^r)\right\}\right\|^2 \\
&\quad - \sum_{r=1}^{T}\sum_{i=1}^{m_r}\alpha_i^r\left\{y_i^r\left[\left(\frac{1}{\mu}\sum_{s=1}^{T}\sum_{j=1}^{m_s}\alpha_j^s\left\{y_j^s\phi(\boldsymbol{x}_j^s)\right\}\right)\cdot\phi(\boldsymbol{x}_i^r)\right]\right\} \\
&\quad - \sum_{r=1}^{T}\sum_{i=1}^{m_r}\alpha_i^r\left\{y_i^r\left[\left(\sum_{j=1}^{m_r}\alpha_j^r\left\{y_j^r\phi_r(\boldsymbol{x}_j^r)\right\}\right)\cdot\phi_r(\boldsymbol{x}_i^r)\right]\right\} \\
&\quad - \sum_{r=1}^{T}\sum_{i=1}^{m_r}\alpha_i^r\left\{-p_i^r\right\} \\
&= \frac{1}{2}\sum_{r=1}^{T}\left\langle\sum_{i=1}^{m_r}\alpha_i^r\left\{y_i^r\phi_r(\boldsymbol{x}_i^r)\right\}, \sum_{i=1}^{m_r}\alpha_i^r\left\{y_i^r\phi_r(\boldsymbol{x}_i^r)\right\}\right\rangle \\
&\quad + \frac{\mu}{2}\left\langle\frac{1}{\mu}\sum_{r=1}^{T}\sum_{i=1}^{m_r}\alpha_i^r\left\{y_i^r\phi(\boldsymbol{x}_i^r)\right\}, \frac{1}{\mu}\sum_{r=1}^{T}\sum_{i=1}^{m_r}\alpha_i^r\left\{y_i^r\phi(\boldsymbol{x}_i^r)\right\}\right\rangle \\
&\quad - \frac{1}{\mu}\left\langle\sum_{r=1}^{T}\sum_{i=1}^{m_r}\alpha_i^r\left\{y_i^r\phi(\boldsymbol{x}_i^r)\right\}, \sum_{r=1}^{T}\sum_{i=1}^{m_r}\alpha_i^r\left\{y_i^r\phi(\boldsymbol{x}_i^r)\right\}\right\rangle \\
&\quad - \sum_{r=1}^{T}\left\langle\sum_{i=1}^{m_r}\alpha_i^r\left\{y_i^r\phi_r(\boldsymbol{x}_i^r)\right\}, \sum_{i=1}^{m_r}\alpha_i^r\left\{y_i^r\phi_r(\boldsymbol{x}_i^r)\right\}\right\rangle \\
&\quad - \sum_{r=1}^{T}\sum_{i=1}^{m_r}\alpha_i^r\left\{-p_i^r\right\} \\
&= -\frac{1}{2\mu}\left\langle\sum_{r=1}^{T}\sum_{i=1}^{m_r}\alpha_i^r\left\{y_i^r\phi(\boldsymbol{x}_i^r)\right\}, \sum_{r=1}^{T}\sum_{i=1}^{m_r}\alpha_i^r\left\{y_i^r\phi(\boldsymbol{x}_i^r)\right\}\right\rangle \\
&\quad - \frac{1}{2}\sum_{r=1}^{T}\left\langle\sum_{i=1}^{m_r}\alpha_i^r\left\{y_i^r\phi_r(\boldsymbol{x}_i^r)\right\}, \sum_{i=1}^{m_r}\alpha_i^r\left\{y_i^r\phi_r(\boldsymbol{x}_i^r)\right\}\right\rangle \\
&\quad + \sum_{r=1}^{T}\sum_{i=1}^{m_r}\alpha_i^r p_i^r
\end{aligned}
$$

Observe that $\boldsymbol{\beta}$ has disappeared from the Lagrangian. Then, the dual problem can be defined as $\min_{\boldsymbol{\alpha}}\Theta(\boldsymbol{\alpha})$ where

$$\Theta(\boldsymbol{\alpha}) = -\mathcal{L}(w^*, {v_1}^*, \ldots, {v_T}^*, {d_1}^*, \ldots, {d_T}^*, \boldsymbol{\xi}^*, \boldsymbol{\alpha}, \boldsymbol{\beta}),$$

and $\boldsymbol{\alpha}$ must fulfill the KKT conditions. The condition (4.10), using that $\alpha_i^r, \beta_i^r \geq 0$, implies $0 \leq \alpha_i^r \leq C$. Taking into account these KKT conditions, the dual problem can

be expressed as

$$\begin{aligned}\min_{\alpha} \quad \Theta(\alpha) = \frac{1}{2\mu}\left\langle \sum_{r=1}^{T}\sum_{i=1}^{m_r}\alpha_i^r\left\{y_i^r\phi(\boldsymbol{x}_i^r)\right\}, \sum_{r=1}^{T}\sum_{i=1}^{m_r}\alpha_i^r\left\{y_i^r\phi(\boldsymbol{x}_i^r)\right\}\right\rangle \\ + \frac{1}{2}\sum_{r=1}^{T}\left\langle \sum_{i=1}^{m_r}\alpha_i^r\left\{y_i^r\phi_r(\boldsymbol{x}_i^r)\right\}, \sum_{i=1}^{m_r}\alpha_i^r\left\{y_i^r\phi_r(\boldsymbol{x}_i^r)\right\}\right\rangle - \sum_{r=1}^{T}\sum_{i=1}^{m_r}\alpha_i^r p_i^r \\ \text{s.t.} \qquad 0 \le \alpha_i^r \le C;\ i = 1,\ldots,m_r; r = 1,\ldots,T \\ \sum_{i=1}^{m_r}\alpha_i^r y_i^r = 0; r = 1,\ldots,T.\end{aligned} \tag{4.11}$$

Where there are task-specific equality constraints that have its origin in Equation (4.9). Using the kernel trick, we can write the dual problem using a vector formulation

$$\begin{aligned}\min_{\alpha} \quad \Theta(\alpha) = \frac{1}{2}\boldsymbol{\alpha}^\intercal\left(\frac{1}{\mu}Q + K\right)\boldsymbol{\alpha} - \boldsymbol{p}\boldsymbol{\alpha} \\ \text{s.t.} \quad 0 \le \alpha_i^r \le C;\ i = 1,\ldots,m_r; r = 1,\ldots,T \\ \sum_{i=1}^{m_r}\alpha_i^r y_i^r = 0; r = 1,\ldots,T.\end{aligned} \tag{4.12}$$

Here Q and K are the common and specific kernel matrices, respectively. The matrix Q is generated using the common kernel, defined as

$$k(x_i^r, x_j^s) = \left\langle \phi(x_i^r), \phi(x_j^s)\right\rangle$$

and K is the block-diagonal matrix built using the kernel

$$k_r(x_i^r, x_j^s) = \delta_{rs}\left\langle \phi_r(x_i^r), \phi_s(x_j^s)\right\rangle$$

that is

$$Q = \begin{pmatrix} \underbrace{Q_{1,1}}_{m_1\times m_1} & \underbrace{Q_{1,2}}_{m_1\times m_2} & \underbrace{Q_{1,3}}_{m_1\times m_3} & \cdots & \underbrace{Q_{1,T}}_{m_1\times m_T} \\ \underbrace{Q_{2,1}}_{m_2\times m_1} & \underbrace{Q_{2,2}}_{m_2\times m_2} & \underbrace{Q_{2,1}}_{m_2\times m_1} & \cdots & \underbrace{Q_{2,T}}_{m_2\times m_T} \\ \vdots & \vdots & \vdots & \ddots & \vdots \\ \underbrace{Q_{T,1}}_{m_T\times m_1} & \underbrace{Q_{T,2}}_{m_T\times m_2} & \underbrace{Q_{T,3}}_{m_T\times m_3} & \cdots & \underbrace{Q_{T,T}}_{m_T\times m_T} \end{pmatrix},$$

where each block $Q_{r,s}$

$$Q_{r,s} = \begin{pmatrix} y_1^r y_1^s k(\boldsymbol{x}_1^r, \boldsymbol{x}_1^s) & y_1^r y_2^s k(\boldsymbol{x}_1^r, \boldsymbol{x}_2^s) & \cdots & y_1^r y_{m_s}^s k(\boldsymbol{x}_1^r, \boldsymbol{x}_{m_s}^s) \\ y_2^r y_1^s k(\boldsymbol{x}_2^r, \boldsymbol{x}_1^s) & y_2^r y_2^s k(\boldsymbol{x}_2^r, \boldsymbol{x}_2^s) & \cdots & y_2^r y_{m_s}^s k(\boldsymbol{x}_2^r, \boldsymbol{x}_{m_s}^s) \\ \vdots & \vdots & \ddots & \vdots \\ y_{m_r}^r y_1^s k(\boldsymbol{x}_{m_r}^r, \boldsymbol{x}_1^s) & y_{m_r}^r y_2^s k(\boldsymbol{x}_{m_r}^r, \boldsymbol{x}_2^s) & \cdots & y_{m_r}^r y_{m_s}^s k(\boldsymbol{x}_{m_r}^r, \boldsymbol{x}_{m_s}^s) \end{pmatrix}; \tag{4.13}$$

and

$$K = \begin{pmatrix} \underbrace{K_{1,1}}_{m_1 \times m_1} & \underbrace{0}_{m_1 \times m_2} & \underbrace{0}_{m_1 \times m_3} & \cdots & \underbrace{0}_{m_1 \times m_T} \\ \underbrace{0}_{m_2 \times m_1} & \underbrace{K_{2,2}}_{m_2 \times m_2} & \underbrace{0}_{m_2 \times m_1} & \cdots & \underbrace{0}_{m_2 \times m_T} \\ \vdots & \vdots & \vdots & \ddots & \vdots \\ \underbrace{0}_{m_T \times m_1} & \underbrace{0}_{m_T \times m_2} & \underbrace{0}_{m_T \times m_3} & \cdots & \underbrace{K_{T,T}}_{m_T \times T} \end{pmatrix},$$

where for each task block K_r we have

$$K_{r,r} = \begin{pmatrix} y_1^r y_1^r k_r(\boldsymbol{x}_1^r, \boldsymbol{x}_1^r) & y_1^r y_2^r k_r(\boldsymbol{x}_1^r, \boldsymbol{x}_2^r) & \cdots & y_1^r y_{m_s}^r k_r(\boldsymbol{x}_1^r, \boldsymbol{x}_{m_r}^r) \\ y_2^r y_1^r k_r(\boldsymbol{x}_2^r, \boldsymbol{x}_1^r) & y_2^r y_2^r k_r(\boldsymbol{x}_2^r, \boldsymbol{x}_2^r) & \cdots & y_2^r y_{m_s}^r k_r(\boldsymbol{x}_2^r, \boldsymbol{x}_{m_r}^r) \\ \vdots & \vdots & \ddots & \vdots \\ y_{m_r}^r y_1^r k_r(\boldsymbol{x}_{m_r}^r, \boldsymbol{x}_1^r) & y_{m_r}^r y_2^r k_r(\boldsymbol{x}_{m_r}^r, \boldsymbol{x}_2^r) & \cdots & y_{m_r}^r y_{m_s}^r k_r(\boldsymbol{x}_{m_r}^r, \boldsymbol{x}_{m_r}^r) \end{pmatrix}. \quad (4.14)$$

Combined, we have a multi-task kernel matrix $\widehat{Q} = (1/\mu)Q + K$, whose corresponding multi-task kernel function can be expressed as

$$\widehat{k}(\boldsymbol{x}_i^r, \boldsymbol{x}_j^s) = \frac{1}{\mu} k(\boldsymbol{x}_i^r, \boldsymbol{x}_j^s) + \delta_{rs} k_r(\boldsymbol{x}_i^r, \boldsymbol{x}_j^s).$$

Here we are using two different kernels: a common one $k(x, \tilde{x})$ and a task-specific one $k_r(x, \tilde{x})$, each being the reproducing kernels for the common and task-specific transformations, respectively. That is, $k(x, \tilde{x}) = \langle \phi(x), \phi(\tilde{x}) \rangle$ and $k_r(x, \tilde{x}) = \langle \phi_r(x), \phi_r(\tilde{x}) \rangle$.

The dual problem (4.12) is very similar to the standard one but we have two major differences: the use of the multi-task kernel matrix $\widehat{Q}$ and the multiple equality constraints. These constraints, which appear in (4.9) are consequence of the specific biases used in the primal problem (4.5). In Cai and Cherkassky (2012) the authors develop a Generalized SMO algorithm to account for these multiple equality constraints.

Analyzing the hyperparameters influence in the dual problem, note that C is an upper bound for the dual coefficients, as in the standard case, but with a different bound for each task; and, the hyperparameter of interest for this MTL formulation, which is μ, scales the common matrix Q. As with the primal formulation, we can define three different cases:

- Reduction to an ITL approach:

$$\mu \to \infty \implies h_r(\hat{x}) = \sum_{i=1}^{m_r} \alpha_i^r y_i^r \{k_r(x_i^r, \hat{x})\} + b_r.$$

  That is the matrix is block-diagonal and optimizing the dual problem is equivalent to optimizing a specific dual problem for each task.

- Reduction to a CTL approach (with task-specific biases):

$$C \to 0, \mu \to 0 \implies h_r(\hat{x}) = \sum_{r=1}^{T} \sum_{i=1}^{m_r} \alpha_i^r y_i^r \{k(x_i^r, \hat{x})\} + b_r.$$

  That is the dual objective function is the standard one for common task learning.

- Pure MTL approach:

$$\mu_{\text{inf}} < \mu < \mu_{\text{sup}} \implies h_r(\hat{x}) = \sum_{r=1}^{T}\sum_{i=1}^{m_r} \alpha_i^r y_i^r \left\{ \frac{1}{\mu} k(x_i^r, \hat{x}) + k_r(x_i^r, \hat{x}) \right\} + b_r.$$

  There is a range of μ, which is unknown, in which the kernel matrix combines the common and specific matrices.

Convex MTL L1-SVM.
The convex MTL primal problem formulation, presented in Ruiz et al. (2019), changes the formulation of the additive MTL SVM but changes its formulation for a convex one that is more interpretable one. The primal problem is

$$\begin{aligned} \underset{w,v_r,\xi}{\arg\min} \quad & J(w, v_r, \xi) = C \sum_{r=1}^{T}\sum_{i=1}^{m_r} \xi_i^r + \frac{1}{2}\sum_{r=1}^{T} \|v_r\|^2 + \frac{1}{2}\|w\|^2 \\ \text{s.t.} \quad & y_i^r \left(\lambda_r \left\{w \cdot \phi(x_i^r) + b\right\} + (1-\lambda_r)\left\{v_r \cdot \phi_r(x_i^r) + b_r\right\}\right) \geq p_i^r - \xi_i^r, \\ & \xi_i^r \geq 0;\ i = 1, \ldots, m_r,\ r = 1, \ldots, T. \end{aligned} \tag{4.15}$$

Here, the former hyperparameter μ used in the regularization is replaced by the hyperparameters λ_r, which are used in the model definition. The prediction model is then

$$h_r(\boldsymbol{x}) = \lambda_r \left\{w \cdot \phi(x_i^r) + b\right\} + (1-\lambda_r)\left\{v_r \cdot \phi_r(x_i^r) + b_r\right\}$$

for regression and

$$h_r(\boldsymbol{x}) = \text{sign}\left(\lambda_r \left\{w \cdot \phi(x_i^r) + b\right\} + (1-\lambda_r)\left\{v_r \cdot \phi_r(x_i^r) + b_r\right\}\right)$$

for classification.

With this convex formulation, the roles of hyperparameters C and λ_r are independent. Hyperparameter C regulates the trade-off between the loss and the margin size of each task-specialized model h_r, while λ_r indicates how specific or common these models are in the range of $[0, 1]$. With $\lambda_r = 0$ we have independent models for each task and for $\lambda_r = 1$ we have a common model for all tasks. In (4.15), depending on the value of hyperparameters C, $\lambda_1, \ldots, \lambda_T$, we can highlight the following situations:

- Reduction to an ITL approach:

$$\lambda_r = 0; r = 1, \ldots, T \implies h_r(\hat{x}) = v_r \cdot \phi_r(\hat{x}) + b_r.$$

- Reduction to a CTL approach:

$$\lambda_r = 1; r = 1, \ldots, T \implies h_r(\hat{x}) = w \cdot \phi(\hat{x}) + b.$$

- Pure MTL approach:

$$0 < \lambda_r < 1; r = 1, \ldots, T \implies h_r(\hat{x}) = \lambda_r(w \cdot \phi(\hat{x}) + b) + (1-\lambda_r)(v_r \cdot \phi_r(\hat{x}) + b_r).$$

Observe that now the cases are not asymptotical but have attainable values, 0 for ITL and 1 for MTL, while all the values in the open $(0, 1)$ yield pure MTL models. Also, the

parameter C no longer interferes with these cases and only λ_r calibrates the specifity of the models. The Lagrangian of problem (4.15) is

$$\begin{aligned}
&\mathcal{L}(w, v_1, \ldots, v_T, b, d_1, \ldots, d_T, \boldsymbol{\xi}, \boldsymbol{\alpha}, \boldsymbol{\beta}) \\
&= C \sum_{r=1}^{T} \sum_{i=1}^{m_r} \xi_i^r + \frac{1}{2} \sum_{r=1}^{T} \|v_r\|^2 + \frac{1}{2} \|w\|^2 \\
&\quad - \sum_{r=1}^{T} \sum_{i=1}^{m_r} \alpha_i^r \left\{ y_i^r \left(\lambda_r \left\{ w \cdot \phi(x_i^r) + b \right\} + (1 - \lambda_r) \left\{ v_r \cdot \phi_r(x_i^r) + b_r \right\} \right) - p_i^r + \xi_i^r \right\} \\
&\quad - \sum_{r=1}^{T} \sum_{i=1}^{m_r} \beta_i^r \xi_i^r,
\end{aligned} \tag{4.16}$$

where $\alpha_i^r, \beta_i^r \geq 0$ are the Lagrange multipliers. Again, $\boldsymbol{\xi}$ represents the vector

$$(\xi_1^1, \ldots, \xi_{m_1}^1, \ldots, \xi_1^T, \ldots, \xi_{m_T}^T)^\intercal$$

and analogously for $\boldsymbol{\alpha}$ and $\boldsymbol{\beta}$.The dual objective function is defined as

$$\begin{aligned}
\Theta(\boldsymbol{\alpha}, \boldsymbol{\beta}) &= \min_{w, v_1, \ldots, v_T, b, d_1, \ldots, d_T, \boldsymbol{\xi}} \mathcal{L}(w, v_1, \ldots, v_T, b, d_1, \ldots, d_T, \boldsymbol{\xi}, \boldsymbol{\alpha}, \boldsymbol{\beta}) \\
&= \mathcal{L}(w^*, {v_1}^*, \ldots, {v_T}^*, b^*, {d_1}^*, \ldots, {d_T}^*, \boldsymbol{\xi}^*, \boldsymbol{\alpha}, \boldsymbol{\beta})
\end{aligned}$$

The gradients with respect to the primal variables are

$$\nabla_w \mathcal{L}|_{w^*, {v_1}^*, \ldots, {v_T}^*, b^*, {d_1}^*, \ldots, {d_T}^*, \boldsymbol{\xi}^*, \boldsymbol{\alpha}, \boldsymbol{\beta}} = 0 \implies w^* - \sum_{r=1}^{T} \lambda_r \sum_{i=1}^{m_r} \alpha_i^r \left\{ y_i^r \phi(x_i^r) \right\} = 0, \tag{4.17}$$

$$\nabla_{v_r} \mathcal{L}|_{w^*, {v_1}^*, \ldots, {v_T}^*, b^*, {d_1}^*, \ldots, {d_T}^*, \boldsymbol{\xi}^*, \boldsymbol{\alpha}, \boldsymbol{\beta}} = 0 \implies {v_r}^* - (1 - \lambda_r) \sum_{i=1}^{m_r} \alpha_i^r \left\{ y_i^r \phi_r(x_i^r) \right\} = 0, \tag{4.18}$$

$$\nabla_b \mathcal{L}|_{w^*, {v_1}^*, \ldots, {v_T}^*, b^*, {d_1}^*, \ldots, {d_T}^*, \boldsymbol{\xi}^*, \boldsymbol{\alpha}, \boldsymbol{\beta}} = 0 \implies \sum_{r=1}^{T} \sum_{i=1}^{m_r} \alpha_i^r y_i^r = 0, \tag{4.19}$$

$$\nabla_{d_r} \mathcal{L}|_{w^*, {v_1}^*, \ldots, {v_T}^*, b^*, {d_1}^*, \ldots, {d_T}^*, \boldsymbol{\xi}^*, \boldsymbol{\alpha}, \boldsymbol{\beta}} = 0 \implies \sum_{i=1}^{m_r} \alpha_i^r y_i^r = 0, \tag{4.20}$$

$$\nabla_{\xi_i^r} \mathcal{L}|_{w^*, {v_1}^*, \ldots, {v_T}^*, b^*, {d_1}^*, \ldots, {d_T}^*, \boldsymbol{\xi}^*, \boldsymbol{\alpha}, \boldsymbol{\beta}} = 0 \implies C - \alpha_i^r - \beta_i^r = 0 \tag{4.21}$$

Using these results and substituting back in the Lagrangian we obtain

$$
\begin{aligned}
&\mathcal{L}(w^*, {v_1}^*, \ldots, {v_T}^*, b^*, {d_1}^*, \ldots, {d_T}^*, \boldsymbol{\xi}^*, \boldsymbol{\alpha}, \boldsymbol{\beta}) \\
&\quad= \frac{1}{2}\sum_{r=1}^{T}\left\|(1-\lambda_r)\sum_{i=1}^{m_r}\alpha_i^r\left\{y_i^r\phi_r(\boldsymbol{x}_i^r)\right\}\right\|^2 + \frac{1}{2}\left\|\sum_{r=1}^{T}\lambda_r\sum_{i=1}^{m_r}\alpha_i^r\left\{y_i^r\phi(\boldsymbol{x}_i^r)\right\}\right\|^2 \\
&\qquad- \sum_{r=1}^{T}\lambda_r\sum_{i=1}^{m_r}\alpha_i^r\left\{y_i^r\left[\left(\sum_{s=1}^{T}\lambda_r\sum_{j=1}^{m_s}\alpha_j^s\left\{y_j^s\phi(\boldsymbol{x}_j^s)\right\}\right)\cdot\phi(\boldsymbol{x}_i^r)\right]\right\} \\
&\qquad- \sum_{r=1}^{T}(1-\lambda_r)\sum_{i=1}^{m_r}\alpha_i^r\left\{y_i^r\left[\left((1-\lambda_r)\sum_{j=1}^{m_r}\alpha_j^r\left\{y_j^r\phi_r(\boldsymbol{x}_j^r)\right\}\right)\cdot\phi_r(\boldsymbol{x}_i^r)\right]\right\} \\
&\qquad- \sum_{r=1}^{T}\sum_{i=1}^{m_r}\alpha_i^r\left\{-p_i^r\right\} \\
&\quad= \frac{1}{2}\sum_{r=1}^{T}\left\langle(1-\lambda_r)\sum_{i=1}^{m_r}\alpha_i^r\left\{y_i^r\phi_r(\boldsymbol{x}_i^r)\right\}, (1-\lambda_r)\sum_{i=1}^{m_r}\alpha_i^r\left\{y_i^r\phi_r(\boldsymbol{x}_i^r)\right\}\right\rangle \\
&\qquad+ \frac{1}{2}\left\langle\sum_{r=1}^{T}\lambda_r\sum_{i=1}^{m_r}\alpha_i^r\left\{y_i^r\phi(\boldsymbol{x}_i^r)\right\}, \sum_{r=1}^{T}\lambda_r\sum_{i=1}^{m_r}\alpha_i^r\left\{y_i^r\phi(\boldsymbol{x}_i^r)\right\}\right\rangle \\
&\qquad- \left\langle\sum_{r=1}^{T}\lambda_r\sum_{i=1}^{m_r}\alpha_i^r\left\{y_i^r\phi(\boldsymbol{x}_i^r)\right\}, \sum_{r=1}^{T}\lambda_r\sum_{i=1}^{m_r}\alpha_i^r\left\{y_i^r\phi(\boldsymbol{x}_i^r)\right\}\right\rangle \\
&\qquad- \sum_{r=1}^{T}\left\langle(1-\lambda_r)\sum_{i=1}^{m_r}\alpha_i^r\left\{y_i^r\phi_r(\boldsymbol{x}_i^r)\right\}, (1-\lambda_r)\sum_{i=1}^{m_r}\alpha_i^r\left\{y_i^r\phi_r(\boldsymbol{x}_i^r)\right\}\right\rangle \\
&\qquad- \sum_{r=1}^{T}\sum_{i=1}^{m_r}\alpha_i^r\left\{-p_i^r\right\} \\
&\quad= -\frac{1}{2}\left\langle\sum_{r=1}^{T}\lambda_r\sum_{i=1}^{m_r}\alpha_i^r\left\{y_i^r\phi(\boldsymbol{x}_i^r)\right\}, \sum_{r=1}^{T}\lambda_r\sum_{i=1}^{m_r}\alpha_i^r\left\{y_i^r\phi(\boldsymbol{x}_i^r)\right\}\right\rangle \\
&\qquad- \frac{1}{2}\sum_{r=1}^{T}(1-\lambda_r)\left\langle\sum_{i=1}^{m_r}\alpha_i^r\left\{y_i^r\phi_r(\boldsymbol{x}_i^r)\right\}, (1-\lambda_r)\sum_{i=1}^{m_r}\alpha_i^r\left\{y_i^r\phi_r(\boldsymbol{x}_i^r)\right\}\right\rangle \\
&\qquad+ \sum_{r=1}^{T}\sum_{i=1}^{m_r}\alpha_i^r p_i^r
\end{aligned}
$$

As with the additive formulation, the dual problem can then be defined as

$$\begin{aligned}\min_{\alpha} \quad \Theta(\alpha) = &\frac{1}{2}\left\langle \sum_{r=1}^{T}\lambda_r \sum_{i=1}^{m_r}\alpha_i^r \left\{y_i^r \phi(\boldsymbol{x}_i^r)\right\}, \sum_{r=1}^{T}\lambda_r \sum_{i=1}^{m_r}\alpha_i^r \left\{y_i^r \phi(\boldsymbol{x}_i^r)\right\}\right\rangle \\ &+ \frac{1}{2}\sum_{r=1}^{T}\left\langle (1-\lambda_r)\sum_{i=1}^{m_r}\alpha_i^r \left\{y_i^r \phi_r(\boldsymbol{x}_i^r)\right\}, (1-\lambda_r)\sum_{i=1}^{m_r}\alpha_i^r \left\{y_i^r \phi_r(\boldsymbol{x}_i^r)\right\}\right\rangle \\ &- \sum_{r=1}^{T}\sum_{i=1}^{m_r}\alpha_i^r p_i^r \\ \text{s.t.} \quad & 0 \leq \alpha_i^r \leq C;\ i = 1, \ldots, m_r; r = 1, \ldots, T \\ & \sum_{i=1}^{m_r}\alpha_i^r y_i^r = 0; r = 1, \ldots, T.\end{aligned} \tag{4.22}$$

And the vector formulation using the kernel matrices is

$$\begin{aligned}\min_{\alpha} \quad & \Theta(\alpha) = \frac{1}{2}\boldsymbol{\alpha}^{\intercal}\left(\Lambda Q \Lambda + (I_n - \Lambda) K (I_n - \Lambda)\right)\boldsymbol{\alpha} - \boldsymbol{p}\boldsymbol{\alpha} \\ \text{s.t.} \quad & 0 \leq \alpha_i^r \leq C;\ i = 1, \ldots, m_r; r = 1, \ldots, T \\ & \sum_{i=1}^{m_r}\alpha_i^r y_i^r = 0; r = 1, \ldots, T.\end{aligned} \tag{4.23}$$

where

$$\Lambda = \operatorname{diag}(\lambda_1, \ldots, \lambda_T)$$

and I_n is the $n \times n$ identity matrix. Here Q and K are the common and specific kernel matrices, respectively. Combined, we have a multi-task kernel matrix

$$\widehat{Q} = \Lambda Q \Lambda + (I_n - \Lambda) K (I_n - \Lambda), \tag{4.24}$$

whose corresponding multi-task kernel function can be expressed as

$$\widehat{k}(\boldsymbol{x}_i^r, \boldsymbol{x}_j^s) = \lambda_r^2 k(\boldsymbol{x}_i^r, \boldsymbol{x}_j^s) + \delta_{rs}(1-\lambda_r)^2 k_r(\boldsymbol{x}_i^r, \boldsymbol{x}_j^s), \tag{4.25}$$

where again we are using the common kernel $k(x, \tilde{x}) = \langle \phi(x), \phi(\tilde{x}) \rangle$ and task-specific kernels $k_r(x, \tilde{x}) = \langle \phi_r(x), \phi_r(\tilde{x}) \rangle$ for $r = 1, \ldots, T$. Then, we can define the kernel matrix as

$$\widehat{Q} = \begin{bmatrix} y_1^1 y_1^1 \widehat{k}(x_1^1, x_1^1) & y_1^1 y_2^1 \widehat{k}(x_1^1, x_2^1) & \ldots & y_1^1 y_{m_T}^T \widehat{k}(x_1^1, x_{m_T}^T) \\ y_2^1 y_1^1 \widehat{k}(x_2^1, x_1^1) & y_2^1 y_2^1 \widehat{k}(x_2^1, x_2^1) & \ldots & y_2^1 y_{m_T}^T \widehat{k}(x_2^1, x_{m_T}^T) \\ \vdots & \vdots & \ddots & \vdots \\ y_{m_T}^T y_1^1 \widehat{k}(x_{m_T}^T, x_1^1) & y_{m_T}^T y_2^1 \widehat{k}(x_{m_T}^T, x_2^1) & \ldots & y_{m_T}^T y_{m_T}^T \widehat{k}(x_{m_T}^T, x_{m_T}^T) \end{bmatrix}.$$

This dual problem is very similar to the one shown in (4.12) where there are also T equality constraints, but the multi-task kernel matrix $\widehat{Q}$ is defined differently, dropping the μ hyperparameter and incorporating the λ_r ones. Studying the influence of λ_r hyperparameters in the dual problem we can describe the following cases:

- Reduction to an ITL approach:

$$\lambda_r = 0; r = 1, \ldots, T \implies h_r(\hat{x}) = \sum_{r=1}^{T} \sum_{i=1}^{m_r} \alpha_i^r y_i^r \left\{k_r(x_i^r, \hat{x})\right\} + b_r.$$

- Reduction to a CTL approach:

$$\lambda_r = 1; r = 1, \ldots, T \implies h_r(\hat{x}) = \sum_{r=1}^{T} \sum_{i=1}^{m_r} \alpha_i^r y_i^r \left\{k(x_i^r, \hat{x})\right\} + b.$$

- Pure MTL approach:

$$0 < \lambda_r < 1; r = 1, \ldots, T \implies$$
$$h_r(\hat{x}) = \sum_{r=1}^{T} \sum_{i=1}^{m_r} \alpha_i^r y_i^r \left\{\lambda_r^2 k(x_i^r, \hat{x}) + (1-\lambda_r)^2 k_r(x_i^r, \hat{x})\right\} + \lambda_r b + (1-\lambda_r) b_r.$$

The properties that are found in the primal formulation are also present in the dual one. All the values of λ_r in the open interval $(0, 1)$ correspond to pure MTL approaches while the extreme values $\lambda_r = 1$ and $\lambda_r = 0$ correspond to CTL and ITL approaches, respectively.

Equivalence Results.
Both the additive and convex MTL SVM approaches solve a similar problem, but there is a change in the formulation to get rid of a regularization hyperparameter μ in favor of those defining convex combination of models, hyperparameters λ_r. Both approaches offer similar properties: ranging the value of their hyperparameters to go from completely common to completely independent models, and passing through pure multi-task models. However, it is not obvious what is the relation between those two approaches. In Ruiz et al. (2019) we provide two propositions to show the equivalence between additive and convex MTL SVM formulations.

Proposition 1. The additive MTL-SVM primal problem with parameters C_{add} and μ (and possibly ϵ), that is,

$$\begin{aligned} \underset{w, v_r, \xi}{\arg\min} \quad & J(w, v_r, \xi) = C_{\text{add}} \sum_{r=1}^{T} \sum_{i=1}^{m_r} \xi_i^r + \frac{1}{2} \sum_{r=1}^{T} \|v_r\|^2 + \frac{\mu}{2} \|w\|^2 \\ \text{s.t.} \quad & y_i^r (w \cdot \phi(x_i^r) + b + v_r \cdot \phi_r(x_i^r) + b_r) \geq p_i^r - \xi_i^r, \\ & \xi_i^r \geq 0;\ i = 1, \ldots, m_r,\ r = 1, \ldots, T, \end{aligned} \tag{4.26}$$

and the convex MTL-SVM primal problem with parameters C_{conv} and $\lambda_1 = \ldots = \lambda_T = \lambda$ (and possibly ϵ), that is,

$$\begin{aligned} \underset{u, u_r, \xi}{\arg\min} \quad & J(u, u_r, \xi) = C_{\text{conv}} \sum_{r=1}^{T} \sum_{i=1}^{m_r} \xi_i^r + \frac{1}{2} \sum_{r=1}^{T} \|u_r\|^2 + \frac{1}{2} \|u\|^2 \\ \text{s.t.} \quad & y_i^r \left(\lambda \left\{u \cdot \phi(x_i^r) + \hat{b}\right\} + (1-\lambda) \left\{u_r \cdot \phi_r(x_i^r) + \hat{d}_r\right\}\right) \geq p_i^r - \xi_i^r, \\ & \xi_i^r \geq 0;\ i = 1, \ldots, m_r,\ r = 1, \ldots, T. \end{aligned} \tag{4.27}$$

where $\lambda \in (0,1)$, are equivalent when $C_{\text{add}} = (1-\lambda)^2 C_{\text{conv}}$ and $\mu = (1-\lambda)^2/\lambda^2$.

Proof. Making the change of variables $w = \lambda u$, $v_r = (1-\lambda)u_r$ and $b_r = \lambda\hat{b} + (1-\lambda)\hat{b_r}$ in the convex primal problem (4.27), we can write it as

$$\begin{aligned}
\underset{w,v_r,\xi}{\arg\min} \quad & J(w, v_r, \xi) = C_{\text{conv}} \sum_{t=1}^{T} \sum_{i=1}^{m_r} \xi_i^r + \frac{1}{2(1-\lambda)^2} \sum_{t=1}^{T} \|v_r\|^2 + \frac{1}{2\lambda^2}\|w\|^2 \\
\text{s.t.} \quad & y_i^r (w \cdot \phi(x_i^r) + v_r \cdot \phi_r(x_i^r) + b_r) \geq p_i^r - \xi_i^r, \\
& \xi_i^r \geq 0, \\
& i = 1, \ldots, m_r, \ t = 1, \ldots, T,
\end{aligned}$$

Multiplying now the objective function by $(1-\lambda)^2$ we obtain the additive MTL-SVM primal problem (4.26) with $\mu = (1-\lambda)^2/\lambda^2$ and $C_{\text{add}} = (1-\lambda)^2 C_{\text{conv}}$. Conversely, we can start at the primal additive problem and make the inverse changes to arrive now to the primal convex problem. □

The previous proposition shows the equivalence between the primal problems, but this result can also be obtained from the dual problems. Consider the dual problem of the convex formulation when $\lambda_1 = \ldots = \lambda_T = \lambda$, and multiplying the objective function by $\frac{1}{(1-\lambda)^2} > 0$ we get

$$\begin{aligned}
\min_{\boldsymbol{\alpha}} \quad & \Theta(\boldsymbol{\alpha}) = \frac{1}{2}\boldsymbol{\alpha}^\intercal \left(\frac{\lambda^2}{(1-\lambda)^2} Q + \frac{(1-\lambda)^2}{(1-\lambda)^2} K \right) \boldsymbol{\alpha} - \frac{1}{(1-\lambda)^2} \boldsymbol{p}\boldsymbol{\alpha} \\
\text{s.t.} \quad & 0 \leq \alpha_i^r \leq C_{\text{conv}}; \ i = 1, \ldots, m_r; r = 1, \ldots, T \\
& \sum_{i=1}^{m_r} \alpha_i^r y_i^r = 0; r = 1, \ldots, T.
\end{aligned} \tag{4.28}$$

Now consider the change of variables $\boldsymbol{\beta} = (1-\lambda)^2\boldsymbol{\alpha}$, then we obtain the problem

$$\begin{aligned}
\min_{\boldsymbol{\beta}} \quad & \Theta(\boldsymbol{\beta}) = \frac{1}{2}\frac{1}{(1-\lambda)^2}\boldsymbol{\beta}^\intercal \left(\frac{\lambda^2}{(1-\lambda)^2} Q + \frac{(1-\lambda)^2}{(1-\lambda)^2} K \right) \frac{1}{(1-\lambda)^2}\boldsymbol{\beta} - \frac{1}{(1-\lambda)^4} \boldsymbol{p}\boldsymbol{\beta} \\
\text{s.t.} \quad & 0 \leq \beta_i^r \leq (1-\lambda)^2 C_{\text{conv}}; \ i = 1, \ldots, m_r; r = 1, \ldots, T \\
& \sum_{i=1}^{m_r} \alpha_i^r y_i^r = 0; r = 1, \ldots, T,
\end{aligned}$$

if we consider again $\mu = (1-\lambda)^2/\lambda^2$ and $C_{\text{add}} = (1-\lambda)^2 C_{\text{conv}}$ and multiply the objective function by $(1-\lambda)^4$ we get the equivalent problem

$$\begin{aligned}
\min_{\boldsymbol{\beta}} \quad & \Theta(\boldsymbol{\beta}) = \frac{1}{2}\boldsymbol{\beta}^\intercal \left(\frac{1}{\mu} Q + K \right) \boldsymbol{\beta} - \boldsymbol{p}\boldsymbol{\beta} \\
\text{s.t.} \quad & 0 \leq \beta_i^r \leq C_{\text{add}}; \ i = 1, \ldots, m_r; r = 1, \ldots, T \\
& \sum_{i=1}^{m_r} \alpha_i^r y_i^r = 0; r = 1, \ldots, T,
\end{aligned}$$

which is the dual problem of the additive formulation.

Finally, observe that the results in Proposition 1 is only valid for λ in the open set $(0,1)$. The results in the extremes of the interval, i.e. $\lambda = 0, 1$, have been already exposed.

When $\lambda = 0$, we obtain an ITL approach, where an independent model is learned for each task. When $\lambda = 1$, the convex formulation is equivalent to a CTL approach, where a single, common model is trained using all tasks.

4.2.2 Extensions to L2 and LS-SVM

The L2-SVM Burges (1998) is a variant of the standard SVM where the hinge loss is replaced by the squared hinge loss in the case of a classification setting, and the epsilon-insensitive loss by the corresponding squared version in the case of regression problems. In both settings a margin where the errors are not penalized is kept, but the errors which are larger than such margin are penalized using its squared value.

The LS-SVM (Suykens and Vandewalle, 1999) is another variant of the standard SVM where the epsilon-insensitive loss is replaced by the squared loss in the case of regression problems, and for classification a regression is made for the negative and positive class.

In this subsection an extension of the convex MTL formulation to both L2 and LS-SVM is presented.

Convex MTL L2-SVM.
The primal problem for the convex MTL L2-SVM, presented in Ruiz et al. (2021), is

$$\begin{aligned} \underset{w,v_r,\xi}{\arg\min} \quad & J(w, v_r, \xi) = \frac{C}{2} \sum_{r=1}^{T} \sum_{i=1}^{m_r} \xi_i^{r\,2} + \frac{1}{2} \sum_{r=1}^{T} \|v_r\|^2 + \frac{1}{2} \|w\|^2 \\ \text{s.t.} \quad & y_i^r \left(\lambda_r \left\{w \cdot \phi(x_i^r) + b\right\} + (1 - \lambda_r) \left\{v_r \cdot \phi_r(x_i^r) + b_r\right\}\right) \geq p_i^r - \xi_i^r . \end{aligned} \tag{4.29}$$

The prediction model is again

$$h_r(\boldsymbol{x}) = \lambda_r \left\{w \cdot \phi(x_i^r) + b\right\} + (1 - \lambda_r) \left\{v_r \cdot \phi_r(x_i^r) + b_r\right\}$$

for regression and

$$h_r(\boldsymbol{x}) = \operatorname{sign} \left(\lambda_r \left\{w \cdot \phi(x_i^r) + b\right\} + (1 - \lambda_r) \left\{v_r \cdot \phi_r(x_i^r) + b_r\right\}\right)$$

for classification.

As in the standard variant, hyperparameter C regulates the trade-off between the loss and the margin size of each task-specialized model h_r, while λ_r indicates how specific or common these models are in the range of $[0, 1]$. With $\lambda_1, \ldots, \lambda_T = 0$ we have independent models for each task and for $\lambda_1, \ldots, \lambda_T = 1$ we have a common model for all tasks.

To obtain the dual problem the Lagrangian of problem (4.29):

$$\begin{aligned} & \mathcal{L}(w, v_1, \ldots, v_T, b, d_1, \ldots, d_T, \boldsymbol{\xi}, \boldsymbol{\alpha}) \\ & = \frac{C}{2} \sum_{r=1}^{T} \sum_{i=1}^{m_r} (\xi_i^r)^2 + \frac{1}{2} \sum_{r=1}^{T} \|v_r\|^2 + \frac{1}{2} \|w\|^2 \\ & \quad - \sum_{r=1}^{T} \sum_{i=1}^{m_r} \alpha_i^r \left\{y_i^r \left(\lambda_r \left\{w \cdot \phi(x_i^r) + b\right\} + (1 - \lambda_r) \left\{v_r \cdot \phi_r(x_i^r) + b_r\right\}\right) - p_i^r + \xi_i^r\right\}, \end{aligned} \tag{4.30}$$

where $\alpha_i^r \geq 0$ are the Lagrange multipliers. Again, $\boldsymbol{\xi}$ represents the vector

$$(\xi_1^1, \ldots, \xi_{m_1}^1, \ldots, \xi_1^T, \ldots, \xi_{m_T}^T)^\intercal$$

and analogously for $\boldsymbol{\alpha}$. The dual objective function is defined as

$$\begin{aligned}\Theta(\boldsymbol{\alpha}) &= \min_{w,v_1,\ldots,v_T,b,d_1,\ldots,d_T,\boldsymbol{\xi}} \mathcal{L}(w, v_1, \ldots, v_T, b, d_1, \ldots, d_T, \boldsymbol{\xi}, \boldsymbol{\alpha}) \\ &= \mathcal{L}(w^*, {v_1}^*, \ldots, {v_T}^*, b^*, {d_1}^*, \ldots, {d_T}^*, \boldsymbol{\xi}^*, \boldsymbol{\alpha})\end{aligned}$$

The gradients with respect to the primal variables are

$$\nabla_w \mathcal{L}|_{w^*,{v_1}^*,\ldots,{v_T}^*,b^*,{d_1}^*,\ldots,{d_T}^*,\boldsymbol{\xi}^*,\boldsymbol{\alpha}} = 0 \implies w^* - \sum_{r=1}^{T} \lambda_r \sum_{i=1}^{m_r} \alpha_i^r \{y_i^r \phi(x_i^r)\} = 0, \tag{4.31}$$

$$\nabla_{v_r} \mathcal{L}|_{w^*,{v_1}^*,\ldots,{v_T}^*,b^*,{d_1}^*,\ldots,{d_T}^*,\boldsymbol{\xi}^*,\boldsymbol{\alpha}} = 0 \implies {v_r}^* - (1-\lambda_r) \sum_{i=1}^{m_r} \alpha_i^r \{y_i^r \phi_r(x_i^r)\} = 0, \tag{4.32}$$

$$\nabla_b \mathcal{L}|_{w^*,{v_1}^*,\ldots,{v_T}^*,b^*,{d_1}^*,\ldots,{d_T}^*,\boldsymbol{\xi}^*,\boldsymbol{\alpha}} = 0 \implies \sum_{r=1}^{T} \sum_{i=1}^{m_r} \alpha_i^r y_i^r = 0, \tag{4.33}$$

$$\nabla_{d_r} \mathcal{L}|_{w^*,{v_1}^*,\ldots,{v_T}^*,b^*,{d_1}^*,\ldots,{d_T}^*,\boldsymbol{\xi}^*,\boldsymbol{\alpha}} = 0 \implies \sum_{i=1}^{m_r} \alpha_i^r y_i^r = 0, \tag{4.34}$$

$$\nabla_{\xi_i^r} \mathcal{L}|_{w^*,{v_1}^*,\ldots,{v_T}^*,b^*,{d_1}^*,\ldots,{d_T}^*,\boldsymbol{\xi}^*,\boldsymbol{\alpha}} = 0 \implies C\xi_i^r - \alpha_i^r = 0. \tag{4.35}$$

Using these results and substituting back in the Lagrangian we obtain

$$
\begin{aligned}
&\mathcal{L}(w^*, {v_1}^*, \ldots, {v_T}^*, b^*, {d_1}^*, \ldots, {d_T}^*, \boldsymbol{\xi}^*, \boldsymbol{\alpha}) \\
&\quad = \frac{C}{2}\frac{1}{C^2}\sum_{r=1}^{T}\sum_{i=1}^{m_r}(\alpha_i^r)^2 \\
&\qquad + \frac{1}{2}\sum_{r=1}^{T}\left\|(1-\lambda_r)\sum_{i=1}^{m_r}\alpha_i^r\left\{y_i^r\phi_r(\boldsymbol{x}_i^r)\right\}\right\|^2 + \frac{1}{2}\left\|\sum_{r=1}^{T}\lambda_r\sum_{i=1}^{m_r}\alpha_i^r\left\{y_i^r\phi(\boldsymbol{x}_i^r)\right\}\right\|^2 \\
&\qquad - \sum_{r=1}^{T}\lambda_r\sum_{i=1}^{m_r}\alpha_i^r\left\{y_i^r\left[\left(\sum_{s=1}^{T}\lambda_r\sum_{j=1}^{m_s}\alpha_j^s\left\{y_j^s\phi(\boldsymbol{x}_j^s)\right\}\right)\cdot\phi(\boldsymbol{x}_i^r)\right]\right\} \\
&\qquad - \sum_{r=1}^{T}(1-\lambda_r)\sum_{i=1}^{m_r}\alpha_i^r\left\{y_i^r\left[\left((1-\lambda_r)\sum_{j=1}^{m_r}\alpha_j^r\left\{y_j^r\phi_r(\boldsymbol{x}_j^r)\right\}\right)\cdot\phi_r(\boldsymbol{x}_i^r)\right]\right\} \\
&\qquad - \sum_{r=1}^{T}\sum_{i=1}^{m_r}\alpha_i^r\left\{-p_i^r\right\} \\
&\quad = \frac{1}{2}\sum_{r=1}^{T}\left\langle(1-\lambda_r)\sum_{i=1}^{m_r}\alpha_i^r\left\{y_i^r\phi_r(\boldsymbol{x}_i^r)\right\}, (1-\lambda_r)\sum_{i=1}^{m_r}\alpha_i^r\left\{y_i^r\phi_r(\boldsymbol{x}_i^r)\right\}\right\rangle \\
&\qquad + \frac{1}{2}\left\langle\sum_{r=1}^{T}\lambda_r\sum_{i=1}^{m_r}\alpha_i^r\left\{y_i^r\phi(\boldsymbol{x}_i^r)\right\}, \sum_{r=1}^{T}\lambda_r\sum_{i=1}^{m_r}\alpha_i^r\left\{y_i^r\phi(\boldsymbol{x}_i^r)\right\}\right\rangle \\
&\qquad - \left\langle\sum_{r=1}^{T}\lambda_r\sum_{i=1}^{m_r}\alpha_i^r\left\{y_i^r\phi(\boldsymbol{x}_i^r)\right\}, \sum_{r=1}^{T}\lambda_r\sum_{i=1}^{m_r}\alpha_i^r\left\{y_i^r\phi(\boldsymbol{x}_i^r)\right\}\right\rangle \\
&\qquad - \sum_{r=1}^{T}\left\langle(1-\lambda_r)\sum_{i=1}^{m_r}\alpha_i^r\left\{y_i^r\phi_r(\boldsymbol{x}_i^r)\right\}, (1-\lambda_r)\sum_{i=1}^{m_r}\alpha_i^r\left\{y_i^r\phi_r(\boldsymbol{x}_i^r)\right\}\right\rangle \\
&\qquad - \sum_{r=1}^{T}\sum_{i=1}^{m_r}\alpha_i^r\left\{-p_i^r\right\} \\
&\quad = -\frac{1}{2}\left\langle\sum_{r=1}^{T}\lambda_r\sum_{i=1}^{m_r}\alpha_i^r\left\{y_i^r\phi(\boldsymbol{x}_i^r)\right\}, \sum_{r=1}^{T}\lambda_r\sum_{i=1}^{m_r}\alpha_i^r\left\{y_i^r\phi(\boldsymbol{x}_i^r)\right\}\right\rangle \\
&\qquad - \frac{1}{2}\sum_{r=1}^{T}(1-\lambda_r)\left\langle\sum_{i=1}^{m_r}\alpha_i^r\left\{y_i^r\phi_r(\boldsymbol{x}_i^r)\right\}, (1-\lambda_r)\sum_{i=1}^{m_r}\alpha_i^r\left\{y_i^r\phi_r(\boldsymbol{x}_i^r)\right\}\right\rangle \\
&\qquad + \sum_{r=1}^{T}\sum_{i=1}^{m_r}\alpha_i^r p_i^r.
\end{aligned}
$$

The corresponding dual problem can be then expressed as

$$\begin{aligned}
\min_{\alpha} \quad \Theta(\alpha) = & \frac{1}{2}\frac{1}{C}\sum_{r=1}^{T}\sum_{i=1}^{m_r}(\alpha_i^r)^2 \\
& + \frac{1}{2}\left\langle \sum_{r=1}^{T}\lambda_r \sum_{i=1}^{m_r}\alpha_i^r \left\{y_i^r \phi(\boldsymbol{x}_i^r)\right\}, \sum_{r=1}^{T}\lambda_r \sum_{i=1}^{m_r}\alpha_i^r \left\{y_i^r \phi(\boldsymbol{x}_i^r)\right\} \right\rangle \\
& + \frac{1}{2}\sum_{r=1}^{T}\left\langle (1-\lambda_r)\sum_{i=1}^{m_r}\alpha_i^r \left\{y_i^r \phi_r(\boldsymbol{x}_i^r)\right\}, (1-\lambda_r)\sum_{i=1}^{m_r}\alpha_i^r \left\{y_i^r \phi_r(\boldsymbol{x}_i^r)\right\} \right\rangle \\
& - \sum_{r=1}^{T}\sum_{i=1}^{m_r}\alpha_i^r p_i^r \\
\text{s.t.} \quad & 0 \leq \alpha_i^r;\ i = 1, \ldots, m_r; r = 1, \ldots, T \\
& \sum_{i=1}^{m_r}\alpha_i^r y_i^r = 0; r = 1, \ldots, T.
\end{aligned} \tag{4.36}$$

Using the kernel trick, we can write the dual problem using a vector formulation

$$\begin{aligned}
\min_{\alpha} \quad & \Theta(\alpha) = \frac{1}{2}\boldsymbol{\alpha}^{\intercal}\left(\left\{\Lambda Q \Lambda + (I_n - \Lambda)\, K\, (I_n - \Lambda)\right\} + \frac{1}{C}I\right)\boldsymbol{\alpha} - \boldsymbol{p}\boldsymbol{\alpha} \\
\text{s.t.} \quad & 0 \leq \alpha_i^r;\ i = 1, \ldots, m_r; r = 1, \ldots, T \\
& \sum_{i=1}^{m_r}\alpha_i^r y_i^r = 0; r = 1, \ldots, T.
\end{aligned} \tag{4.37}$$

As in the convex MTL L1-SVM, we are using the matrix

$$\Lambda = \operatorname{diag}(\lambda_1, \ldots, \lambda_T)$$

and the $n \times n$ identity matrix I_n. Note that instead of having the box constraints for the dual coefficients α_i^r we add a diagonal term to the MTL kernel matrix $\widehat{Q}$, as defined in (4.24), so the matrix that is used is $\widehat{Q} + \frac{1}{C}I_n$.

The difference between the convex MTL based on the L1-SVM and this one, based on the L2-SVM, can be seen in the primal formulation, where the square of the errors is penalized, and, therefore, no inequality constraint is needed for the ξ_i^r variables. This is reflected in the dual problem, where there is no longer an upper bound for the dual coefficients, but a diagonal term is added to the kernel matrix, which acts as a soft constraint for the size of these dual coefficients.

Convex MTL LS-SVM.
The primal problem for the convex MTL LS-SVM, presented in Ruiz et al. (2021), is

$$\begin{aligned}
\underset{w, v_r, \xi}{\arg\min} \quad & J(w, v_r, \xi) = \frac{C}{2}\sum_{r=1}^{T}\sum_{i=1}^{m_r}(\xi_i^r)^2 + \frac{1}{2}\sum_{r=1}^{T}\|v_r\|^2 + \frac{1}{2}\|w\|^2 \\
\text{s.t.} \quad & y_i^r\left(\lambda_r\left\{w \cdot \phi(x_i^r) + b\right\} + (1-\lambda_r)\left\{v_r \cdot \phi_r(x_i^r) + b_r\right\}\right) = p_i^r - \xi_i^r.
\end{aligned} \tag{4.38}$$

Observe that it differs with the L1-SVM from (4.15) and L2-SVM from (4.29) The prediction model is again

$$h_r(\boldsymbol{x}) = \lambda_r \{w \cdot \phi(x_i^r) + b\} + (1 - \lambda_r) \{v_r \cdot \phi_r(x_i^r) + b_r\}$$

for regression and

$$h_r(\boldsymbol{x}) = \text{sign} \left(\lambda_r \{w \cdot \phi(x_i^r) + b\} + (1 - \lambda_r) \{v_r \cdot \phi_r(x_i^r) + b_r\}\right)$$

for classification.

As in the standard variant, hyperparameter C regulates the trade-off between the loss and the margin size, while λ_r indicates how specific or common these models are in the range of $[0, 1]$. With $\lambda_1, \ldots, \lambda_T = 0$ we have independent models for each task and for $\lambda_1, \ldots, \lambda_T = 1$ we have a common model for all tasks.

To obtain the dual problem the Lagrangian of problem (4.38):

$$\begin{aligned}
&\mathcal{L}(w, v_1, \ldots, v_T, b, d_1, \ldots, d_T, \boldsymbol{\xi}, \boldsymbol{\alpha}) \\
&= \frac{C}{2} \sum_{r=1}^{T} \sum_{i=1}^{m_r} (\xi_i^r)^2 + \frac{1}{2} \sum_{r=1}^{T} \|v_r\|^2 + \frac{1}{2} \|w\|^2 \\
&\quad - \sum_{r=1}^{T} \sum_{i=1}^{m_r} \alpha_i^r \left\{y_i^r \left(\lambda_r \{w \cdot \phi(x_i^r) + b\} + (1 - \lambda_r) \{v_r \cdot \phi_r(x_i^r) + b_r\}\right) - p_i^r + \xi_i^r\right\},
\end{aligned} \tag{4.39}$$

where $\alpha_i^r \in \mathbb{R}$ are the Lagrange multipliers. Observe that, although the Lagrangian is identical to the one of the L2-SVM, the non-negativity condition is no longer required for the dual coefficients. Again, $\boldsymbol{\xi}$ represents the vector

$$(\xi_1^1, \ldots, \xi_{m_1}^1, \ldots, \xi_1^T, \ldots, \xi_{m_T}^T)^\intercal$$

and analogously for $\boldsymbol{\alpha}$. The dual objective function is defined as

$$\begin{aligned}
&\min_{w, v_1, \ldots, v_T, b, d_1, \ldots, d_T, \boldsymbol{\xi}} \mathcal{L}(w, v_1, \ldots, v_T, b, d_1, \ldots, d_T, \boldsymbol{\xi}, \boldsymbol{\alpha}) \\
&= \mathcal{L}(w^*, {v_1}^*, \ldots, {v_T}^*, b^*, {d_1}^*, \ldots, {d_T}^*, \boldsymbol{\xi}^*, \boldsymbol{\alpha})
\end{aligned}$$

The gradients with respect to the primal variables are

$$\nabla_w \mathcal{L}|_{w^*, {v_1}^*, \ldots, {v_T}^*, b^*, {d_1}^*, \ldots, {d_T}^*, \boldsymbol{\xi}^*, \boldsymbol{\alpha}} = 0 \implies w^* - \sum_{r=1}^{T} \lambda_r \sum_{i=1}^{m_r} \alpha_i^r \{y_i^r \phi(x_i^r)\} = 0, \tag{4.40}$$

$$\nabla_{v_r} \mathcal{L}|_{w^*, {v_1}^*, \ldots, {v_T}^*, b^*, {d_1}^*, \ldots, {d_T}^*, \boldsymbol{\xi}^*, \boldsymbol{\alpha}} = 0 \implies {v_r}^* - (1 - \lambda_r) \sum_{i=1}^{m_r} \alpha_i^r \{y_i^r \phi_r(x_i^r)\} = 0, \tag{4.41}$$

$$\nabla_b \mathcal{L}|_{w^*, {v_1}^*, \ldots, {v_T}^*, b^*, {d_1}^*, \ldots, {d_T}^*, \boldsymbol{\xi}^*, \boldsymbol{\alpha}} = 0 \implies \sum_{r=1}^{T} \sum_{i=1}^{m_r} \alpha_i^r y_i^r = 0, \tag{4.42}$$

$$\nabla_{d_r} \mathcal{L}|_{w^*, {v_1}^*, \ldots, {v_T}^*, b^*, {d_1}^*, \ldots, {d_T}^*, \boldsymbol{\xi}^*, \boldsymbol{\alpha}} = 0 \implies \sum_{i=1}^{m_r} \alpha_i^r y_i^r = 0, \tag{4.43}$$

$$\nabla_{\xi_i^r} \mathcal{L}|_{w^*, {v_1}^*, \ldots, {v_T}^*, b^*, {d_1}^*, \ldots, {d_T}^*, \boldsymbol{\xi}^*, \boldsymbol{\alpha}} = 0 \implies C\xi_i^r - \alpha_i^r = 0. \tag{4.44}$$

Since all $\alpha_i^r \in \mathbb{R}$ are feasible, we can also write the corresponding KKT conditions as

$$\frac{\partial \mathcal{L}}{\partial \alpha_i^r} = 0 \implies y_i^r \left(\lambda_r \left\{w \cdot \phi(x_i^r) + b\right\} + (1-\lambda_r)\left\{v_r \cdot \phi_r(x_i^r) + b_r\right\}\right) = p_i^r - \xi_i^r,$$

and, using Equations (4.40) and (4.41) to substitute w and v_r, and (4.44) to replace ξ_i^r, we can express this condition as

$$\begin{aligned} & y_i^r \left(\lambda_r \left\{\left\langle \sum_{s=1}^{T} \lambda_s \sum_{j=1}^{m_s} \alpha_j^s y_j^s \phi(x_j^s), \phi(x_i^r)\right\rangle\right\}\right) \\ & \quad y_i^r \left((1-\lambda_r)\left\{\left\langle (1-\lambda_r) \sum_{j=1}^{m_r} \alpha_j^r y_j^r \phi_r(x_j^r), \phi_r(x_i^r)\right\rangle + b_r\right\}\right) = p_i^r - \frac{1}{C}\alpha_i^r \\ \implies & \left(\lambda_r \left\{\sum_{s=1}^{T} \lambda_s \sum_{j=1}^{m_s} \alpha_j^s y_i^r y_j^s k(x_j^s, x_i^r) + y_i^r b\right\}\right) \\ & \left((1-\lambda_r)\left\{(1-\lambda_r)\sum_{j=1}^{m_r} \alpha_j^r y_i^r y_j^r k_r(x_j^r, x_i^r) + y_i^r b_r\right\}\right) + \frac{1}{C}\alpha_i^r = p_i^r. \end{aligned} \tag{4.45}$$

These equations, alongside those corresponding to the conditions (4.42) can be expressed as the following system of equations

$$\left[\begin{array}{c|c|c} 0 & \mathbf{0}_T^\intercal & \boldsymbol{y}^\intercal \\ \hline \mathbf{0}_T & 0_{T\times T} & A^\intercal Y \\ \hline \boldsymbol{y} & YA & \widehat{Q} + \frac{1}{C} I_n \end{array}\right] \begin{bmatrix} b \\ d_1 \\ \vdots \\ d_T \\ \boldsymbol{\alpha} \end{bmatrix} = \begin{bmatrix} 0 \\ \mathbf{0}_T \\ \boldsymbol{p} \end{bmatrix}, \tag{4.46}$$

where $\mathbf{0}_T$ is the zero vector of length T, $0_{T\times T}$ is the $T \times T$ zero matrix, and we use the matrices

$$\underset{T\times N}{A^\intercal} = \begin{bmatrix} \overbrace{1\ldots1}^{m_1} & \ldots & \overbrace{0\ldots0}^{m_T} \\ \ddots & \ddots & \ddots \\ 0\ldots0 & \ldots & 1\ldots1 \end{bmatrix}, \quad \underset{N\times N}{Y} = \begin{bmatrix} y_1^1 & 0 & \ldots & 0 \\ 0 & y_2^1 & \ldots & 0 \\ \vdots & \vdots & \ddots & \vdots \\ 0 & 0 & \ldots & y_{m_T}^T \end{bmatrix}.$$

Again, $\widehat{Q}$ is the convex MTL kernel matrix defined in (4.24) and, as in the L2-SVM, a diagonal term $\frac{1}{C} I_n$ is added.

In contrast to the L1 and L2-SVM, where the dual problem is a convex quadratic optimization problem, in the LS-SVM case the dual problem is a system of equations. In the primal problem, the inequalities are replaced by equalities, which removes the bounds of the dual coefficients, thus leading to a problem that can be solved as a linear system of equations.

4.2.3 Optimal Convex Combination of Pre-trained Models

A natural alternative to the convex MTL formulation that we have developed is to directly combine pre-trained models in a convex manner. That is, given a model $g(\cdot)$ trained with the data from all tasks, and task-specific models $g_r(\cdot)$ that have been trained

with only the data from the corresponding task, for each task $r = 1, \ldots, T$ we can define the combination

$$h_r(\cdot) = \lambda_r g(\cdot) + (1 - \lambda_r) g_r(\cdot).$$

These are models that combines a common and task-specific models that have been trained separately. Since both $g(\cdot)$ and $g_r(\cdot)$ are fixed functions, the training phase only involves the process of learning the parameters $\lambda_r, r = 1, \ldots, T$. The goal is to select the parameters λ_r that minimize the training error

$$\sum_{r=1}^{T} \sum_{i=1}^{m_r} \ell(\lambda_r g(x_i^r) + (1 - \lambda_r) g_r(x_i^r), y_i^r),$$

which depends on the choice of the loss function ℓ. In Ruiz et al. (2021) we consider the training error with four popular loss functions:

- Training error using hinge loss (classification)

$$\sum_{r=1}^{T} \sum_{i=1}^{m_r} \left[1 - y_i^r \left\{\lambda_r g(x_i^r) + (1 - \lambda_r) g_r(x_i^r)\right\}\right]_+ .$$

- Training error using squared hinge loss (classification)

$$\sum_{r=1}^{T} \sum_{i=1}^{m_r} \left[1 - y_i^r \left\{\lambda_r g(x_i^r) + (1 - \lambda_r) g_r(x_i^r)\right\}\right]_+^2 .$$

- Training error using absolute loss (regression)

$$\sum_{r=1}^{T} \sum_{i=1}^{m_r} \left| y_i^r - \left\{\lambda_r g(x_i^r) + (1 - \lambda_r) g_r(x_i^r)\right\}\right| .$$

- Training error using squared loss (regression)

$$\sum_{r=1}^{T} \sum_{i=1}^{m_r} \left(y_i^r - \left\{\lambda_r g(x_i^r) + (1 - \lambda_r) g_r(x_i^r)\right\}\right)^2 .$$

Observe that using these training errors we can cover the kernel methods that we have considered. The L1-SVM uses the hinge loss for the classification error and the absolute error can be seen as a special case of the regression error when $\epsilon = 0$. The L2-SVM used the squared hinge loss for classification and, again, the squared loss is a special case of the regression error when $\epsilon = 0$. Finally, the squared loss function is used in the LS-SVM for both regression and classification.

Unified Formulation.
For simplicity, we consider the following renaming of error terms in the classification errors, that is those using hinge and squared hinge loss,

$$1 - \left\{\lambda_r g(x_i^r) + (1 - \lambda_r) g_r(x_i^r)\right\} y_i^r = \lambda_r \left\{y_i^r (g_r(x_i^r) - g(x_i^r))\right\} + 1 - y_i^r g_r(x_i^r) = \lambda_r c_i^r + d_i^r,$$

where we are using the variables

$$c_i^r = y_i^r(g_r(x_i^r) - g(x_i^r)),\ d_i^r = 1 - y_i^r g_r(x_i^r). \tag{4.47}$$

Also, for regression, where the absolute and squared losses are used,

$$\lambda_r g(x_i^r) + (1-\lambda_r)g_r(x_i^r) - y_i^r = \lambda_r\left\{g(x_i^r) - g_r(x_i^r)\right\} + \left\{g_r(x_i^r) - y_i^r\right\} = \lambda_r c_i^r + d_i^r,$$

where we are using the change of variables

$$c_i^r = g(x_i^r) - g_r(x_i^r),\ d_i^r = g_r(x_i^r) - y_i^r. \tag{4.48}$$

Recall that the functions $g(\cdot)$ and $g_r(\cdot)$ are fixed, and we want to learn the optimal parameters $\lambda_1^*, \ldots, \lambda_T^*$. Also, observe that each particular λ_r is only present in the training error terms concerning task r. That is, using the change of variables (4.47) and (4.48), we can consider the for each task $r = 1, \ldots, T$ the problem

$$\arg\min_{\lambda_r \in [0,1]} \mathcal{J}(\lambda_r) = \sum_{i=1}^{m_r} u(\lambda_r c_i^r + d_i^r),$$

where, for a simpler formulation we remove the task index, that is

$$\arg\min_{\lambda \in [0,1]} \mathcal{J}(\lambda) = \sum_{i=1}^{m} u(\lambda c_i + d_i), \tag{4.49}$$

where u can be different functions depending on the selected loss: the positive part for the hinge loss, the squared positive part for the squared hinge loss, and the absolute and squared functions for their corresponding losses.

These functions, except for the squared loss, are not differentiable in their whole domain, but piece-wise differentiable, so we will use the subdifferential when necessary. That is, let $\lambda_{(1)} < \ldots < \lambda_{(p)}$ be the sorted list of points where $\mathcal{J}$ is not differentiable, we will refer to these points as elbows. To find the optimal parameters λ_r^* we will consider the subdifferential of $\mathcal{J}(\lambda)$ in the elbows, that is, the set $\partial\mathcal{J}(\lambda) = \{c \in \mathbb{R}, \mathcal{J}(z) - \mathcal{J}(\lambda) \leq c(z-\lambda)\ \forall z \in (0,1)\}$. Using the generalizad Fermat theorem,

$$\lambda^* = \arg\min_{0 \leq \lambda \leq 1} \mathcal{J}(\lambda) \iff (0 \in \partial\mathcal{J}(\lambda^*) \text{ and } \lambda^* \in (0,1)) \text{ or } \lambda^* = 0 \text{ or } \lambda^* = 1.$$

To compute $\partial\mathcal{J}(\lambda)$ we use that all functions $u(\lambda c_i + d_i)$ share the same domain, that is, $\lambda \in [0,1]$, and therefore the subdifferential of the sum is the sum of subdifferentials.

Moreover, a result that is common for the linear loss functions is presented in Ruiz et al. (2021, Proposition 1).

Proposition 2. For the absolute value and hinge losses, $\partial J(\lambda)$ is single valued and constant between the elbows λ_j. Moreover, if $\partial J(\lambda) = J'(\lambda) = \gamma$ for some λ between two consecutive distinct elbows, i.e., $\lambda_{(j)} < \lambda < \lambda_{(j+1)}$, then $\gamma \in \partial J(\lambda_{(j)})$ and $\gamma \in \partial J(\lambda_{(j+1)})$.

This proposition states that in the case the linear losses considered, absolute and hinge losses, we find the optimal value λ^* in the elbows. In the following subsections we show how to select the optimal parameters λ_r^*, i.e. those minimizing the training error, with each of the losses considered.

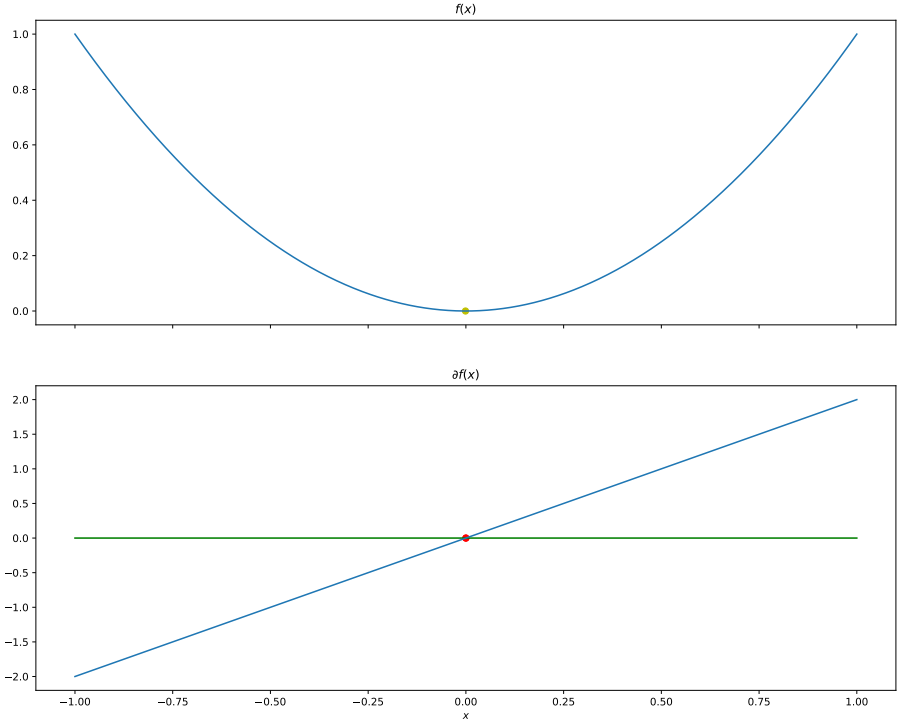

FIGURE 4.1: Squared value function (top) and its corresponding subgradient (bottom). The green line represents the 0 constant function. The yellow dot indicates the point minimizing the function.

Squared loss.
This is the simplest case, since the squared function, $f(x) = x^2$, is differentiable, and its derivative is $\nabla f(x) = 2x$; both are shown in Figure 4.1. Using the formulation of (4.49), the training error corresponding to the squared loss is

$$\arg\min_{\lambda \in [0,1]} \mathcal{J}(\lambda) = \sum_{i=1}^{m} (\lambda c_i + d_i)^2 . \tag{4.50}$$

In this case, $\mathcal{J}(\lambda)$ is a differentiable function, and its gradient is

$$\mathcal{J}'(\lambda) = \sum_{i=1}^{m} 2c_i(\lambda c_i + d_i).$$

Solving $\mathcal{J}'(\lambda) = 0$ results in

$$\lambda' = -\frac{\sum_{i=1}^{m} d_i c_i}{\sum_{i=1}^{m} (c_i)^2},$$

and the optimum is hence $\lambda^* = \max(0, \min(1, \lambda'))$.

In Figure 4.2 the error function using 10 random pairs (c_i, d_i) and its corresponding differential is shown.

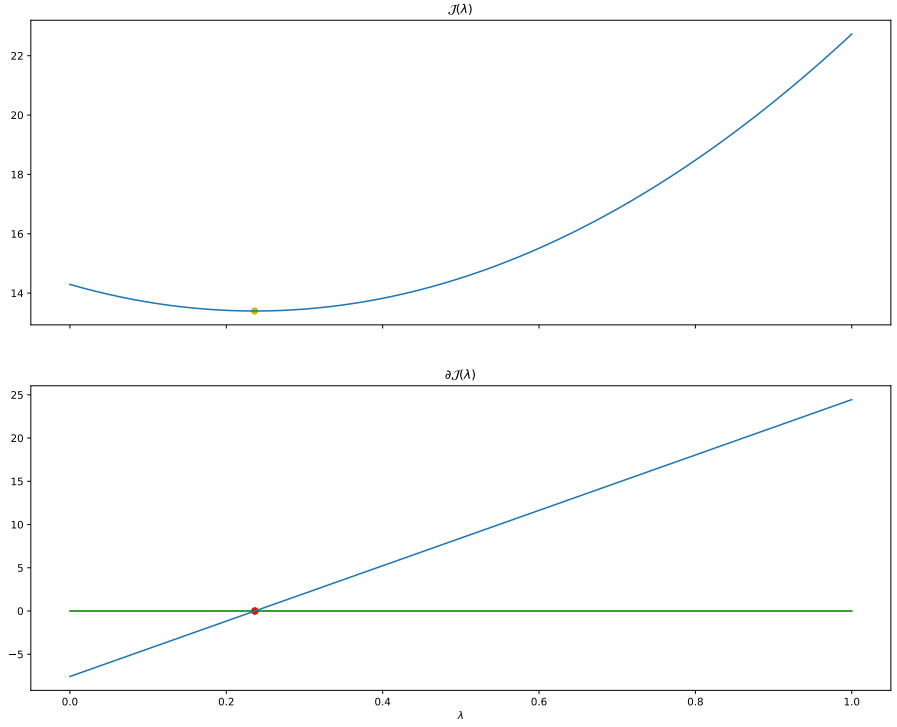

FIGURE 4.2: Error using squared loss function (top) and its corresponding subgradient (bottom). The green line represents the 0 constant function. The yellow dot is the point minimizing the error, and whose corresponding subgradient contains the value 0.

Absolute loss.
The absolute function

$$f(x) = \begin{cases} -x & x \leq 0, \\ x & x > 0 \end{cases}$$

is not differentiable at 0, but the subgradient can be expressed at any point as

$$f(x) = \begin{cases} -1 & x < 0, \\ [-1, 1] & x = 0, , \\ 1 & x > 0 \end{cases}$$

which is illustrated in Figure 4.3. Using the formulation of (4.49), the training error corresponding to the absolute value loss is

$$\arg\min_{\lambda \in [0,1]} \mathcal{J}(\lambda) = \sum_{i=1}^{m} |\lambda c_i + d_i| \,. \tag{4.51}$$

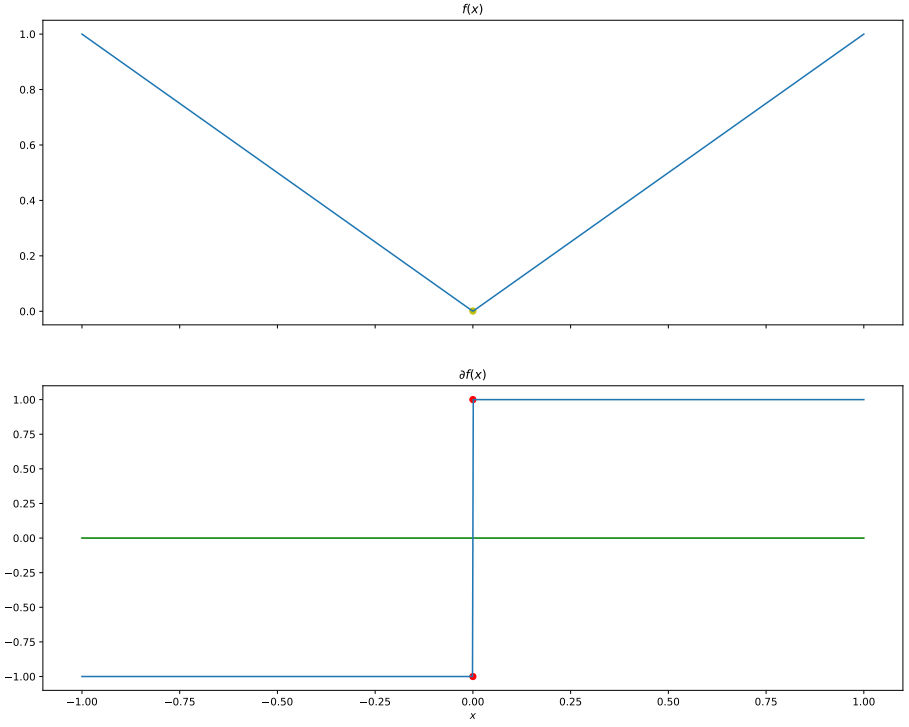

FIGURE 4.3: Absolute value function (top) and its corresponding subgradient (bottom). The green line represents the 0 constant function. The yellow dot indicates the point minimizing the function.

Observe that in each term of the sum the subdifferential is

$$\partial \left|\lambda c_i + d_i\right| = \begin{cases} -\left|c_i\right| & , \lambda c_i + d_i < 0 \\ \left[-\left|c_i\right|, \left|c_i\right|\right] & , \lambda c_i + d_i = 0 \\ \left|c_i\right| & , \lambda c_i + d_i > 0 \end{cases}$$

The elbows are obtained using the values $\frac{-d_i}{c_i}$, that can be clipped and sorted to get $\lambda_{(1)} < \ldots < \lambda_{(m)}$. In Ruiz et al. (2021, Proposition 2) we present a result to get the optimal λ^*.

Proposition 3 (Optimal λ^* with absolute value loss). In problem (4.51) $\lambda^* = 0$ is optimal iff

$$-\sum_{j:\lambda_{(j)}<0} |c_j| + \sum_{j:\lambda_{(j)}>0} |c_j| < 0.$$

If this condition does not hold, $\lambda^* \in (0, 1)$ is optimal iff λ^* is a feasible elbow, that is, $0 \leq \lambda^* = \lambda_{(k)} \leq 1$ for some $k = 1, \ldots, m$, and

$$-\sum_{j:\lambda_{(j)}<\lambda_{(k)}} |c_j| + \sum_{j:\lambda_{(j)}>\lambda_{(k)}} |c_j| \in \left[-\left|c_k\right|, \left|c_k\right|\right]. \tag{4.52}$$

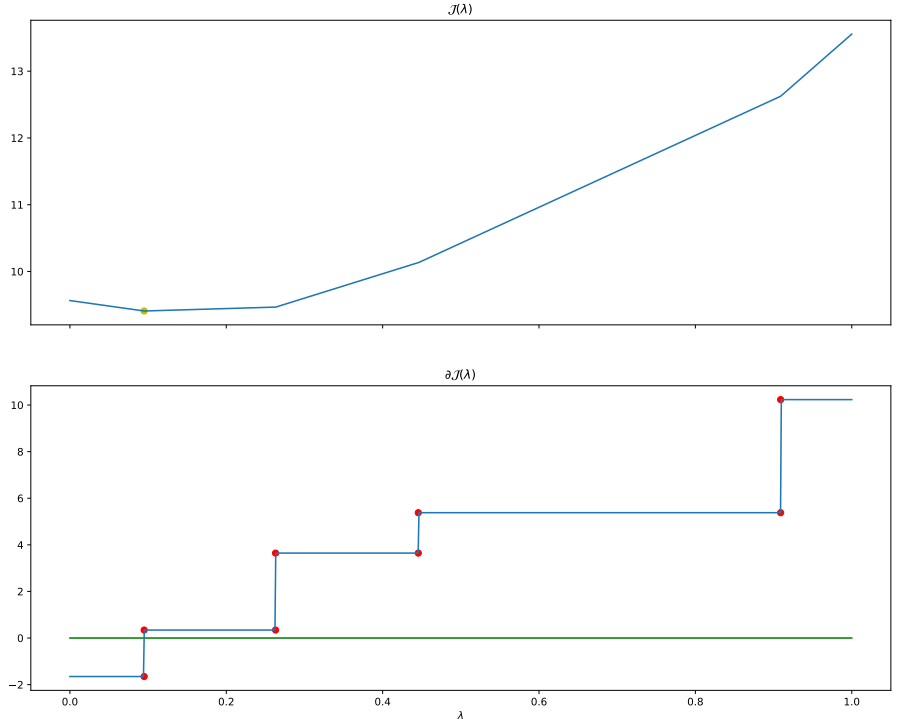

FIGURE 4.4: Error using absolute loss function (top) and its corresponding subgradient (bottom). The green line represents the 0 constant function. Red dots mark the extremes of the subdifferential intervals of non-differentiable points. The yellow dot is the point minimizing the error, and whose corresponding subgradient contains the value 0.

If none of the previous conditions hold, then $\lambda^* = 1$ is optimal.

The result of this proposition is depicted in Figure 4.4, where the error and its corresponding subgradient is computed for 10 random pairs (c_i, d_i).

Hinge loss.
The positive part function

$$f(x) = \begin{cases} 0 & x \leq 0, \\ x & x > 0 \end{cases}$$

is not differentiable at 0, but, again, the subgradient can be expressed at any point as

$$f(x) = \begin{cases} 0 & x < 0, \\ [0,1] & x = 0, , \\ 1 & x > 0 \end{cases}$$

which is illustrated in Figure 4.5. Using the formulation of (4.49), the training error

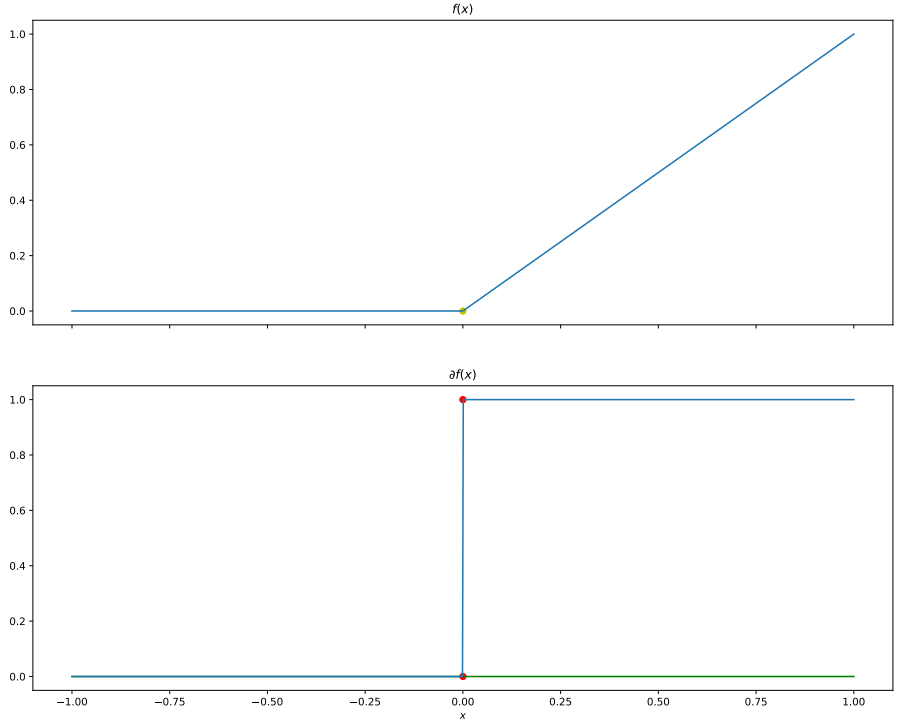

FIGURE 4.5: Positive part function (top) and its corresponding subgradient (bottom). The green line represents the 0 constant function. The yellow dot indicates the point minimizing the function.

corresponding to the hinge loss is

$$\arg\min_{\lambda\in[0,1]} \mathcal{J}(\lambda) = \sum_{i=1}^{m} [\lambda c_i + d_i]_+ . \tag{4.53}$$

Observe that in each term of the sum the subdifferential is

$$\partial\,[\lambda c_i + d_i]_+ = \begin{cases} 0 & , \lambda c_i + d_i < 0 \\ [\min(0, c_i), \max(0, c_i)] & , \lambda c_i + d_i = 0 \\ c_i & , \lambda c_i + d_i > 0 \end{cases} .$$

That is, the elbows are related to the values $\frac{-d_i}{c_i}$, that can be clipped and sorted to obtain the elbows $\lambda_{(1)} < \ldots < \lambda_{(m)}$. In Ruiz et al. (2021, Proposition 2) we present a result to get the optimal λ^*.

Proposition 4 (Optimal λ^* with hinge loss). In (4.53), $\lambda^* = 0$ is optimal iff

$$-\sum_{j:\lambda_{(j)}<0} \max(0, c_{(j)}) - \sum_{\lambda_{(j)}>0} \min(0, c_{(j)}) \leq 0. \tag{4.54}$$

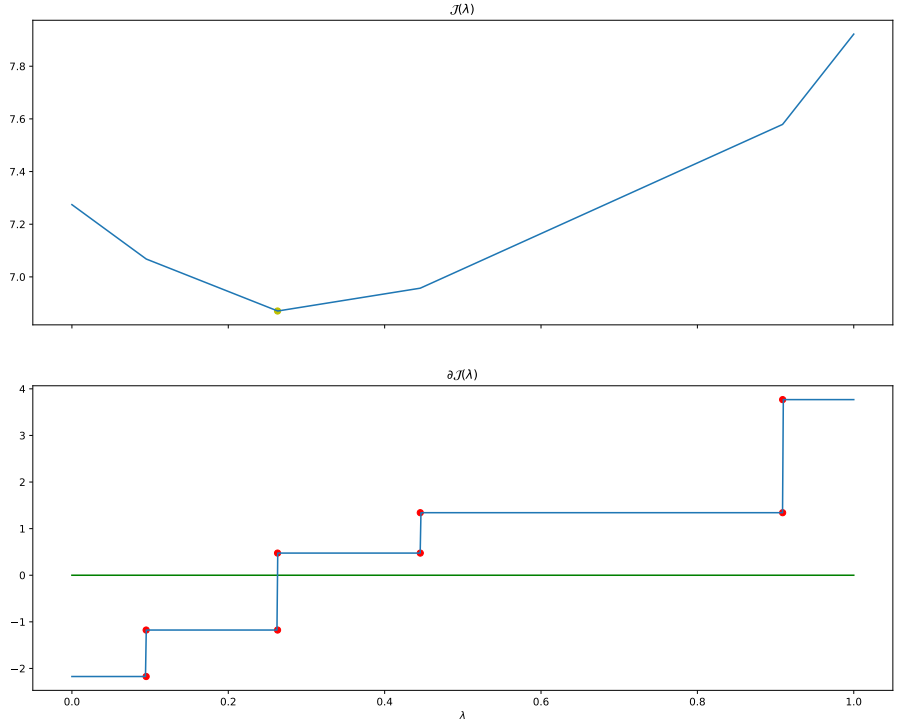

FIGURE 4.6: Error using hinge loss function (top) and its corresponding subgradient (bottom). The green line represents the 0 constant function. Red dots mark the extremes of the subdifferential intervals of non-differentiable points. The yellow dot is the point minimizing the error, and whose corresponding subgradient contains the value 0.

If this condition does not hold, a value $\lambda^* \in (0,1)$ is optimal for problem (4.53) iff $\lambda^* \in \{0,1\}$ or λ^* is a feasible elbow, that is, $0 \leq \lambda^* = \lambda_{(k)} \leq 1$ for some $k = 1,\ldots,m$, and

$$-\sum_{j:\lambda_{(j)}<\lambda_{(k)}} \max(0, c_{(j)}) - \sum_{j:\lambda_{(j)}>\lambda_{(k)}} \min(0, c_{(j)}) \in \left[\min(0, c_{(k)}), \max(0, c_{(k)})\right]. \quad (4.55)$$

If none of the previous conditions hold, then $\lambda^* = 1$ is optimal.

Again, the results of the proposition are illustrated in Figure 4.6, where 10 pairs (c_i, d_i) are randomly sampled, and the corresponding error function $\mathcal{J}(\lambda)$ and its subgradient are shown.

Squared hinge loss.
The squared positive part function is

$$f(x) = \begin{cases} 0 & x \leq 0, \\ x^2 & x > 0 \end{cases}$$

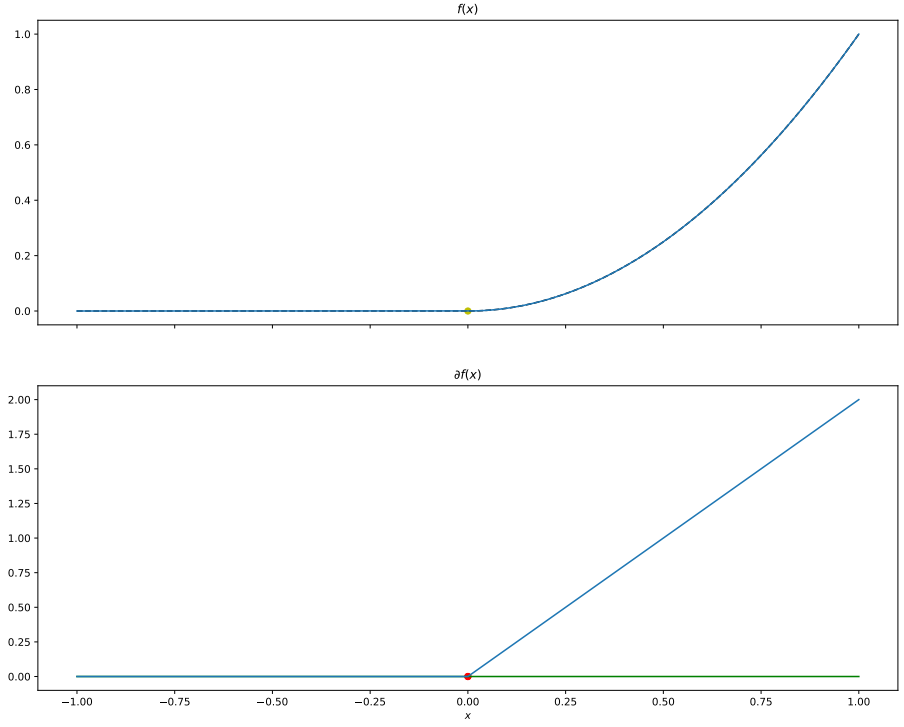

FIGURE 4.7: Positive part function (top) and its corresponding subgradient (bottom). The green line represents the 0 constant function. The yellow dot indicates the point minimizing the function.

and its gradient can be expressed at any point as

$$f(x) = \begin{cases} 0 & x \leq 0, \\ 2x & x > 0 \end{cases},$$

which is illustrated in Figure 4.5. Although the gradient can be defined at any point, the definition by parts makes it difficult to obtain results. Using the formulation of (4.49), the training error corresponding to the hinge loss is

$$\arg\min_{\lambda \in [0,1]} \mathcal{J}(\lambda) = \sum_{i=1}^{m} [\lambda c_i + d_i]_+^2 . \tag{4.56}$$

In each term of the sum the subdifferential is

$$\partial \, [\lambda c_i + d_i]_+^2 = \begin{cases} 0 & , \lambda c_i + d_i \leq 0 \\ 2c_i(\lambda c_i + d_i) & , \lambda c_i + d_i > 0 \end{cases} .$$

The elbows are again related to the values $\frac{-d_i}{c_i}$, that can be clipped and sorted to obtain the elbows $\lambda_{(1)} < \ldots < \lambda_{(m)}$. In Ruiz et al. (2021, Proposition 2) we give a result to get the optimal λ^* when using the squared hinge loss.

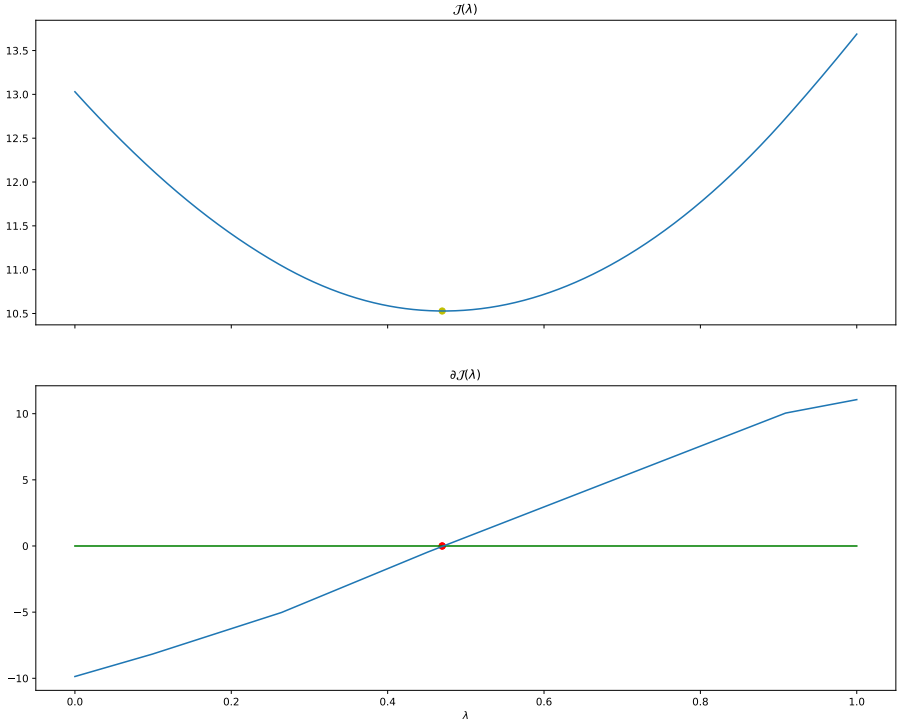

FIGURE 4.8: Error using squared hinge loss function (top) and its corresponding subgradient (bottom). The green line represents the 0 constant function. The yellow dot is the point minimizing the error, and whose corresponding subgradient contains the value 0.

Proposition 5 (Optimal λ^* with squared hinge loss). In (4.56), $\lambda^* = 0$ is optimal iff

$$-\frac{\sum_{j:\lambda_j<0} \max(0, c_j)d_j + \sum_{j:\lambda_j>0} \min(0, c_j)d_j}{\sum_{j:\lambda_j<0} \max(0, c_j)^2 + \sum_{j:\lambda_j>0} \min(0, c_j)^2} < 0.$$

If this condition does not hold, consider the extended sorted list of feasible elbows $\lambda_{(p-1)} = 0 \leq \lambda_{(p)} \leq \ldots, \lambda_{(q)} \leq \lambda_{(q+1)} = 1$, with $1 \leq p, q \leq m$, and define for $k = p-1, \ldots, q$ $\widehat{\lambda}_k$ as

$$\widehat{\lambda}_k = -\frac{\sum_{j:\lambda_{(j)}<\lambda_{(k)}} \max(0, c_j)d_j + \sum_{j:\lambda_{(j)}>\lambda_{(k)}} \min(0, c_j)d_j}{\sum_{j:\lambda_{(j)}<\lambda_{(k)}} \max(0, c_j)^2 + \sum_{j:\lambda_{(j)}>\lambda_{(k)}} \min(0, c_j)^2}. \tag{4.57}$$

Then, if $\lambda_k \leq \widehat{\lambda}_k \leq \lambda_{k+1}$ for some $\widehat{\lambda}_k$, then $\lambda^* = \widehat{\lambda}_k$ is optimal. Finally, if none of the previous conditions holds, (4.56) has a minimum at $\lambda^* = 1$.

As with the other losses, the error function and respective gradient for 10 random pairs (c_i, d_i) are represented in Figure 4.8.

4.2.4 Experiments

In this subsection we show the experiments used to test the convex MTL formulation with kernel models, which have been presented in (Ruiz et al., 2019) and (Ruiz et al., 2021). First, following the work in (Ruiz et al., 2019), experiments comparing convex and additive MTL formulations in the L1-SVM are described. Then, the experiments of (Ruiz et al., 2021) are exposed, where all convex MTL models using L1, L2 and LS-SVMs as well as optimal convex combination of pre-trained models are compared using multiple real problems.

Before diving into the results, some technical details have to be explained. The convex MTL formulation, as presented in Equation (4.15), uses task-specific hyperparameters λ_r, as well as common and task-specific kernels, with their corresponding hyperparameters; however, the selection of hyperparameters is always a challenge because of the curse of dimensionality. To select the hyperparameters $p_1, \ldots, p_L$ of a learning algorithm using CV the following problem is solved:

$$p_1^*, \ldots, p_L^* = \underset{p_i \in \mathcal{S}_{p_i}, i=1,\ldots,L}{\arg\min} \sum_{j=1}^{F} \rho(\mathcal{A}(p_1, \ldots, p_L; (X^j_{\text{train}}, y^j_{\text{train}})); (X^j_{\text{val}}, y^j_{\text{val}})), \tag{4.58}$$

where ρ is some measure, $\mathcal{A}$ is our choice of learning algorithm; $p_1, \ldots, p_L$ are the parameters on which $\mathcal{A}$ depends and $\mathcal{S}_{p_i}$ a feasible space for the parameter p_i; and $(X^j_{\text{train}}, y^j_{\text{train}}), (X^j_{\text{val}}, y^j_{\text{val}})$ are the training and validation sets, respectively. We are using F folds, that is, for $j = 1, \ldots, F$ we select different training and validation sets and we train our algorithm $\mathcal{A}$ on the training set $(X^j_{\text{train}}, y^j_{\text{train}})$, then we use ρ to measure the wellness of our model on $(X^j_{\text{val}}, y^j_{\text{val}})$. Observe that our search space is the product space $\mathcal{S}_{p_1} \times \ldots \times \mathcal{S}_{p_L}$, so the difficulty of selecting an optimal combination of hyperparameters scales exponentially with the number of such parameters.

In a standard Gaussian kernel SVM, the definition of the problem depends on two hyperparameters: C and γ. In the L1 and L2-SVM for regression problems we also add a third parameter: ϵ. That is, to select the hyperparameters of a standard SVM for a single task we have to solve the problem

$$C^*, \gamma^*(, \epsilon^*) = \underset{\substack{C \in \mathcal{S}_C; \\ \gamma \in \mathcal{S}_\gamma; \\ (\epsilon \in \mathcal{S}_\epsilon);}}{\arg\min} \sum_{j=1}^{F} \rho(\mathcal{A}(C, \gamma(, \epsilon); (X^j_{\text{train}}, y^j_{\text{train}})); (X^j_{\text{val}}, y^j_{\text{val}})),$$

which is typically feasible by using a grid search method in the space $\mathcal{S}_C \times \mathcal{S}_\gamma (\times \mathcal{S}_\epsilon)$.

However, using the convex MTL formulation, we have the following hyperparameters: the regularization parameter C; the common kernel width γ, and task-specific ones $\gamma_1, \ldots, \gamma_T$; and the convex combination parameters $\lambda_1, \ldots, \lambda_T$; and possibly the ϵ parameter. That is, there are at least $2T + 2$ hyperparameters that have to be selected. Even with $T = 2$, a search space of dimension 6 is computationally unfeasible to cover.

To solve this difficulty and select the optimal parameters for the convex MTL formulation we follow the following strategy. For the kernel widths, we proceed as follows: we first hyperparametrize the corresponding CTL and ITL kernel models, which have a common and task-specific kernel widths, respectively. Observe that in the CTL approach where a single virtual task is solved and in the ITL approach, where we solve the tasks independently, we have 2 or 3 parameters. We solve problems, which are represented in Equation (4.58), using standard methods, and we obtain optimal common C^*, γ^* and

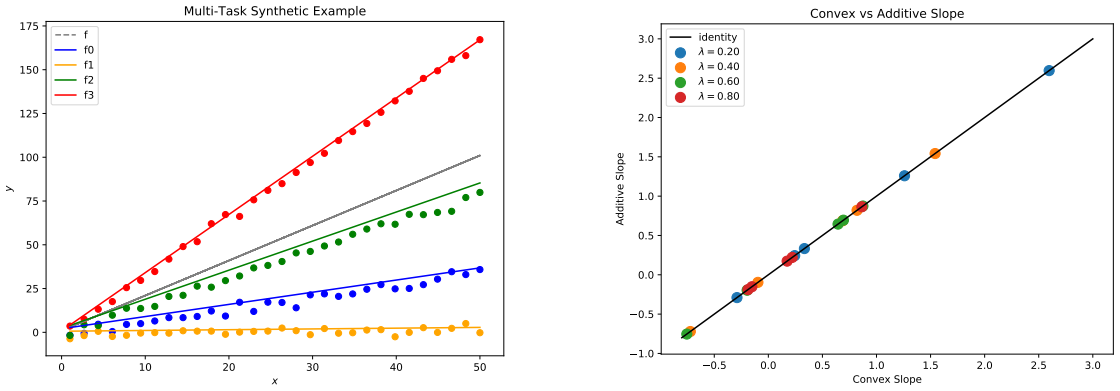

FIGURE 4.9: Left: Synthetic example dataset, where the data of each task (corresponding to a different function f_i) are represented with a different color. Right: Comparison of the weights obtained by the convex and additive approaches.

task-specific ones C_r^*, γ_r^* for $r = 1, \ldots, T$. Then, we reutilize the optimal widths for these models, and fix them in the MTL one. Moreover, for the convex combination parameters we use a single λ for all tasks, that is, $\lambda_1 = \ldots = \lambda_T = \lambda$. With these considerations, the problem to select the remaining hyperparameters is

$$C^*, \lambda^*(, \epsilon^*) = \underset{\substack{C \in \mathcal{S}_C; \\ \lambda \in \mathcal{S}_\lambda; \\ (\epsilon \in \mathcal{S}_\epsilon);}}{\arg\min} \sum_{j=1}^{F} \rho(\mathcal{A}(C, \lambda, \gamma^*, \gamma_1^*, \ldots, \gamma_T^*(, \epsilon); (X_{\text{train}}^j, y_{\text{train}}^j)); (X_{\text{val}}^j, y_{\text{val}}^j)),$$

where we have a maximum of 3 hyperparameters.

These are the two adjustments that we make to carry out the experiments shown in this subsection. The first adjustment concerning kernel widths does not change the model definition, but it assumes that kernel widths that are good for CTL or ITL models are good for the MTL one. This assumption is a sensible one, since kernel widths are not that descriptive of the model but of the data used. The combined data from all tasks, which is used in CTL approach, is well "characterized" by a width σ^* so we expect that this width is also useful for the common part of the MTL model. The same reasoning applies to task-specific data and ITL approach. The second adjustment does change the models definition, using a single λ that determines the specifity of all models. However, we expect that the possible difference in specifity among tasks can be corrected in the training process by selecting larger task-specific weights v_r if necessary.

Comparison of Convex and Additive Formulations.
In (Ruiz et al., 2019), we illustrate the results of equivalence between the additive and convex formulations in an empirical way. To do this we generate a synthetic problem, shown in Figure 4.9, left, as a four linear regression tasks problem. We use four different functions f_0, f_1, f_2, f_3 by considering a base function $f(x) = 2x - 1$ with slope $m = 2$ and bias $n = 1$, then we sample $z_m^r, z_n^r \sim N(0, 1)$ for each task $r = 0, \ldots, 3$ and create the r-th slope and bias by adding these Gaussian samples, i.e., $m_r = m + z_m^r$ and $n_r = n + z_n^r$. Also, we sample the noise σ_r for each task uniformly in $(0, 5)$. Then, the r-th task consists on estimating m_r and n_r from data. To do this, for each task we uniformly sample 30 points $x_i^r \in [1, 50)$, and the target values are defined as $y_i^r = f_r(x_i^r) + \epsilon_r^i$ where $\epsilon_r^i \sim N(0, \sigma_r)$. Combining all tasks, there are 120 data points, 30 for each task, that we split randomly in

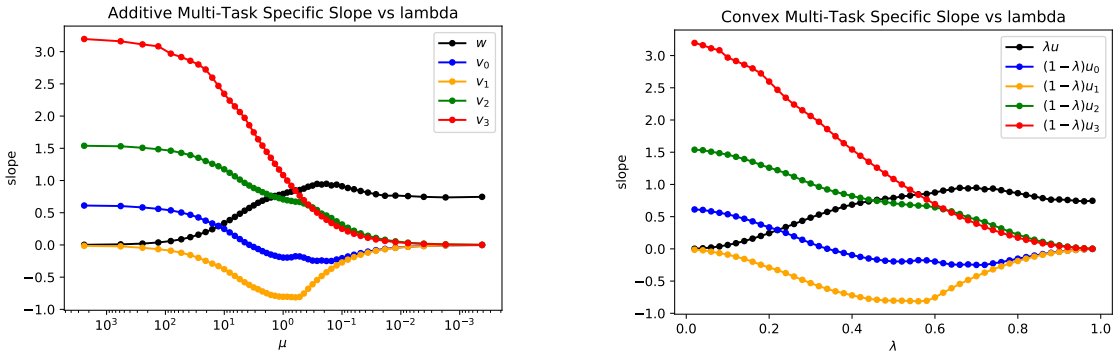

FIGURE 4.10: Convex (right) and additive (left) MTLSVR slope estimates weights as a function of λ. We represent the common part of the models, w for the additive and λu for the convex, as well as each task specific deviation v_t and $(1-\lambda)u_t$.

a stratified way: two thirds, i.e. 80 points are used for training, and the rest are used for testing purposes; in this division, the task size proportions are kept constant, that is 1/4 for each task, in both the train and test sets. With this synthetic problem, we train four convex MTL models corresponding to values of $\lambda \in \{0.2, 0.4, 0.6, 0.8\}$; and we also train the corresponding equivalent additive MTL models, in which we set $\mu = (1-\lambda)/\lambda^2$ and $C_{\text{add}} = (1-\lambda)^2 C_{\text{conv}}$, as shown in Proposition 1. Our goal is to compare the influence of μ with that of λ in the final models that are obtained. To do that, we need C to be small enough so the regularization and, therefore, μ are relevant; the value $C_{\text{conv}} = 10^{-2}$ is found to be useful. We also consider linear kernels, so we can obtain the primal coefficients, that is, the slopes, and compare those obtained using the additive and convex formulations. In Figure 4.9, right, we show the estimated slopes for each of the λ values considered with a different color. In the x axis we represent the convex slopes and in the y axis the additive ones. There are four dots of each color, corresponding to each of the tasks considered in our synthetic problem. We can observe that all dots lie in the diagonal line corresponding to the identity function, as we expected from the equivalence result from Proposition 1.

To further compare the two formulations, to visualize how the change on the hyper-parameters imposes a change on the final models. Using the already described synthetic problem of Figure 4.9, left, we select values of λ ranging from 0 to 1, and their corresponding values $\mu = (1-\lambda)^2/\lambda^2$, and fit convex and additive MTL linear SVMs using these values. In Figure 4.10 we show the coefficients obtained for the common and task-specific parts with the additive formulation (left) and convex one (right). We can observe how both graphics show a similar behaviour, with the common model starting in 0 when μ is large or $\lambda = 0$, and, as μ decreases and λ grow, the task-specific parts go to zero and the common model reaches the optimal value for CTL. However, two facts are noticeable, the first one is the range of hyperparameters needed for each formulation; while the convex formulation always uses $[0, 1]$, with the additive formulation it seems that $(10^{-3}, 10^3)$ is useful in this problem, but we cannot extrapolate to other problems; the second one is the smoother transition of the convex formulation, where the changes are steadily made, while with the additive one the changes look more abrupt.

Performance of Convex MTL and Optimal Convex Combination.
To test the performance of the convex MTL formulation, in (Ruiz et al., 2019) we also conduct experiments with real problems, which are extended in (Ruiz et al., 2021).

Models. Considering that LX can stand for L1, LS or LS, we use the following approaches:

- Common Task Learning LX-SVM (CTL-LX): A single LX-SVM which is fitted using data from all the tasks and does not use of the task information.
- Independent Task Learning LX-SVM (ITL-LX): Multiple task-specific LX-SVMs, each of which is fitted with the data from its own task.
- Direct Convex Combination of LX-SVMs (cvxCMB-LX): A combination of the best CTL-LX and ITL-LX as described in Subsection 4.2.3.
- Convex Multi-Task Learning LX-SVM (cvxMTL-LX): The Convex MTL formulations shown in Subsection 4.2.1 for the L1-SVM and in Subsection 4.2.2 for the L2- and LS-SVM.

Problems. To compare these approaches we will use several regression and classification problems. We use a total of six regression problems:

- majorca: The goal is to predict the photovoltaic energy production of a park installed in Mallorca. The tasks are defined as the energy prediction at each hour with sunlight (we remove the night hours).
- tenerife: The goal is to predict the photovoltaic energy production of a park installed in Tenerife. The tasks are defined as the energy prediction at each hour with sunlight (we remove the night hours).
- boston: This is the housing problem in Boston, where the goal is to predict house prices, and the tasks are defined as the predictions in different areas of the city. In Boston we have the houses that are next to the river and those that are not.
- california: This is the housing problem in California, where the goal is also to predict house prices. Here the tasks correspond to 4 different areas of the city, related to their distance to the sea.
- abalone: The goal is to predict the number of rings of a specie of marine molluscs. The tasks are male, female or infant.
- crime: The goal is to predict the number of crimes per 100.000 habitants in the U.S., the tasks are the prediction of the crime rate in different states.

For the classification setting, we consider eight problems, six of which are generated by applying different task definitions to two different problems.

- landmine: This is a binary classification problem in which the goal is to detect landmines. Detection of different types of landmines determines a different task each.
- binding: This is a binary classification problem where the goal is to determine if a given molecule will bind peptides. Different molecules define different tasks.
- adult: The goal is to predict whether the salary of a particular person is greater than 50K based on sociocultural data. We can define different tasks dividing the population by either gender or race, so we have the problems:

TABLE 4.1: Sample sizes, dimensions and number of tasks of the datasets used.

Dataset	Size	No. feat.	No. tasks	Avg. task size	Min. t. s.	Max. t. s.
majorca	15 330	765	14	1095	1095	1095
tenerife	15 330	765	14	1095	1095	1095
california	19 269	9	5	3853	5	8468
boston	506	12	2	253	35	471
abalone	4177	8	3	1392	1307	1527
crime	1195	127	9	132	60	278
binding	32 302	184	47	687	59	3089
landmine	14 820	10	28	511	445	690
adult_(G)	48 842	106	2	24 421	16 192	32 650
adult_(R)	48 842	103	5	9768	406	41 762
adult_(G, R)	48 842	101	10	4884	155	28 735
compas_(G)	3987	11	2	1993	840	3147
compas_(R)	3987	9	4	997	255	1918
compas_(G, R)	3987	7	8	498	50	1525

TABLE 4.2: Hyperparameters, grids used to select them (when appropriate) and hyperparameter selection method for each model.

	Grid	CTL-L1,2	ITL-L1,2	cvxMTL-L1,2	CTL-LS	ITL-L,S	cvxMTL-LS
C	$\{4^k : -2 \leq k \leq 6\}$	CV	CV	CV	CV	CV	CV
ϵ	$\left\{\frac{\sigma}{4^k} : 1 \leq k \leq 6\right\}$	CV	CV	CV	-	-	-
γ_c	$\left\{\frac{4^k}{d} : -2 \leq k \leq 3\right\}$	CV	-	CTL-L1,2	CV	-	CTL-LS
γ_s^r	$\left\{\frac{4^k}{d} : -2 \leq k \leq 3\right\}$	-	CV	ITL-L1,2	-	CV	ITL-LS
λ	$\{0.1k : 0 \leq k \leq 10\}$	-	-	CV	-	-	CV

  - ad_{G}: dividing by gender
  - ad_{R}: dividing by race
  - ad_{G, R}: dividing by both gender and race

- compas: The goal is to predict whether the COMPAS algorithm will assign "low" or "high" scores of recidivism to a particular subject. We can also divide the sample by either race or gender, so we obtain:
  - comp_{G}: dividing by gender
  - comp_{R}: dividing by race
  - comp_{G, R}: dividing by both gender and race

The characteristics of some of the problems considered are present in Table 3.1 but, considering the different task definitions for compas and adult we give a more complete table in Table 4.1.

Experimental Procedure. To obtain the experimental results, we have to select the optimal hyperparameters for each model in a training-validation set and measure its performance on a test set. To do this, we follow the adjustments and experimental procedure described at the beginning of this subsection: reusing the kernel widths from CTL and ITL approaches and limiting the convex MTL formulation to a single parameter λ. In all models considered we use Gaussian kernels, so all features have been scaled to the $[0, 1]$ interval. As previously explained, the hyperparameters for the CTL and ITL approaches in the classification setting are $\{C, \gamma\}$ for all variants L1, L2 and LS-SVM. In the regression setting we have $\{C, \gamma, \epsilon\}$ for the L1 and L2 variants, and $\{C, \gamma\}$ for the LS-SVM. After selecting the optimal kernel widths in the CTL approach σ^*, and the task-specific widths σ_r^* in the ITL approach, we use these values to fix them in the convex

MTL formulation. Then, the hyperparameters that we are considering for CV search in the convex MTL approaches in the classification settings are $\{C, \lambda\}$ for all variants, while in the regression problems they are $\{C, \lambda, \epsilon\}$ for the L1 and L2 variants and $\{C, \lambda\}$ for the LS-SVM. The optimal combination approaches do not have proper hyperparameters, since λ can be considered a training parameter. In all problems, the hyperparameters considered are selected with a grid search using a task-stratified 3-fold CV. That is, given a training-validation set, we divide it in three different folds where the task proportions are kept constant, and we use two of these folds for training the model and evaluate its performance in the remaining one. In the regression problems, we will measure the validation performance using the MAE, see Table 4.3, and MSE, see Table 4.4. Observe that the objective function of L1-SVM based models is more aligned with minimizing the MAE, while those of L2 and LS-SVM based models are more related to minimizing the MSE. In the classification problems, see Table 4.5, we will consider the F1 score to deal with the class-imbalance ratio that we find, for example, in the landmine dataset where we have 200 negative examples for every 13 positive ones. In Table 4.2 we show for each hyperparameter of the considered approaches if they are selected using a CV procedure or recycling them from other approach, as well as the grids used for the CV search.

We have explained how we select the hyperparameters given a training-validation set, but it is necessary also to describe how we get the final results that we show on tables. In every problem, except for majorca and tenerife, we will consider three external folds, each with the internal three folds for cross-validation. That is, the whole dataset of each problem is first divided in three task-stratified external folds: F_1, F_2, F_3; then, two folds will form the training-validation set and the third one will be used as the test set. All folds have the same task proportions. There are three different combinations to do this division: $\{F_1, F_2; F_3\}, \{F_1, F_3; F_2\}$ and $\{F_2, F_3; F_1\}$, where the first two folds form the train-validation set and the other one is the test set. In each train-validation set we follow the procedure described above to select the optimal hyperparameters, and the performance model with the optimal hyperparameters will be tested in the remaining fold, i.e., the test set.

The problems of majorca and tenerife have a temporal dependency, so it is not possible to use training data from a time that is ahead of that of the test or validation data. Therefore, we use data from years 2013, 2014 and 2015, each corresponding to train, validation and test sets, respectively. We consider different metrics to measure the test performance. Therefore, in every problem, except majorca and tenerife, for each metric we obtain three different scores, each corresponding to a different test set, so we will show the mean and standard deviation of such scores. In majorca and tenerife we obtain a single test score corresponding to data from the year 2015. For the regression problems, in Tables 4.3 and 4.4, we show both the MAE and R2 score, closely related to MSE, obtained in the test set, and for classification, in Table 4.5, we show the F1 and the accuracy scores.

Results. The tables with the numerical results have three blocks, one for each variant L1, L2 or LS-SVMs, and, in each block, for each problem we show in bold the model with best test results. We also provide a statistical significant ranking based on the Wilcoxon test. The Wilcoxon test is a pairwise test that checks whether the difference of two samples has its median in 0, i.e., the distribution is symmetric around 0. Instead of showing every Wilcoxon test result between all pairs of models, which would result in a 12×12 matrix difficult to interpret, we take the following approach. We first sort the models, according to some criterion, and test the significance between one model

TABLE 4.3: Test MAE (top) and R2 score (bottom) and Wilcoxon-based ranking for the models selected using the MAE for hyperparametrization. The best models are shown in bold.

	maj.	ten.	boston	california	abalone	crime
			MAE			
ITL-L1	5.087 (6)	5.743 (3)	2.341±0.229 **(1)**	36883.582±418.435 (2)	1.481±0.051 (3)	0.078±0.001 (2)
CTL-L1	5.175 (7)	5.891 (5)	**2.192±0.244 (1)**	41754.337±270.908 (6)	1.482±0.050 (3)	0.078±0.001 (2)
cvxCMB-L1	**5.047** (5)	**5.340 (1)**	2.239±0.255 **(1)**	36880.238±420.417 **(1)**	1.470±0.052 (2)	0.077±0.002 (2)
cvxMTL-L1	5.050 (5)	5.535 (2)	2.206±0.292 **(1)**	**36711.383±343.333 (1)**	**1.454±0.048 (1)**	**0.074±0.002 (1)**
ITL-L2	4.952 (3)	**5.629** (3)	2.356±0.300 **(1)**	37374.618±433.511 (5)	1.498±0.054 (4)	0.079±0.002 (2)
CTL-L2	5.193 (7)	6.107 (8)	**2.083±0.136 (1)**	42335.612±163.773 (8)	1.503±0.047 (5)	0.080±0.002 (2)
cvxCMB-L2	4.869 (3)	5.963 (6)	2.089±0.128 **(1)**	37374.618±433.511 (4)	1.494±0.050 (4)	0.077±0.003 (2)
cvxMTL-L2	**4.854** (2)	5.784 (4)	2.089±0.134 **(1)**	**37202.603±419.166** (3)	**1.482±0.049** (3)	**0.077±0.002** (2)
ITL-LS	4.937 (3)	5.649 (3)	2.204±0.116 **(1)**	37348.347±441.240 (4)	1.496±0.051 (4)	0.079±0.002 (2)
CTL-LS	5.193 (7)	6.005 (7)	**2.072±0.143 (1)**	42259.492±146.825 (7)	1.502±0.052 (5)	0.079±0.002 (2)
cvxCMB-LS	4.977 (4)	**5.593** (3)	2.081±0.146 **(1)**	37339.179±430.288 (4)	1.486±0.049 (4)	0.079±0.002 (2)
cvxMTL-LS	**4.824 (1)**	5.754 (4)	2.077±0.152 **(1)**	**37231.043±420.992** (4)	**1.478±0.050** (3)	**0.076±0.002** (2)
			R2			
ITL-L1	0.845 (6)	0.901 (7)	0.821±0.041 (2)	0.699±0.009 (7)	0.543±0.022 (8)	0.732±0.021 (3)
CTL-L1	0.837 (9)	0.901 (6)	0.854±0.036 **(1)**	0.639±0.006 (10)	0.559±0.014 (6)	0.740±0.027 (3)
cvxCMB-L1	0.844 (6)	0.905 (4)	0.845±0.053 **(1)**	0.699±0.009 (6)	0.555±0.018 (7)	0.741±0.029 (3)
cvxMTL-L1	**0.846** (4)	**0.908** (2)	**0.858±0.057 (1)**	**0.703±0.007** (6)	**0.568±0.012** (5)	**0.760±0.024** (2)
ITL-L2	0.846 (5)	0.906 (3)	0.836±0.045 (2)	0.707±0.009 (5)	0.565±0.025 (6)	0.743±0.017 (3)
CTL-L2	0.840 (8)	0.901 (8)	**0.889±0.017 (1)**	0.645±0.005 (9)	0.574±0.013 (4)	0.744±0.028 (3)
cvxCMB-L2	0.850 (3)	0.900 (9)	0.885±0.013 **(1)**	0.707±0.009 (4)	0.571±0.018 (4)	0.755±0.024 (3)
cvxMTL-L2	**0.863** (2)	**0.908 (1)**	0.888±0.015 **(1)**	**0.709±0.008** **(1)**	**0.580±0.014** (3)	**0.762±0.028 (1)**
ITL-LS	0.849 (3)	0.907 (3)	0.856±0.008 **(1)**	0.707±0.009 (3)	0.573±0.015 (4)	0.743±0.022 (3)
CTL-LS	0.838 (9)	0.904 (5)	**0.894±0.015 (1)**	0.646±0.005 (8)	0.576±0.016 (4)	0.746±0.032 (3)
cvxCMB-LS	0.843 (7)	0.907 (2)	0.886±0.024 **(1)**	0.707±0.009 (2)	0.581±0.012 (2)	0.746±0.021 (3)
cvxMTL-LS	**0.863 (1)**	**0.910 (1)**	0.890±0.016 **(1)**	**0.709±0.008** (2)	**0.581±0.015 (1)**	**0.763±0.028 (1)**

and next in the sorting order. Then we create a new significant ranking, the ranking increases only if this difference is significant. For example, if there are no significant differences between the first and second model, according the sorting order, they both obtain the ranking of 1.

In the regression tables, apart from the test scores, we provide a Wilcoxon-based ranking for each problem. To apply the Wilcoxon test, in each problem we sort the models (using all blocks) according to their mean score. Then, we test if the difference between each model and the next one in the ranking is significant. To do this, we take the list of errors committed by each model in the test set, that is, $e_1 = y - \hat{y_1}$ and $e_2 = y - \hat{y_2}$ are the list of errors of each model. Then, we use the Wilcoxon test to check if $e_1 - e_2$ is centered around 0. If the null hypothesis is rejected at a 5% level, then we say that the difference is significant. The results for regression problems are shown in Table 4.3, where the best parameters are selected according to the MAE validation score, and in Table 4.4, where the MSE is used as the validation metric. Although we cannot pick a single overall winner, we can still draw some conclusions from the tables. Note that the convex MTL approaches usually perform better, obtaining the best result in 11 out of 18 MAE blocks and 16 out of 18 R2 blocks of Table 4.3; in Table 4.4 it obtains 12 out of 18 MAE blocks and 15 out of 18 R2 blocks. Also, a convex MTL approach obtains the single best overall model in four problems, while ties for the first place in boston and, only in tenerife ends up as second, after the cvxCMB-L1 model.

The classification results, in Table 4.5 show a similar behavior. In this table, the ranking is not computed for each problem, but in general, computing the mean of scores across all problems. This mean score is used to rank the models, which is the second left-most column, and, using the Wilcoxon-based procedure we produce a statistical significant ranking shown in the last column. Now, the Wilcoxon tests are done with

TABLE 4.4: Test MAE (top) and R2 score (bottom) and Wilcoxon-based ranking for the models selected using the MSE for hyperparametrization. The best models are shown in bold.

	maj.	ten.	boston	california	abalone	crime
			MAE			
ITL-L1	5.087 (7)	5.743 (3)	2.437±0.281 (3)	36941.516±450.767 (1)	1.480±0.058 (3)	0.079±0.002 (3)
CTL-L1	5.175 (8)	5.891 (7)	2.315±0.192 (2)	41857.602±235.021 (6)	1.479±0.047 (3)	0.078±0.000 (2)
cvxCMB-L1	**4.920** (4)	5.743 (4)	2.315±0.192 (3)	**36941.476±450.711 (1)**	1.471±0.057 (2)	0.079±0.002 (2)
cvxMTL-L1	5.050 (6)	**5.535 (1)**	**2.244±0.150** (1)	36999.003±360.445 (2)	**1.455±0.046 (1)**	**0.074±0.001 (1)**
ITL-L2	4.924 (5)	5.752 (5)	2.437±0.324 (3)	37407.929±461.878 (5)	1.497±0.050 (5)	0.079±0.002 (2)
CTL-L2	5.193 (8)	6.107 (9)	2.096±0.112 (1)	42335.612±163.773 (7)	1.504±0.048 (6)	0.079±0.002 (2)
cvxCMB-L2	**4.813 (1)**	**5.623** (3)	2.116±0.131 (1)	37398.940±449.498 (5)	1.495±0.051 (5)	0.078±0.003 (2)
cvxMTL-L2	4.854 (4)	5.784 (6)	**2.082±0.130** (1)	**37356.599±390.629** (4)	**1.481±0.041** (4)	**0.076±0.000** (2)
ITL-LS	4.937 (5)	5.649 (3)	2.326±0.231 (3)	37385.244±403.331 (4)	1.495±0.045 (5)	0.079±0.002 (2)
CTL-LS	5.193 (8)	6.005 (8)	**2.072±0.143 (1)**	42339.063±156.624 (7)	1.504±0.043 (6)	0.078±0.002 (2)
cvxCMB-LS	**4.820** (2)	5.578 (2)	2.136±0.106 (1)	37377.005±391.694 (4)	1.491±0.048 (5)	0.078±0.002 (2)
cvxMTL-LS	4.824 (3)	**5.754** (6)	2.090±0.090 (1)	**37232.918±397.866** (3)	**1.478±0.042** (3)	**0.076±0.000** (2)
			R2			
ITL-L1	0.845 (6)	0.901 (9)	0.800±0.050 (3)	0.703±0.009 (8)	0.534±0.053 (10)	0.732±0.017 (4)
CTL-L1	0.837 (7)	0.901 (8)	0.860±0.026 (2)	0.642±0.006 (10)	0.564±0.011 (8)	0.748±0.017 (3)
cvxCMB-L1	**0.852** (4)	0.901 (10)	0.860±0.026 (3)	0.703±0.009 (7)	0.550±0.036 (9)	0.733±0.018 (3)
cvxMTL-L1	0.846 (5)	**0.908** (5)	**0.871±0.019** (1)	**0.705±0.008** (6)	**0.573±0.011** (7)	**0.764±0.019** (1)
ITL-L2	0.850 (4)	0.906 (6)	0.819±0.053 (3)	0.707±0.009 (4)	0.573±0.020 (6)	0.744±0.018 (3)
CTL-L2	0.840 (6)	0.901 (11)	0.886±0.014 (1)	0.645±0.005 (9)	0.574±0.013 (6)	0.747±0.025 (3)
cvxCMB-L2	0.857 (3)	**0.910 (1)**	0.883±0.016 (1)	0.707±0.009 (2)	0.574±0.021 (5)	0.751±0.029 (3)
cvxMTL-L2	**0.863** (2)	0.908 (4)	**0.887±0.015** (1)	**0.708±0.007** (2)	**0.581±0.011** (2)	**0.768±0.020 (1)**
ITL-LS	0.849 (4)	0.907 (5)	0.841±0.028 (3)	0.707±0.009 (5)	0.577±0.012 (4)	0.743±0.021 (3)
CTL-LS	0.838 (7)	0.904 (7)	**0.894±0.015 (1)**	0.645±0.005 (9)	0.575±0.012 (4)	0.754±0.022 (3)
cvxCMB-LS	0.856 (3)	0.909 (3)	0.877±0.009 (1)	0.707±0.009 (3)	0.580±0.013 (3)	0.750±0.024 (3)
cvxMTL-LS	**0.863 (1)**	**0.910** (2)	0.890±0.014 (1)	**0.710±0.008 (1)**	**0.582±0.011 (1)**	**0.763±0.019** (2)

samples of size 8, the number of classification problems, so it is more difficult to find significant differences. The convex MTL approaches get 18 out of 24 F1 blocks and 22 out 26 accuracy blocks. The best overall model is the cvxMTL-L2, while the other convex MTL models are tied with it in the significant ranking. In any case, the Wilcoxon test here uses a very small sample size and is given only for illustration purposes.

4.3 Convex Multi-Task Learning with Neural Networks

The convex MTL formulation is easily applicable and interpretable, so it has good properties for kernel models, but also for a broader class of learning models. Neural networks, in particular deep ones, have had a massive success in multiple applications. Moreover, they are very flexible models whose architecture can be adapted to fulfill different goals. In this section we show how to use our convex formulation for MTL with neural networks.

In Chapter 3 we have reviewed the taxonomy for MTL methods, and the approaches can be broadly grouped in three categories: feature-based, parameter-based and combination-based. We also show in Subsection 3.4.4 some of the most famous approaches to MTL with neural networks. Most of these approaches can fit in the feature-based category, where the shared layers are fully or partially shared to obtain a latent representation that is useful for all tasks, as shown in Figure 4.11; see for example Caruana (1997); Misra et al. (2016); Ruder et al. (2017). Some approaches rely also on a parameter-based view, where the parameters of each task-specific network are regularized together so that they are close in some sense, see Long and Wang (2015); Yang and Hospedales (2017b). However, to the best of my knowledge, the first purely

TABLE 4.5: Test F1 (top) and accuracy (bottom) scores, global and block-wise Wilcoxon-based rankings for classification problems. The best models in each block are shown in bold.

	comp_(G)	comp_(R)	comp_(G,R)	ad_(G)	ad_(R)	ad_(G,R)	landmine	binding	mean	rank	Wil.
					F1						
ITL-L1	0.625	**0.639**	0.630	**0.659**	0.653	0.657	0.231	0.867	0.620	10	1
CTL-L1	0.623	0.638	0.638	0.657	0.650	0.653	0.255	0.901	0.627	7	1
cvxCMB-L1	0.616	0.638	0.638	0.658	0.650	0.653	**0.270**	0.901	**0.628**	6	1
cvxMTL-L1	**0.627**	0.636	**0.640**	**0.659**	**0.655**	**0.659**	0.242	**0.907**	**0.628**	5	1
ITL-L2	0.636	0.623	0.607	**0.668**	**0.666**	**0.668**	0.256	0.867	0.624	8	3
CTL-L2	**0.640**	0.647	**0.651**	0.665	0.661	0.659	**0.270**	0.903	0.637	2	2
cvxCMB-L2	0.629	0.640	0.645	0.666	0.662	0.661	**0.270**	0.903	0.634	3	2
cvxMTL-L2	0.634	**0.651**	0.650	**0.668**	**0.666**	**0.668**	0.263	**0.909**	**0.639**	1	1
ITL-LS	**0.631**	0.622	0.608	**0.659**	**0.659**	**0.660**	0.243	0.867	0.619	12	2
CTL-LS	0.628	**0.644**	**0.649**	0.650	0.653	0.647	0.230	0.853	0.619	11	2
cvxCMB-LS	0.630	0.635	0.642	0.657	0.658	0.654	0.238	0.873	0.623	9	2
cvxMTL-LS	0.630	0.641	0.648	**0.659**	**0.659**	0.659	**0.257**	**0.906**	**0.632**	4	1
					Accuracy						
ITL-L1	0.750	0.749	0.746	0.852	0.851	**0.853**	**0.941**	0.790	0.817	11	3
CTL-L1	**0.757**	0.759	**0.763**	0.852	0.847	0.849	0.938	0.850	0.827	6	2
cvxCMB-L1	0.754	0.759	**0.763**	0.852	0.847	0.849	0.935	0.850	0.826	7	2
cvxMTL-L1	0.753	**0.760**	**0.763**	**0.853**	**0.852**	**0.853**	0.933	**0.861**	**0.829**	5	1
ITL-L2	0.754	0.762	0.751	**0.856**	**0.855**	**0.856**	**0.942**	0.791	0.821	8	2
CTL-L2	**0.762**	0.765	**0.767**	0.854	0.853	0.851	0.933	0.853	0.830	3	1
cvxCMB-L2	0.757	0.764	0.766	0.854	0.853	0.853	0.934	0.853	0.829	4	1
cvxMTL-L2	0.753	**0.766**	0.766	**0.856**	**0.855**	**0.856**	0.933	**0.864**	**0.831**	1	1
ITL-LS	0.754	0.761	0.750	**0.851**	**0.850**	**0.851**	0.943	0.791	0.819	9	2
CTL-LS	**0.757**	**0.764**	0.766	0.845	0.847	0.842	0.914	0.750	0.811	12	3
cvxCMB-LS	0.754	**0.764**	0.765	0.849	**0.850**	0.848	0.925	0.793	0.818	10	3
cvxMTL-LS	**0.757**	**0.764**	**0.767**	**0.851**	**0.850**	**0.851**	**0.944**	**0.858**	**0.830**	2	1

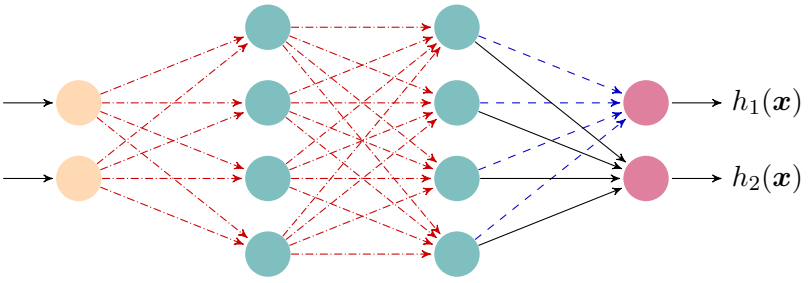

FIGURE 4.11: *Hard Sharing* Neural Network for two tasks and a two-dimensional input. Assuming a sample belonging to task 1 is used, the updated shared weights are represented in red, and in blue the updated specific weights. The input neurons are shown in yellow, the hidden ones in cyan and the output ones in magenta.

combination-based approach to MTL with neural networks is presented in Ruiz et al. (2022), where we use a convex combination of neural networks.

4.3.1 Model Definition

Using the formulation of (4.1), we use neural networks to the model the common part

$$g(x_i^r; w, \Theta) = w^\intercal f(x_i^r; \Theta) + b,$$

and task-specific parts

$$g_r(x_i^r; w_r, \Theta_r) = w_r^\intercal f_r(x_i^r; \Theta_r) + b_r.$$

Here Θ and Θ_r are the sets of hidden weights, w, w_r are the output weights of the common and specific networks, respectively, and b and b_r the output biases. Observe that the feature transformations $f(x_i^r;\Theta)$ and $f_r(x_i^r;\Theta_r)$ are not fixed like $\phi(x_i^r)$ and $\phi_r(x_i^r)$ in the kernel methods, instead, here, they are automatically learned in the training process. The full MTL models are then

$$h_r(x_i^r) = \lambda\{w^\intercal f(x_i^r;\Theta) + b\} + (1-\lambda)\{w_r^\intercal f_r(x_i^r;\Theta_r) + b_r\}. \tag{4.59}$$

This formulation offers multiple combinations since we can model each common or independent function using different architectures for $f(\cdot;\Theta)$ or $f_r(\cdot;\Theta_r)$. For example, we can use a network with a larger number of parameters for the common part, since it will be fed with more data, and simpler networks for the task-specific parts. Even different types of neural networks, such as fully connected and convolutional, can be combined depending on the characteristics of each task. This combination of neural networks can also be interpreted as an implementation of the LUPI paradigm (Vapnik and Izmailov, 2015) shown in Subsection 3.2.4, i.e., the common network captures the privileged information for each of the tasks, since it can learn from more sources.

4.3.2 Training Procedure

The regularized risk corresponding to the convex MTL neural networks is

$$R_{\boldsymbol{z}} = \sum_{r=1}^{T}\sum_{i=1}^{m} \ell(h_r(x_i^r), y_i^r) + \frac{\mu}{2}\left(\|w\|^2 + \sum_{r=1}^{T}\|w_r\|^2 + \Omega(\Theta) + \Omega(\Theta_r)\right). \tag{4.60}$$

Here, h_r is defined as in equation (4.59), and $\Omega(\Theta)$ and $\Omega(\Theta_r)$ represents the L_2 regularization of the set of hidden weights of the common and specific networks, respectively. Given a loss function $\ell(\hat{y}, y)$ and a pair (x_i^t, y_i^t) from task t, we use the chain rule to compute the gradient of the loss function with respect to some parameters $\mathcal{P}$:

$$\nabla_{\mathcal{P}}\ell(h_t(x_i^t), y_i^t) = \frac{\partial}{\partial \hat{y}_i^t}\ell(\hat{y}_i^t, y_i^t)|_{\hat{y}_i^t = h_t(x_i^t)} \nabla_{\mathcal{P}} h_t(x_i^t). \tag{4.61}$$

Recall that we are using the formulation

$$h_t(x_i^t) = \lambda\{w^\intercal f(x_i^t;\Theta) + b\} + (1-\lambda)\{w_t^\intercal f_t(x_i^t;\Theta_t) + b_t\},$$

where we make a distinction between output weights w, w_t and hidden parameters Θ, Θ_t. Then, the corresponding gradients of h_t needed to compute the loss gradients are

$$\begin{aligned}
&\nabla_w h_t(x_i^t) = \lambda\{f(x_i^t,\Theta)\}, && \nabla_\Theta h_t(x_i^t) = \lambda\{w^\intercal \nabla_\Theta f(x_i^t,\Theta)\};\\
&\nabla_{w_t} h_t(x_i^t) = (1-\lambda)\{f_t(x_i^t,\Theta)\}, && \nabla_{\Theta_t} h_t(x_i^t) = (1-\lambda)\{w^\intercal \nabla_{\Theta_t} f_t(x_i^t,\Theta_t)\};\\
&\nabla_{w_r} h_t(x_i^t) = 0, && \nabla_{\Theta_r} h_t(x_i^t) = 0, \text{ for } r \neq t.
\end{aligned} \tag{4.62}$$

Putting all together, the gradient of the loss with respect to w, for example, is

$$\nabla_w \ell(h_t(x_i^t), y_i^t) = \ell(\hat{y}_i^t, y_i^t)|_{\hat{y}_i^t = h_t(x_i^t)} \lambda\{f(x_i^t,\Theta),\}$$

and the same for the rest of parameters. Observe that the convex combination information is transferred in the back-propagation, the loss gradients with respect to common parameters are scaled by λ, while those of the task-specific parameters are scaled by

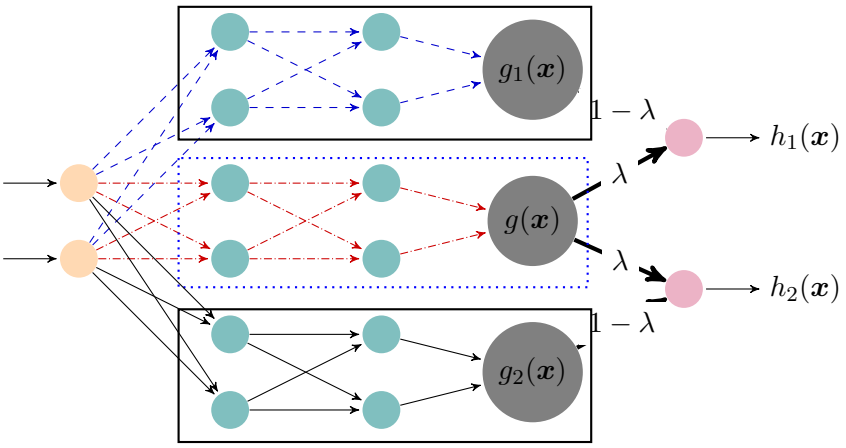

FIGURE 4.12: Convex MTL neural network for two tasks and a two-dimensional input. Assuming a sample belonging to task 1 is used, the updated shared weights are represented in red, and in blue the updated specific weights. Specific networks are framed in black boxes and the common one in a blue box. The input neurons are shown in yellow, the hidden ones in cyan (except those in grey), and the output ones in magenta. We use the grey color for hidden neurons containing the intermediate functions that will be combined for the final output: $g_1(\boldsymbol{x})$, $g_2(\boldsymbol{x})$ and $g(\boldsymbol{x})$. The thick lines are the hyperparameters λ and $1-\lambda$ of the convex combination.

$(1-\lambda)$. Moreover, the regularization of each set of parameters, i.e., $\{w\}, \Theta$ and $\{w_r\}, \Theta_r$, is done independently, so their gradients can be computed in the standard way. During the back propagation procedure, we only update the parameters that have been used in the forward pass, with possibly different learning rates for each network. That is, given an example (x_i^t, y_i^t), when using vanilla SGD the update rules for the common network parameters would be

$$\begin{aligned} w^{\tau+1} &\leftarrow w^{\tau} + \eta \left[\frac{\partial}{\partial \hat{y}_i^t} \ell(\hat{y}_i^t, y_i^t)|_{\hat{y}_i^t = h_t(x_i^t)} \lambda \{ f(x_i^t, \Theta) \} + \mu w^{\tau} \right], \\ \Theta^{\tau+1} &\leftarrow \Theta^{\tau} + \eta \left[\frac{\partial}{\partial \hat{y}_i^t} \ell(\hat{y}_i^t, y_i^t)|_{\hat{y}_i^t = h_t(x_i^t)} \lambda \{ w^{\intercal} \nabla_{\Theta} f(x_i^t, \Theta) \} + \mu \{ \nabla_{\Theta} \Omega(\Theta) \} \right]; \end{aligned} \tag{4.63}$$

while the update rules for t-th task network parameters would be

$$\begin{aligned} w_t^{\tau+1} &\leftarrow w_t^{\tau} + \eta_t \left[\frac{\partial}{\partial \hat{y}_i^t} \ell(\hat{y}_i^t, y_i^t)|_{\hat{y}_i^t = h_t(x_i^t)} (1-\lambda) \{ f(x_i^t, \Theta) \} + \mu w_t^{\tau} \right], \\ \Theta_t^{\tau+1} &\leftarrow \Theta_t^{\tau} + \eta_t \left[\frac{\partial}{\partial \hat{y}_i^t} \ell(\hat{y}_i^t, y_i^t)|_{\hat{y}_i^t = h_t(x_i^t)} (1-\lambda) \{ w^{\intercal} \nabla_{\Theta_t} f(x_i^t, \Theta_t) \} + \mu \{ \nabla_{\Theta_t} \Omega(\Theta_t) \} \right]; \end{aligned} \tag{4.64}$$

and the parameters from the rest of task-specific network are not updated. That is, no specific algorithm has to be developed for training the convex MTL NN. In (4.63) and (4.64) we have shown the update rules for vanilla SGD, but any other algorithm, e.g., Adam, can be used scaling properly the loss gradients.

4.3.3 Implementation Details

Our implementation of the convex MTL neural network is based on `PyTorch` (Paszke et al., 2019). Although we include the gradients expressions in equation (4.62), the

Input: $X_{\text{mb}}, t_{\text{mb}}$ // Minibatch data and task labels
Output: f // Forward pass for the minibatch
Data: λ // Parameter of convex combination
Data: $g; g_1, \ldots, g_T$ // Modules of the common and specific networks
for $x_i, t_i \in (X_{mb}, t_{mb})$ **do**
  $f_i \leftarrow \lambda g(x_i) + (1 - \lambda) g_{t_i}(x_i)$ // Convex combination
end

Algorithm 1: Forward pass for Convex MTL neural network.

`PyTorch` package implements automatic differentiation, so the gradients are not explicitly implemented. Instead, we implement each network, common or specific, using (possibly different) `PyTorch` modules. In the forward pass of the network, the output for an example x_i^r from task r is computed using a pass of the common module and the corresponding specific module, combining both passes with the convex formulation to obtain the final output $h_r(x_i^r)$. In the training phase, in which minibatches are used, the full minibatch is passed through the common model, but the minibatch is task-partitioned, where each partition is passed through its corresponding specific module. By doing this, when using examples from the r-th task only the parameters corresponding to common module and its corresponding specific one are updated. Moreover, as mentioned above, with the adequate forward pass, the `PyTorch` package automatically computes the scaled gradients in the training phase.

In Algorithm 1 we show the pseudo-code of the forward pass of the convex MTL neural network. Here, g and $g_1, \ldots, g_T$ are the common and task-specific modules, whose outputs are combined. We do not show the backward pass because we rely on PyTorch automatic differentiation.

4.3.4 Experiments

Problems Description.
To test the Convex MTL neural networks we use four Multi-Task image datasets: var-MNIST, rot-MNIST, based on MNIST (LeCun et al., 1998), and var-FMNIST, rot-FMNIST, based on fashion-MNIST (Xiao et al., 2017). The MNIST and fashion-MNIST datasets are both composed of 70 000 examples of 28×28 grey-scale images. The MNIST dataset contains images of handwritten numbers, while the fashion-MNIST has images of clothes and fashion-related objects. Both are used as classification problems, where the images have to be classified in one of 10 possible classes. These classes are balanced in both datasets. To generate the Multi-Task image datasets that we use, we take the images from MNIST or fashion-MNIST and use either the *variations* procedure or the *rotation* one.

For the var-MNIST and var-FMNIST we use the *variations* procedure. Inspired by the work of Bergstra and Bengio (2012), we consider three transformations:

- *random*: adding random noise to the original image.
- *image*: adding a random patch of another image to the original image.
- *standard*: no transformations are applied to the original image.

Then, we use a random split to divide the original datasets in three groups. Each group is applied one of the transformations defined, so we get three tasks: two with 23 333 examples and the third one with 23 334.

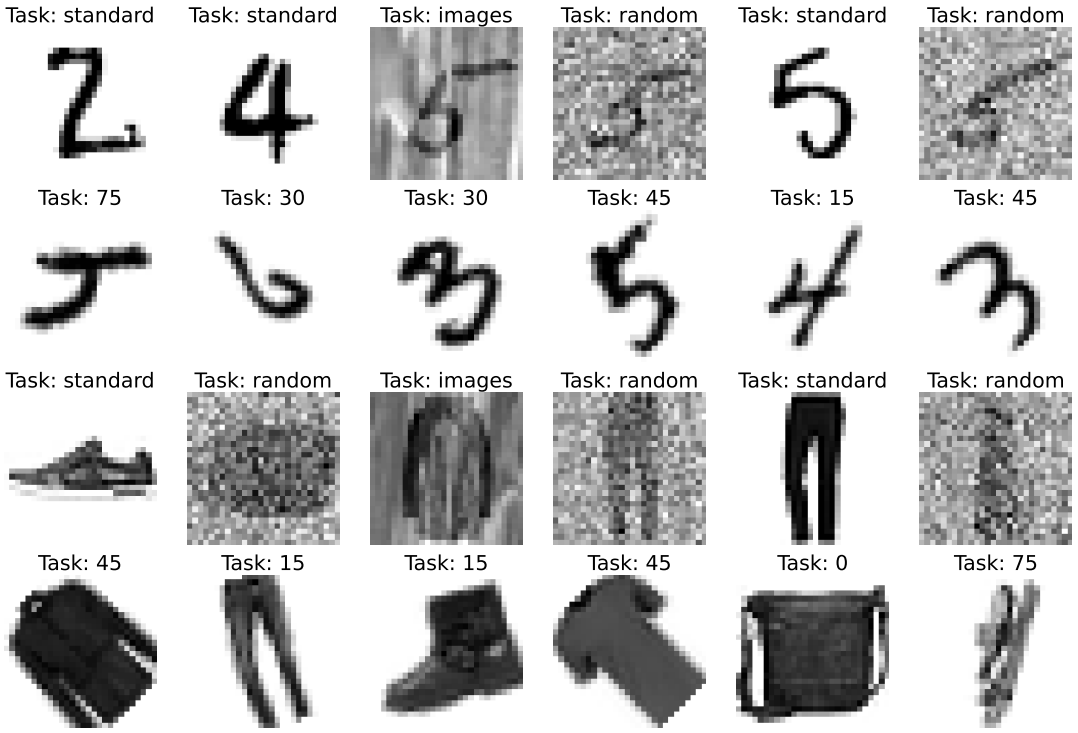

FIGURE 4.13: Images of the four classification problems used. Each image has a title indicating the corresponding task. The rows correspond to var-MNIST, rot-MNIST, var-FMNIST and rot-FMNIST (from top to bottom).

For the rot-MNIST and rot-FMNIST we use the *rotations* procedure. Using the definitions of Ghifary et al. (2015), we consider six transformations:

- *0*: rotating 0° the original image.
- *15*: rotating 15° the original image.
- *30*: rotating 30° the original image.
- *45*: rotating 45° the original image.
- *60*: rotating 60° the original image.
- *75*: rotating 75° the original image.

Again, we use a random split to divide the original datasets in six groups and each group is applied one of the transformations defined, so we get six tasks: four with 11 667 examples and two with 11 666.

In Figure 4.13 we show examples of the four MTL image problems that we generate, with the corresponding task annotation for each one.

Experimental Procedure.
For testing the performance of our proposal we consider the following models:

- ctlNN: a CTL-based neural network, that is, a single network for all tasks.
- itlNN: an ITL-based neural network, that is, an independent network for each task.

Table 4.6: Test Accuracy with Majority Voting.

	var-MNIST	rot-MNIST	var-FMNIST	rot-FMNIST
ctINN	0.964	0.973	0.784	0.834
itINN	0.968	0.981	0.795	0.873
hsNN	0.971	0.980	0.770	0.852
cvxmtINN	**0.974** ($\lambda^* = 0.6$)	**0.984** ($\lambda^* = 0.8$)	**0.812** ($\lambda^* = 0.6$)	**0.880** ($\lambda^* = 0.6$)

- hsNN: a MTL-based neural network using the hard sharing strategy. That is, a single neural network is used for all tasks, where the first layers are shared among tasks, but a task-specific output layer is used for each task.
- cvxmtINN: a MTL-based neural network using the convex formulation we propose.

All of these models are based on convolutional network, which we will name convNet, whose architecture is based on the Spatial Transformer Network (Jaderberg et al., 2015) used in Pytorch[1]. The architecture of convNet consists, in this order, on two convolutional layers of kernel size 5, with 10 and 20 output channels each; then a dropout layer, followed by a max pooling layer, and two hidden layers with 320 and 50 neurons. After this, the output layers follow.

In the ctINN, we use a single network with the convNet architecture with 10 output neurons, one for each class. In the itINN, an independent network, with the convNet architecture and 10 output neurons, is used for each task. For the hsNN, a single network with the convNet architecture is used, but we have a group of 10 output neurons for each task in the problem. For example, if we are using of the *rotation*-based problems, we would have 60 output neurons, but only the group of 10 corresponding to each task is used with each example. In the cvxmtINN we use a network with the convNet architecture and 10 output neurons to model the common network and each of the task-specific networks. That is, given an example from task r, the 10 common output neurons and the r-th task-specific ones are combined to obtain the final output.

We use the AdamW algorithm (Loshchilov and Hutter, 2019) to train all the models considered, and the weight decay parameter μ for each model is selected using a CV-based search over the values $\{10^{-4}, 10^{-3}, 10^{-2}, 10^{-1}, 10^{0}\}$. The rest of the parameters, which are part of the architecture, are fixed and set to the default values: the dropout rate is 0.5 and we use a 2×2 max pooling layer with a stride of 2. The cvxmtINN model also has λ as a hyperparameter, and it is selected, alongside μ, using a CV grid search, where the grid for λ is $\{0, 0.2, 0.4, 0.6, 0.8, 1\}$.

The train and test sets are generates using a task-stratified split of 70% and 30%, respectively. The CV grid searches are carried out using the training set, where we use a 5-fold CV scheme. These folds are task-stratified, that is, all have the same task proportions. Also, since the problems are class-balanced and the sample size is reasonably large, the folds are expected to be class-balanceda as well.

Results.

To get more accurate results, less sensitive to randomness, we train each model 5 different times. To do this, once the optimal hyperparameters have been selected using the CV in the training set, we refit the model with these hyperparameters using the whole training

[1] www.pytorch.org/tutorials/intermediate/spatial_transformer_tutorial.html

Table 4.7: Test Mean Categorical Cross Entropy.

	var-MNIST	rot-MNIST	var-FMNIST	rot-FMNIST
ctlNN	1.274 ± 0.143	1.145 ± 0.039	2.369 ± 0.183	1.757 ± 0.075
itlNN	1.072 ± 0.029	0.873 ± 0.058	2.356 ± 0.130	1.598 ± 0.042
hsNN	1.087 ± 0.253	0.898 ± 0.073	3.067 ± 0.888	1.888 ± 0.075
cvxmtlNN	$\mathbf{0.924 \pm 0.024}$ ($\lambda^* = 0.6$)	$\mathbf{0.831 \pm 0.029}$ ($\lambda^* = 0.8$)	$\mathbf{2.147 \pm 0.090}$ ($\lambda^* = 0.6$)	$\mathbf{1.482 \pm 0.063}$ ($\lambda^* = 0.6$)

set. That is, the CV is done only once for each model in each problem, but then we repeat 5 times the procedure of training the network over the whole training set.

Although maximizing the accuracy is ultimately the goal in classification problems, it is not a differentiable measure, so we use the categorical cross entropy instead as the loss function to train the networks. Both measures are correlated, but they do not represent exactly the same behavior. We will show the results using both for completeness.

Since we have 5 instances of each model, a typical strategy to combine their predictions is majority voting. We perform this majority voting directly using the logits, in the output neurons, of each instance and averaging them, so we have 10 values, one for each class. In Table 4.6 we show the test accuracy, using the logits average already described, for each of the approaches considered. Other approach to visualize these results is to compute the categorical cross entropy directly on the averaged logits, which we show in Table 4.7. In both tables we also show the optimal values for λ selected in the CV.

Our proposal, the cvxmtlNN model, obtains the best results in all the problems, either in terms of accuracy or cross entropy. The ITL approach comes second in all problems, except for the accuracy score in var-MNIST, where the hsNN is second and itlNN goes third. The hsNN model goes third in the rest of problems, while the ctlNN gets the worst results consistently in all problems, sometimes by a large margin. By looking at the tables, it seems that a CTL approach is not able to capture the different properties of each task at once. On the other hand, the ITL approach obtains good results, because it is specialized in each task. Considering the optimal values for λ, there are, however, common information shared among the tasks. These values fall far from the margins, so neither the CTL nor the ITL are optimal approaches. This is reflected in the tables, where the cvxMTLNN outperforms consistently ctlNN and itlNN. We can assume, then, that the information learned by the common network and the task-specific ones is complementary, because their combination lead to better results. The hard sharing approach, although better than a CTL one, seems to be too rigid to effectively capture the differences among different tasks, so it is frequently surpassed by the ITL network.

4.4 Application to Renewable Energy Prediction

A transition towards renewable energies is taking place, with particular interest for solar and wind generation, which implies a demand for accurate energy production forecasts to be made for the transmission system operators, wind and solar farm managers and market agents. These forecasts can be made at different time horizons: very short (up to one hour), short (up to a few hours), or medium-long (one or more days ahead). In this application of our convex MTL techniques to renewable energies forecast, we will focus wit the latter, in particular, the hourly, day-ahead prediction, that is, the prediction of tomorrow, at each hour, is predicted today.

Machine Learning (ML), like in others forecasting problems, have an increasing presence in the energy prediction approaches. The usage of ML models require choosing the predictive features that will be used, which depends on the time horizon of interest. For short-term forecast, past values of energy production and real time meteorological data can be used; however, for longer horizons, the most common features are numerical weather predictions (NWP), that can be provided by entities such as the European Centre for Medium-Range Weather Forecasts, which is the one used in this work. For the hourly day-ahead predictions of interest here, we use the NWP forecasts of the ECMWF run at 00 UTC in a given day to predict the hourly energy productions the day before. That is, using the NWP of 00 UTC, the energy generation predictions are given for each hour from 24 to 47h.

After the selection of predictive features, the ML method better suited for the problem at hand has to be selected. Also, each method has a set of hyperparameters that influence on its behaviour and have to be adjusted in each case. In the case of interest here, there are two possibilities: using local models for single installations or global models for multiple installations within a geographic area.

Anyway, any ML approach has to deal with the changing behaviour of a wind or solar farm, which can be altered substantially according to different conditions or time. In the PV energy production this is obvious, since different times of the day, from sunrise to sunset, have very different behaviours; but there are also seasonal effects that affect the energy generation in the solar farms. For wind energy, it is more difficult to define the variables that determine different scenarios. The energy velocity forecast is the most relevant variable for energy generation, but it is important to take into account the power curve of wind turbines, which has three different response zones: one for low speed and near zero production, an intermediate one with power growing with wind velocity and one with maximum constant power up to the cut-off speed. The angle in which this wind incide is also important, since the turbines of a farm have a specific direction. Finally, the assymetrical wind velocities between the day and night period can also affect the energy production.

One way to deal with this different behaviour scenarios is to apply a MTL model, where the models built are specialized in each scenario but all scenarios are used in the learning process. In this Section a convex MTL approach will be used for wind and solar energy forecasting. To do this, it is necessary to define the tasks of interest on each case, which are described in the following subsections. In the first subsection the experimental methodology is described, showing how the models are chosen and the hyperparameters are selected. Then, the next two subsection presents the approach and the detailed task definitions used for solar and wind energy, respectively, as well as the results to judge the resultant performance.

4.4.1 Experimental Methodology.

Here we describe the methodology that we have followed to conduct the experiments of renewable energy prediction. For the solar and wind energy we use the same procedure. In each problem, we have a train, validation and test sets, each corresponding to one year of data. In the solar energy problems we have 2013, 2014 and 2015 as train, validation and test sets, respectively; while for wind energy problems we use 2016, 2017 and 2018. For both solar and wind problems we use different definition of tasks. To define these tasks we use only the training data, which partition the data, then, with these tasks'

TABLE 4.8: Hyperparameters, grids used to find them (when appropriate), and hyperparameter selection method for each model. Here, d is the number of dimensions of the data and σ is the standard deviation of the target.

Par.	Grid	ctlSVR	itlSVR	cvxMTL
C	$\left\{10^k : -1 \leq k \leq 6\right\}$	CV	CV	CV
ϵ	$\left\{\frac{\sigma}{2^k} : 1 \leq k \leq 6\right\}$	CV	CV	CV
γ	$\left\{\frac{4^k}{d} : -2 \leq k \leq 3\right\}$	CV	-	ctlSVR
γ_r	$\left\{\frac{4^k}{d} : -2 \leq k \leq 3\right\}$	-	CV	itlSVR
λ	$\left\{10^{-1}k : 0 \leq k \leq 10\right\}$	-	-	CV

definition, we apply them to get the tasks of the validation and test examples. For example, if we use the wind velocity to define three tasks, we study the velocities of the training examples to set the boundaries that define each task; then, we use this definitions on the validation and test sets. We will represent the task definition applied with the nomenclature: (taskDef)_modelName, where taskDef is a name for the task definition and modelName is the name of the model.

We consider three different models based on the standard Gaussian kernel SVR:

- ctlSVR: a CTL model, that is, a single SVR for all tasks. Its set of hyperparameters is $\{C, \gamma, \epsilon\}$, where C is the regularization trade-off parameter, γ is the kernel width, and ϵ the width of the error insensitive area.

- itlSVR: an ITL model, that is, an independent SVR for each task. For each task, we have standard SVR with its hyperparameters: $\{C_r, \gamma_r, \epsilon_r\}$ for $r = 1, \ldots, T$.

- mtlSVR: a convex MTL model, as shown in Subsection 4.2.1, with its corresponding set of hyperparameters is $\{C, \epsilon, \gamma, \gamma_1, \ldots, \gamma_T, \lambda_1, \ldots, \lambda_T\}$, where γ is the kernel width of the common part and γ_r the one of the r-th specific part; also, λ_r is the convex combination parameter corresponding to the r-th task.

Although the CTL approach does not use the tasks information, the ITL and MTL models depend on the task definition that we use. For example, prediction at different hours can define different tasks, where the possible values are, for example, (hour=14) or (hour=12). The models using this task definition will be named (hour)_itlSVR and (hour)_mtlSVR. Since each task definition partition the data, we can also use multiple task definitions, combining them and creating finer partitions. We will name (taskDef1,...,taskDefM) the combination of task definitions taskDef1, ..., taskDefM. For example, consider the (hour) definition, which, in our definition consider 14 different hours, hence, 14 tasks; and consider the season definition, which considers the prediction in each season as a different task, hence, four tasks. The combined definition (hour, season) generates 14×4 possible tasks, whose values can be, for example, (hour = 12, season = summer). The models using this combination will be named (hour, season)_itlSVR or (hour, season)_mtlSVR.

As explained in Subsection 4.2.1, the cost of methods to select the optimal hyperparameters scale exponentially with the dimension, so it is not feasible to use a CV grid search, for example, if we have more than 3 hyperparameters. In the ctlSVR and itlSVR it is not a problem, since we have 3 hyperparameters, for the common, single SVR, and for the task-independent ones, respectively. We use then a CV grid search, using as train and validation sets described above. However, to find the hyperparameters of mtlSVR we

have to make some adjustements, as shown in Subsection 4.2.4. First, we use a convex MTL formulation with a single λ parameter, common to all tasks. Second, we use the optimal kernel widths selected in validation for the CTL and ITL approaches as the widths in the MTL approach. That is, we get the optimal common γ^* and task-specific $\gamma_1^*, \ldots, \gamma_T^*$, and fix them in the mtlSVR model, not including them in the grid search procedure. Then, we use a CV grid search to find the optimal values of the remaining hyperparameters, that is, $\{C, \epsilon, \lambda\}$. In Table 4.8 we show the method to obtain each hyperparameter, as well as the grids used in the CV grid search procedures. We use the MAE as the validation metric, because is the most natural to the ϵ-insensitive loss that is used in the SVRs.

The whole procedure to get the final scores is:

1. **Scaling the target and normalizing the features.** We scale the target values to $[0, 1]$ and we normalize each feature, so it has 0 mean and a standard deviation of 1. This is done using the training data only. For the target scale, we select the target minimum and maximum values of the training set, that is, $y_{\min} = 0$, when no energy is produced, and $y_{\max}$ is the maximum capacity of the park.

2. **Using a CV grid search to select the optimal hyperparameters.** This is done using the train and validation sets, with the grids and adjustements already explained. We use the MAE as our validation metric.

3. **Predict on the test set and rescale to the original scale.** That is, we use the corresponding model $f(\cdot)$ to compute the prediction of the normalized i-th test example from task r, $\tilde{x}_i^r$, as $f(\tilde{x}_i^r)$. Then, we rescale it back to obtain the final prediction $\hat{y}_i^r = f(x_i^r) \times (y_{\max} - y_{\min}) + y_{\min}$

4. **Compute the test score.** Using the target values y_i^r and their corresponding predictions, $\hat{y}_i^r$, we measure the performance of our model using both MAE and MSE.

The whole process is carried out using a `Pipeline` object, where we make use of class `StandardScaler` to normalize the data, and `TransformedTargetRegressor` class to scale the targets. All these classes are part of the *scikit-learn* library.

To put our results in perspective, we also show the errors of simple persistence models and of multilayer perceptrons. For the perceptron we use the `MLPRegressor` class of *scikit-learn*. The architecture for both problems consists on fully connected networks with two hidden layers, with 100 and 50 neurons. We train these networks using the L-BFGS solver with a maximum of 800 iterations a tolerance of 10^{-10}. The regularization hyperparameter is selected using a CV grid search, as those described above, where the grid is $\left\{4^k : -2 \leq j \leq 3\right\}$.

4.4.2 Solar Energy

The goal is to predict the hourly energy production in two parks, located in the islands of Majorca and Tenerife, and name the corresponding problems as majorca and tenerife, respectively. In this subsection the experiments with these solar problems are presented, using the experimental procedure already shown. First a description of the problems is given and the data used, then the results are given and analyzed.

Data and Tasks.
For both problems, majorca and tenerife, the same variables, extracted from the Numerical Weather Prediction (NWP), are used. These variables, extracted from NWP predictions made by the European Center for Medium Weather Forecasts (ECMWF; ECMWF (1975)), are:

- Surface net solar radiation (SSR).
- Surface solar radiation downwards (SSRD).
- Total Cloud Cover (TCC).
- Temperature at 2 meters (T2M).
- Module of the speed of wind at 10 meters (v10).

The radiation variables SSR, solar radiation, and SSRD, solar radiation plus the diffuse radiation scattered by the atmosphere, as well as the TCC, have all a direct impact on PV production. The T2M and v10 features are also considered because they influence the conversion of photon energy into electrical one, and also the overall performance of PV stations.

To collect these features, geographical grids with a $0.125°$ spatial resolution are considered. For majorca, the grid has its northeast coordinates at $(2°, 40°)$, and its southwest coordinates at $(4°, 39°)$. For tenerife, the coordinates are $(-17.5°, 28.75°)$ for the northeast corner, and $(-15.5°, 27.75°)$ for the southwest one. That is, both grids have a longitude width of 2 degrees and a latitude height of 1 degree. With the spatial resolution considered, this results in a total number of $17 \times 9 = 153$ grid points; since we use five variables at every point, the total dimension of our data is thus $5 \times 153 = 765$.

Observe that we obtain large dimensional patterns, where the features might be highly correlated. That is, a feature, SSR for example, measured in one point of the grid and another close point might be very correlated, since the grids are squares with sides of about 12 km. This correlation will affect those models based on matrix-vector computations, such as linear models, which are the most obvious, but, also, to some extent, to neural networks. Although Ridge or Tikhonov regularization can alleviate this issue for these models, the kernel-methods, such as the kernel SVMs, seems better suited for these kind of problems. When we use kernel methods, such as the Gaussian kernel $\exp -\gamma \|x - y\|^2$, the algorithm learns using the distances among patterns $\|x - y\|$, instead of its features. These distances scale linearly with the dimension of data, that is, consider the features scaled to $[0, 1]$, then a rough estimate of the distance between two patterns would be d. In the extreme case where all features are equal, i.e. $x_j = x_1$ for all $j = 1, \ldots, d$; then, $\|x - x'\| = d(x_1 - x'_1)$. However, this influence of the dimension can be easily controlled by γ, and, if selected properly, should not affect the performance of a Gaussian SVR.

Recall that we use data from years 2013, 2014 and 2015 as train, validation and test sets, respectively. We show the errors in both total MWh and as percentages, in the range $[0, 100]$ of the total install PV power in each photovoltaic park, 72.46 MW in majorca and 107.68 MW in tenerife. We remove night data for obvious reasons and make predictions between 06 UTC and 19 UTC for `majorca` and between 07 UTC and 20 UTC for `tenerife`. The hour of the day has a direct influence on the solar radiation, and, therefore, on energy production. Also, the season of the year has a similar impact on the production. This leads to two obvious task definitions:

- `hour`: The prediction at each hour is defined as a different task; there are thus 14 tasks in `majorca` (from 06 to 19 UTC) and `tenerife` (from 07 to 20 UTC).
- `season`: The prediction at each season is defined as different task. With a slight abuse of language, the definitions for each season used are: Spring, from 16 February to 15 May; Summer, from 16 May to 15 August; Autumn, from 16 August to 15 November; and Winter, from 16 November to 15 February.

In Subfigures 4.14a and 4.14b the hourly averages of the PV energy in MWh are shown for majorca and tenerife. Also, in Subfigures 4.14c and 4.14d the monthly averages, colored by season.

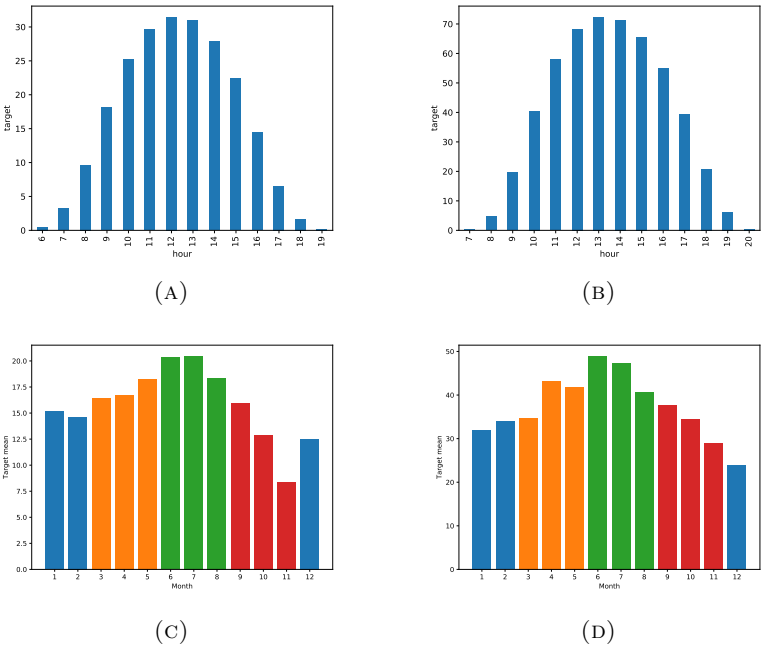

(A) (B) (C) (D)

FIGURE 4.14: Hourly photovoltaic energy mean in `majorca` a and `tenerife` b measured in MWh. Photovoltaic energy monthly averages for `majorca` c and `tenerife` d , colored using the tasks defined using the season and measured in MWh. All the histograms have been computed using data from year 2016.

TABLE 4.9: Test MAEs (left), test MSEs (center), and optimal mixing λ^* (right) of the solar energy models considered in `majorca`. Base units are either MWh or percentages (%). The best model errors are shown in bold.

	MAE			**MSE**			$\boldsymbol{\lambda^*}$
	MWh	%	rank	MWh	‰	Rank	
ctISVR	5.265	7.265	(6)	59.322	112.985	(6)	-
(season)_itISVR	5.305	7.384	(7)	59.591	113.498	(7)	-
(season)_mtISVR	**4.884**	**6.740**	**(1)**	53.222	101.366	(2)	0.4
(hour)_itISVR	5.083	7.015	(4)	54.540	103.877	(3)	-
(hour)_mtISVR	4.957	6.840	(2)	**52.614**	**100.208**	**(1)**	0.3
(hour, season)_itISVR	5.250	7.251	(5)	57.927	110.328	(5)	-
(hour, season)_mtISVR	5.038	6.952	(3)	54.601	103.992	(4)	0.3

TABLE 4.10: Test MAEs (left), test MSEs (center), and optimal mixing λ^* (right) of the solar energy models considered in `tenerife`. Base units are either MWh or percentages (%). The best model errors are shown in bold. The positions with hyphens correspond to the model ranked first in terms of MAE or MSE, as indicated by its column.

	MAE			**MSE**			$\boldsymbol{\lambda^*}$
	MWh	%	Rank	MWh	‰	Rank	
ctlSVR	5.786	5.373	(5)	88.323	76.174	(5)	-
(season)_itlSVR	5.930	5.545	(6)	97.454	84.611	(6)	-
(season)_mtlSVR	5.579	5.181	(4)	86.227	74.366	(3)	0.8
(hour)_itlSVR	5.403	5.018	(2)	86.686	74.762	(4)	-
(hour)_mtlSVR	**5.376**	**4.993**	**(1)**	**84.207**	**72.624**	**(1)**	0.7
(hour, season)_itlSVR	6.025	5.554	(7)	104.536	90.297	(7)	-
(hour, season)_mtlSVR	5.494	5.102	(3)	85.440	73.687	(2)	0.7

TABLE 4.11: Wilcoxon p-values for absolute (left) and quadratic (right) errors.

	MAE		**MSE**	
	`majorca`	`tenerife`	`majorca`	`tenerife`
ctlSVR	0.014 (4)	0.000 (5)	0.081 (4)	0.000 (5)
(season)_itlSVR	0.008 (5)	0.636 (5)	0.215 (4)	0.354 (5)
(season)_mtlSVR	—— (1)	0.000 (4)	0.036 (2)	0.000 (3)
(hour)_itlSVR	0.693 (2)	0.006 (2)	0.000 (3)	0.000 (4)
(hour)_mtlSVR	0.067 (1)	—— (1)	—— (1)	—— (1)
(hour, season)_itlSVR	0.000 (3)	0.000 (6)	0.000 (4)	0.098 (5)
(hour, season)_mtlSVR	0.000 (2)	0.000 (3)	0.745 (3)	0.000 (2)

Experimental Results.
In Tables 4.9 and 4.10 we show the numerical results for majorca and tenerife, respectively. We give the test MAE, which is the most natural metric for SVRs, as well as the MSE. In the case of percentages, for MAE, we give the percentage corresponding to the total installed power, and for the MSE, the permyriad, that is per 10 000, of the installed power. We also show the rankings in terms of MAE or MSE, and the optimal hyperparameter λ^* selected in the CV for the MTL models.

To show statistical significance the Wilcoxon test is used, but instead of testing every pair of models, the rankings of Tables 4.9 and 4.10 are used. The Wilcoxon test is applied between each model and the next in ranking at the 0.05 level, to determine if the difference is significant. The test is applied over the list of errors commited by each model in the patterns of the test set. When the null hypothesis of the Wilcoxon test is refused, it implies that the distribution of the difference between the errors does not have its median at 0. In Table 4.11, we show the p-values of the pairwise tests. If the p-value is smaller than the level considered level of 0.05, then the different between models is considered significant. With these procedure, a new significant ranking, shown in Table 4.11, is generated: starting from the best model, we compare each model with the next best one, and we increase the ranking only if the difference is significant. For example, in Table 4.9, in terms of MAE, the first model, (season)_mtlSVR, is tested against the second one, (hour)_mtlSVR. In Table 4.11, we show the p-value corresponding to that test, which is 0.067, and since it is larger than the level 0.05, the ranking is not increased and both models have the same significant ranking.

Looking at the tables, it is easy to see that the MTL approaches obtain the best results in both problems, while ctlSVR has the worst performance in `tenerife` and second worst in `majorca`. ITL models are more difficult to interpret, although they are always behind their corresponding MTL approaches, they can obtain good results, like the (hour)_itlSVR in majorca which is second; but they can also have bad performances, like the (season)_itlSVR in tenerife.

The λ^* values can help to understand this behaviour. In both problems, the selected values lie far from the extremes 0 or 1, which distances the MTL approaches from the CTL or ITL ones. If these values are optimal, then the CTL or ITL equivalent models, with $\lambda = 1$ and $\lambda = 0$, respectively, obtain a worse result in validation. This is reflected also in the test set, as shown in the tables. Also, it is noticeable that the optimal values for majorca are all smaller than 0.5, which can be intepreted as models with a stronger common part, while in tenerife, the optimal values are larger than 0.5 which reflects stronger independent parts. Although the MTL approaches get the best results with any task definition, the (hour) definition seems to work best than the (season) one. The (hour)_mtlSVR gets a second best result, which is not significantly worse than the best one in majorca, and the single best result in tenerife.

For completeness the scores of persistence models and a neural network are given. The persistence forecasts are obtained by predicting at each hour the target value 24 hours prior. By doing this, the MAE scores for majorca are 5.776 MWh and 7.766 MWh, which scaled to $[0, 100]$ correspond to 7.97% and 7.21%; which are an 18% and 44% error increase of the best MTL models. The neural network errors are 5.140 MWh and 5.763 MWh, that is, 7.09% and 5.35% of the total PV installed. While this results are still competitive, this performance is worse than those of the convex MTL models proposed.

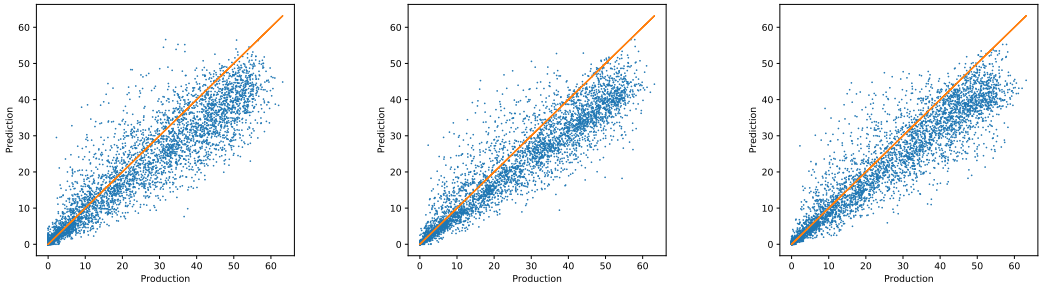

(A) (B) (C)

FIGURE 4.15: Real energy production against prediction made by the best CTL a, ITL b, and MTL c models in `majorca` in terms of MAE; the perfect prediction line is shown in orange. The units of the axis are MWh.

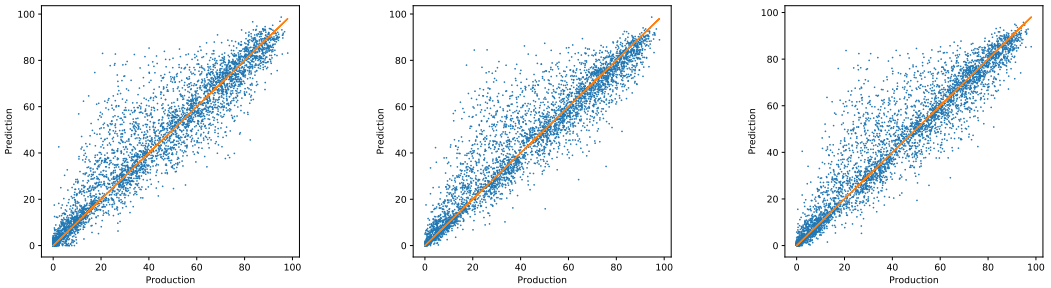

(A) (B) (C)

FIGURE 4.16: Real energy production against prediction made by the best CTL a, ITL b, and MTL c models in `tenerife` in terms of MAE; the perfect prediction line is shown in orange. The units of the axis are MWh.

To get a better understanding of the results we plot the predictions against the target values of the CTL model and the best ITL and MTL ones. In the case of majorca, we plot the predictions ctlSVR, (hour)_itlSVR and (season)_mtlSVR in Figure 4.15. From these scatter plots it seems that the CTL approach has a larger deviation in its predictions, while the ITL one has a bias, that is, it systematically underestimates the prediction corresponding to larger values of energy production. The MTL approach seems to correct, to a certain degree, this bias of the ITL model, while preserving a smaller variance than the CTL one. For tenerife we plot the predictions of ctlSVR, (hour)_itlSVR and (hour)_mtlSVR, which are shown in Figure 4.16. It is more difficult to interpret the plots in this case, although it is possible to highlight that the MTL approach seems less prone to overestimate the production at lower values than either the CTL or ITL models.

4.4.3 Wind Energy

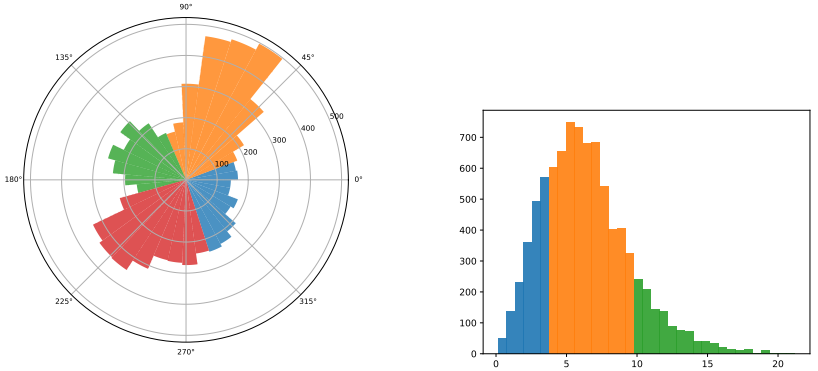

(A) (B)

FIGURE 4.17: Histograms of wind. a Histogram of wind angles derived from NWP data for the year 2016 in Sotavento colored by task angle. b Histogram of wind velocity derived from NWP data for the year 2016 and measured in m/s in Sotavento colored by task velocity.

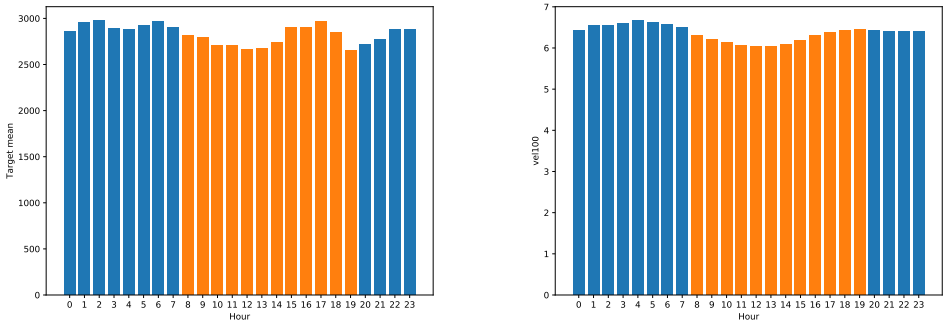

(A) (B)

FIGURE 4.18: Histograms of wind. a Hourly mean measured in kWh of generated energy during the year 2016 in Sotavento colored by task timeOfDay. b Hourly mean of velocity in Sotavento derived from NWP data for the year 2016 and measured in m/s at 100 m colored by task timeOfDay.

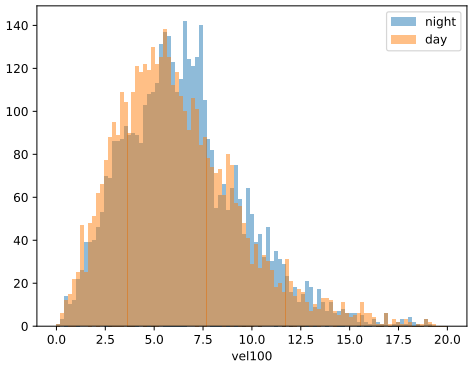

FIGURE 4.19: Histograms of the velocity of wind at 100m derived from NWP data for the year 2016 and measured in m/s during the day and night in Sotavento.

Data and Tasks.
We want to predict the wind energy production at the Sotavento wind park located in Galicia, Spain. The variables from the NWP that we consider as predictors are:

- Eastward component of the wind at 10 m (U10).
- Northward component of the wind at 10 m (V10).
- Module of velocity of the wind at 10 m.
- Eastward component of the wind at 100 m (U100).
- Northward component of the wind at 100 m (V100).
- Module of velocity of the wind at 100 m.
- Surface Pressure (sp).
- 2 meter temperature (2t)

These variables are collected in a grid, which is approximately centered at the farm, with northeast and southwest coordinates at $(-9.5°, 44°)$ and $(-6°, 42.25°)$, respectively, and a spatial resolution of $0.125°$. This results in a grid with 435 points, that, with the 8 variables considered at each point, gives a total number of 3480 predictive features. We scale the energy productions values to $[0, 100]$ using the maximum power installed (17.56 MW), which corresponds to the value 100. Recall that we have three years of data: 2016, 2017 and 2018, which are used as train, validation and test sets. Although there are no obvious task definitions, we consider three different criteria:

- angle: Here the wind angle at a height of $100m$ is considered, which is obtained from the U100 and V100 variables. First, the most frequent angle is estimated, which is $56°$, and then, we use it as the center of the first quadrant. That is, the patterns that correspond to the first task as those whose wind angle lies between 11 and $101°$ The other three quadrants, corresponding to a task each, are defined by the remaining sectors of $90°$. The histogram of wind angles, and the defined quadrants in different colors, are shown in Figure 4.17a

- velocity: Here the wind velocity at a height of $100m$ is considered, which is again obtained from the U100 and V100 variables. The speed boundaries selected to define three tasks are 4 and 10m/s, which, for an ideal generator, are approximately the starting point of wind energy generation and its maximum power plateau, before cut-off speed. In Figure 4.17b the histrogram of velocities is shown with the task regions colored.

- timeOfDay: Here the 24 hours of a day are divided in two 12 hours periods: a day period between 08 and 19 UTC, and a night one between 20 to 07 UTC. In Figures 4.18a and 4.18b the hourly average energy production and wind speed are shown, with the hours colored according to the two tasks defined. In Figure 4.19 the histograms of wind velocity in the night and day periods are shown.

For these task definitions, it is necessary to perform an analysis of the data, which is done only using the train set, corresponding to 2016. The tasks in this case are not as clear as that defined for the solar energy. For the angle and velocity definitions some differences across tasks in the histograms can be found, but not definitive ones. For the timeOfDay definition, the two histograms of Figure 4.19 look very similar. Moreover, the boundaries of the tasks are set in a way that is partially arbitrary, and a bad selection of tasks could lead to poor results.

TABLE 4.12: Test MAEs (left), MSEs scores (center), and optimal mixing λ^* (right) of the Sotavento wind energy models considered. The best model errors are shown in bold.

	MAE	**MSE**	$\boldsymbol{\lambda^*}$
ctlSVR	**6.132** (1)	90.228 (2)	-
(velocity)_itlSVR	6.211 (7)	93.363 (7)	-
(velocity)_mtlSVR	6.208 (6)	93.199 (6)	0
(timeOfDay)_itlSVR	6.283 (9)	93.594 (9)	-
(timeOfDay)_mtlSVR	**6.132** (1)	90.228 (2)	1
(timeOfDay, velocity)_itlSVR	6.341 (11)	97.250 (11)	-
(timeOfDay, velocity)_mtlSVR	6.312 (10)	94.774 (10)	0.4
(timeOfDay, angle)_itlSVR	6.266 (8)	93.517 (8)	-
(timeOfDay, angle)_mtlSVR	**6.132** (1)	90.228 (2)	1
(timeOfDay, angle, velocity)_itlSVR	6.410 (12)	102.031 (12)	-
(timeOfDay, angle, velocity)_mtlSVR	**6.132** (1)	90.228 (2)	1
(angle)_itlSVR	6.170 (4)	91.586 (4)	-
(angle)_mtlSVR	6.135 (2)	**90.026** (1)	0.9
(angle, velocity)_itlSVR	6.173 (5)	92.529 (5)	-
(angle, velocity)_mtlSVR	6.168 (3)	90.990 (3)	0.7

TABLE 4.13: Wilcoxon p-values and corresponding ranking for absolute (right) and quadratic (left) wind energy errors in Sotavento. The positions with hyphens correspond to the model ranked first in terms of MAE or MSE, as indicated by its column.

	MAE	**MSE**
ctlSVR	—— (1)	—— (2)
(velocity)_itlSVR	0.570 (3)	0.150 (3)
(velocity)_mtlSVR	0.356 (3)	0.466 (3)
(timeOfDay)_itlSVR	0.195 (4)	0.258 (4)
(timeOfDay)_mtlSVR	—— (1)	—— (2)
(timeOfDay, velocity)_itlSVR	0.941 (4)	0.021 (5)
(timeOfDay, velocity)_mtlSVR	0.428 (4)	0.650 (4)
(timeOfDay, angle)_itlSVR	0.000 (4)	0.015 (4)
(timeOfDay, angle)_mtlSVR	—— (1)	—— (2)
(timeOfDay, angle, velocity)_itlSVR	0.090 (4)	0.024 (6)
(timeOfDay, angle, velocity)_mtlSVR	—— (1)	—— (2)
(angle)_itlSVR	0.855 (3)	0.644 (3)
(angle)_mtlSVR	0.035 (2)	—— (1)
(angle, velocity)_itlSVR	0.253 (3)	0.465 (3)
(angle, velocity)_mtlSVR	0.018 (3)	0.001 (3)

Experimental Results.
In Table 4.12 the MAE and MSE scores are shown, and also the ranking is given in parentheses. Unlike the solar energy case, here the CTL approach seems to better suited than using an ITL one. This is also reflected in the selection of λ^* values, that are close to 1, the CTL equivalent case, in the models that get best results, see all the models using $\lambda^* = 1$, which are equivalent to ctlSVR but also the cases of (angle)_mtlSVR and (angle, velocity)_mtlSVR, that are second and third using $\lambda^* = 0.9$ and $\lambda^* = 0.7$. Those models

who put the emphasis on the independent parts, like (timeOfDay, velocity)_mtlSVR, and, of course, the ITL approaches, get worse results. As with the solar energy problems, the statistical significance of the results is tested using the Wilcoxon test. As before, using the ranking of Table 4.12, the significance of the difference between one model and its immediate succesor is tested. In Table 4.13 the p-values of these Wilcoxon tests are given, and the statistical significant ranking is shown. Recall that two models have different significant ranking only if the Wilcoxon test hypothesis is refused. The CTL approach obtains the best results, being the best model in terms of MAE and second best in terms of MSE. Nevertheless, the equivalent MTL approaches that use $\lambda^* = 1$ trivially tie at first place, these are (timeOfDay)_mtlSVR, (timeOfDay, angle)_mtlSVR and (timeOfDay, angle, velocity)_mtlSVR; while the (angle)_mtlSVR gets the second best MAE score. When the MSE scores are analyzed, the roles are reversed, the (angle)_mtlSVR gets the best result, and the ctlSVR and the equivalents MTL approaches are second.

This advantage of the CTL approach can find its roots on poorly defined tasks, which do not have a strong relation with the energy production. Also, the definition of the tasks is made using the train set, data from year 2016, which may not be useful to the validation or test years. Nevertheless, the MTL approaches, having the possibility of blending to either CTL or ITL approaches get the best results too.

In this wind energy problem, the persistence forecasts, which again predict the energy production the previous day at the same hour, obtain an error of 15.64%, which is quite large and represent a 150% increase on the lowest error using SVRs. This is not unusual, since the wind velocity or angle between two different days are not necessarily correlated. With the neural network regressor, the error is a 6.66%, which is also greater than any of the models considered.

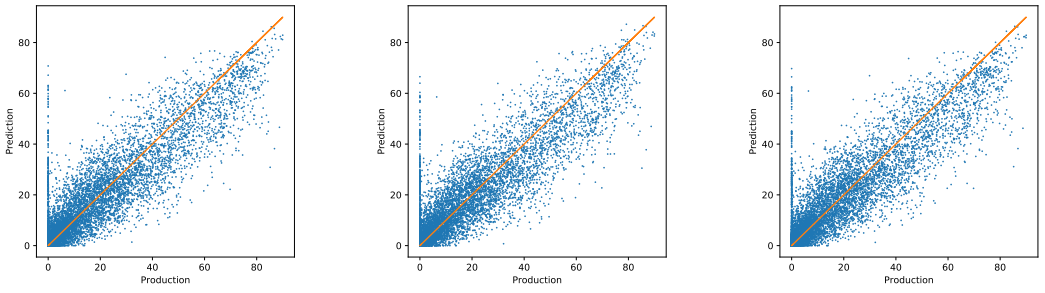

(A) (B) (C)

FIGURE 4.20: Real energy production against prediction made by the best CTL a, ITL b, and MTL c models for Sotavento; the perfect prediction line is shown in orange. The units of the axis are percentages points of the total PV energy installed.

Again, we plot the predictions agains the target values of the CTL model and best ITL, (angle)_itlSVR, and pure MTL, (angle)_mtlSVR approaches. The presence of points with zero production is noticeable, but this is relatively frequent in wind energy. It can be caused either by energy curtailments or by maintenance periods of the wind farm. Also, it is appreciable the frequency of small production values, below 20 %, which is due to the approximate Weibull distribution of wind speeds, where small speed values have higher frequencies. With these considerations, it is difficult to compare the plots and find significant differences in model performance.

4.5 Conclusions

In this chapter, we have...

Chapter 5

Adaptive Graph Laplacian for Multi-Task Learning

5.1 Introduction

5.2 Graph Laplacian Multi-Task Support Vector Machine

In **?** we proposed a convex formulation of the Graph Laplacian MTL SVM which includes a common regularization term and whose primal problem is

$$\begin{aligned} \underset{\boldsymbol{w},\boldsymbol{v}_1,\ldots,\boldsymbol{v}_T,b,\boldsymbol{\xi}}{\arg\min} \quad & \sum_{r=1}^{T} C_r \sum_{i=1}^{n_r} \xi_i^r + \frac{\nu}{2} \sum_{r=1}^{T} \sum_{s=1}^{T} A_{rs} \|\boldsymbol{v}_r - \boldsymbol{v}_s\|^2 + \frac{1}{2} \sum_r \|\boldsymbol{v}_r\|^2 + \frac{1}{2} \|\boldsymbol{w}\|^2 \\ \text{s.t.} \quad & y_i^r(\lambda(\boldsymbol{w} \cdot \boldsymbol{x}_i^r) + (1-\lambda)(\boldsymbol{v}_r \cdot \boldsymbol{x}_i^r) + b_r) \geq p_i^r - \xi_i^r, \\ & \xi_i^r \geq 0,\ i = 1,\ldots,n_r,\ r = 1,\ldots,T. \end{aligned} \tag{5.1}$$

The corresponding Lagrangian is

$$\begin{aligned} &\mathcal{L}(\boldsymbol{w}, \boldsymbol{v}_r, b_r, \xi_i^r, \boldsymbol{\alpha}, \boldsymbol{\beta}) \\ &= \sum_{r=1}^{T} C_r \sum_{i=1}^{n_r} \xi_i^r + \frac{\nu}{2} \sum_{r=1}^{T} \sum_{s=1}^{T} A_{rs} \|\boldsymbol{v}_r - \boldsymbol{v}_s\|^2 + \frac{1}{2} \sum_r \|\boldsymbol{v}_r\|^2 + \frac{1}{2} \|\boldsymbol{w}\|^2 \\ &\quad - \sum_{r=1}^{T} \sum_{i=1}^{n_r} \alpha_i^r [y_i^r(\lambda(\boldsymbol{w} \cdot \boldsymbol{x}_i^r) + (1-\lambda)(\boldsymbol{v}_r \cdot \boldsymbol{x}_i^r) + b_r) - p_i^r + \xi_i^r] - \sum_{r=1}^{T} \sum_{i=1}^{n_r} \beta_i^r \xi_i^r. \end{aligned} \tag{5.2}$$

Taking derivatives

$$\begin{aligned}
\frac{\partial \mathcal{L}}{\partial \boldsymbol{w}} = 0 &\implies \boldsymbol{w} = \lambda \sum_{r=1}^{T} \sum_{i=1}^{m_r} \alpha_i^r y_i^r x_i^r \ , \\
\frac{\partial \mathcal{L}}{\partial \boldsymbol{v}_r} = 0 &\implies \boldsymbol{v}_r + \sum_{s=1}^{T} (L_{rs} + L_{sr})(\boldsymbol{v}_r^* - \boldsymbol{v}_s^*) = \sum_{i=1}^{m_r} \alpha_i^r y_i^r x_i^r \ , \\
\frac{\partial \mathcal{L}}{\partial b_r} = 0 &\implies \sum_{i=1}^{m_r} \alpha_i^r y_i^r = 0 \ , \\
\frac{\partial \mathcal{L}}{\partial \xi_i^r} = 0 &\implies C_r - \alpha_i^r - \beta_i^r = 0 \ .
\end{aligned}$$

Observe that

$$\begin{aligned}
\boldsymbol{v}^\intercal (I_T \otimes I_d) \boldsymbol{v} &= \sum_{r=1}^{T} \|v_r\|^2 \, , \\
\boldsymbol{v}^\intercal (L \otimes I_d) \boldsymbol{v} &= \frac{1}{2} \sum_{r=1}^{T} \sum_{s=1}^{T} A_{rs} \|v_r - v_s\|^2 \, ,
\end{aligned}$$

Proof:

$$\begin{aligned}
\boldsymbol{v}(L \otimes I_d)\boldsymbol{v} &= \boldsymbol{v}(D \otimes I_d)\boldsymbol{v} - \boldsymbol{v}(A \otimes I_d)\boldsymbol{v} \\
&= \sum_{r=1}^{T} \sum_{s=1}^{T} D_{rs} v_r^\intercal v_s - \sum_{r=1}^{T} \sum_{s=1}^{T} A_{rs} v_r^\intercal v_s \\
&= \sum_{r=1}^{T} D_{rr} v_r^\intercal v_r - \sum_{r=1}^{T} \sum_{s=1}^{T} A_{rs} v_r^\intercal v_s \\
&= \sum_{r=1}^{T} \sum_{s=1}^{T} A_{rs} v_r^\intercal v_r - \sum_{r=1}^{T} \sum_{s=1}^{T} A_{rs} v_r^\intercal v_s \\
&= \sum_{r=1}^{T} \sum_{s=1}^{T} A_{rs} (v_r^\intercal v_r - v_r^\intercal v_s)
\end{aligned}$$

If A is symmetric, that is $A_{rs} = A_{sr}$, then

$$\begin{aligned}
\sum_{r=1}^{T}\sum_{s=1}^{T} A_{rs}(v_r^\intercal v_r - v_r^\intercal v_s) &= \sum_{r=1}^{T}\sum_{s=r}^{T}\{A_{rs}(v_r^\intercal v_r - v_r^\intercal v_s) + A_{sr}(v_s^\intercal v_s - v_s^\intercal v_r)\} \\
&= \sum_{r=1}^{T}\sum_{s=r}^{T}\{(A_{rs} + A_{sr})(v_r^\intercal v_r + v_s^\intercal v_s - 2v_r^\intercal v_s)\} \\
&= \sum_{r=1}^{T}\sum_{s=r}^{T}\{(A_{rs} + A_{sr})\,\|w_r - w_s\|^2\} \\
&= \frac{1}{2}\sum_{r=1}^{T}\sum_{s=1}^{T}\{(A_{rs} + A_{sr})\,\|w_r - w_s\|^2\} \\
&= \sum_{r=1}^{T}\sum_{s=1}^{T}\{A_{rs}\,\|w_r - w_s\|^2\}.
\end{aligned}$$

5.3 Adaptive Graph Laplacian Algorithm

If we want to learn A from data we would like the matrix to meet some requirements:

- A has to be symmetric, so we can express the regularizer using the Laplacian in the dual form.
- The rows of A add up to 1.

5.4 Experiments

5.5 Conclusions

In this chapter, we have...

Bibliography

Agarwal, A., III, H. D., and Gerber, S. (2010). Learning multiple tasks using manifold regularization. In Lafferty, J. D., Williams, C. K. I., Shawe-Taylor, J., Zemel, R. S., and Culotta, A., editors, *Advances in Neural Information Processing Systems 23: 24th Annual Conference on Neural Information Processing Systems 2010. Proceedings of a meeting held 6-9 December 2010, Vancouver, British Columbia, Canada*, pages 46–54. Curran Associates, Inc.

Akhiezer, N. I. and Glazman, I. M. (1961). Theory of linear operators in hilbert space.

Álvarez, M. A., Rosasco, L., and Lawrence, N. D. (2012). Kernels for vector-valued functions: A review. *Found. Trends Mach. Learn.*, 4(3):195–266.

Ando, R. K. and Zhang, T. (2005). A framework for learning predictive structures from multiple tasks and unlabeled data. *J. Mach. Learn. Res.*, 6:1817–1853.

Argyriou, A., Clémençon, S., and Zhang, R. (2013). Learning the graph of relations among multiple tasks. *HAL*.

Argyriou, A., Evgeniou, T., and Pontil, M. (2006). Multi-task feature learning. In Schölkopf, B., Platt, J. C., and Hofmann, T., editors, *Advances in Neural Information Processing Systems 19, Proceedings of the Twentieth Annual Conference on Neural Information Processing Systems, Vancouver, British Columbia, Canada, December 4-7, 2006*, pages 41–48. MIT Press.

Argyriou, A., Evgeniou, T., and Pontil, M. (2008). Convex multi-task feature learning. *Mach. Learn.*, 73(3):243–272.

Argyriou, A., Micchelli, C. A., Pontil, M., and Ying, Y. (2007). A spectral regularization framework for multi-task structure learning. In Platt, J. C., Koller, D., Singer, Y., and Roweis, S. T., editors, *Advances in Neural Information Processing Systems 20, Proceedings of the Twenty-First Annual Conference on Neural Information Processing Systems, Vancouver, British Columbia, Canada, December 3-6, 2007*, pages 25–32. Curran Associates, Inc.

Baldassarre, L., Rosasco, L., Barla, A., and Verri, A. (2012). Multi-output learning via spectral filtering. *Mach. Learn.*, 87(3):259–301.

Bartlett, P. L. and Mendelson, S. (2002). Rademacher and gaussian complexities: Risk bounds and structural results. *J. Mach. Learn. Res.*, 3:463–482.

Barzilai, A. and Crammer, K. (2015). Convex multi-task learning by clustering. In Lebanon, G. and Vishwanathan, S. V. N., editors, *Proceedings of the Eighteenth International Conference on Artificial Intelligence and Statistics, AISTATS 2015, San Diego, California, USA, May 9-12, 2015*, volume 38 of *JMLR Workshop and Conference Proceedings*. JMLR.org.

Baxter, J. (2000). A model of inductive bias learning. *Journal of artificial intelligence research*, 12:149–198.

Ben-David, S. and Borbely, R. S. (2008). A notion of task relatedness yielding provable multiple-task learning guarantees. *Mach. Learn.*, 73(3):273–287.

Ben-David, S. and Schuller, R. (2003). Exploiting task relatedness for mulitple task learning. In Schölkopf, B. and Warmuth, M. K., editors, *Computational Learning Theory and Kernel Machines, 16th Annual Conference on Computational Learning Theory and 7th Kernel Workshop, COLT/Kernel 2003, Washington, DC, USA, August 24-27, 2003, Proceedings*, volume 2777 of *Lecture Notes in Computer Science*, pages 567–580. Springer.

Bergstra, J. and Bengio, Y. (2012). Random search for hyper-parameter optimization. *J. Mach. Learn. Res.*, 13:281–305.

Bonilla, E. V., Chai, K. M. A., and Williams, C. K. I. (2007). Multi-task gaussian process prediction. In Platt, J. C., Koller, D., Singer, Y., and Roweis, S. T., editors, *Advances in Neural Information Processing Systems 20, Proceedings of the Twenty-First Annual Conference on Neural Information Processing Systems, Vancouver, British Columbia, Canada, December 3-6, 2007*, pages 153–160. Curran Associates, Inc.

Burges, C. J. C. (1998). A tutorial on support vector machines for pattern recognition. *Data Min. Knowl. Discov.*, 2(2):121–167.

Cai, F. and Cherkassky, V. (2009). SVM+ regression and multi-task learning. In *International Joint Conference on Neural Networks, IJCNN 2009, Atlanta, Georgia, USA, 14-19 June 2009*, pages 418–424. IEEE Computer Society.

Cai, F. and Cherkassky, V. (2012). Generalized SMO algorithm for svm-based multitask learning. *IEEE Trans. Neural Networks Learn. Syst.*, 23(6):997–1003.

Caruana, R. (1997). Multitask learning. *Mach. Learn.*, 28(1):41–75.

Cavallanti, G., Cesa-Bianchi, N., and Gentile, C. (2010). Linear algorithms for online multitask classification. *J. Mach. Learn. Res.*, 11:2901–2934.

Chen, J., Liu, J., and Ye, J. (2010). Learning incoherent sparse and low-rank patterns from multiple tasks. In Rao, B., Krishnapuram, B., Tomkins, A., and Yang, Q., editors, *Proceedings of the 16th ACM SIGKDD International Conference on Knowledge Discovery and Data Mining, Washington, DC, USA, July 25-28, 2010*, pages 1179–1188. ACM.

Chen, J., Tang, L., Liu, J., and Ye, J. (2009). A convex formulation for learning shared structures from multiple tasks. In Danyluk, A. P., Bottou, L., and Littman, M. L., editors, *Proceedings of the 26th Annual International Conference on Machine Learning, ICML 2009, Montreal, Quebec, Canada, June 14-18, 2009*, volume 382 of *ACM International Conference Proceeding Series*, pages 137–144. ACM.

Chen, J., Zhou, J., and Ye, J. (2011). Integrating low-rank and group-sparse structures for robust multi-task learning. In Apté, C., Ghosh, J., and Smyth, P., editors, *Proceedings of the 17th ACM SIGKDD International Conference on Knowledge Discovery and Data Mining, San Diego, CA, USA, August 21-24, 2011*, pages 42–50. ACM.

Ciliberto, C., Mroueh, Y., Poggio, T. A., and Rosasco, L. (2015). Convex learning of multiple tasks and their structure. In Bach, F. R. and Blei, D. M., editors, *Proceedings of the 32nd International Conference on Machine Learning, ICML 2015, Lille, France, 6-11 July 2015*, volume 37 of *JMLR Workshop and Conference Proceedings*, pages 1548–1557. JMLR.org.

Crammer, K. and Mansour, Y. (2012). Learning multiple tasks using shared hypotheses. In Bartlett, P. L., Pereira, F. C. N., Burges, C. J. C., Bottou, L., and Weinberger, K. Q., editors, *Advances in Neural Information Processing Systems 25: 26th Annual Conference on Neural Information Processing Systems 2012. Proceedings of a meeting held December 3-6, 2012, Lake Tahoe, Nevada, United States*, pages 1484–1492.

Dinuzzo, F. (2013). Learning output kernels for multi-task problems. *Neurocomputing*, 118:119–126.

ECMWF (1975). European Center for Medium–range Weather Forecasts. http://www.ecmwf.int/.

Evgeniou, T., Micchelli, C. A., and Pontil, M. (2005). Learning multiple tasks with kernel methods. *J. Mach. Learn. Res.*, 6:615–637.

Evgeniou, T. and Pontil, M. (2004). Regularized multi–task learning. In Kim, W., Kohavi, R., Gehrke, J., and DuMouchel, W., editors, *Proceedings of the Tenth ACM SIGKDD International Conference on Knowledge Discovery and Data Mining, Seattle, Washington, USA, August 22-25, 2004*, pages 109–117. ACM.

Fung, G. and Mangasarian, O. L. (2001). Proximal support vector machine classifiers. In Lee, D., Schkolnick, M., Provost, F. J., and Srikant, R., editors, *Proceedings of the seventh ACM SIGKDD international conference on Knowledge discovery and data mining, San Francisco, CA, USA, August 26-29, 2001*, pages 77–86. ACM.

Ghifary, M., Kleijn, W. B., Zhang, M., and Balduzzi, D. (2015). Domain generalization for object recognition with multi-task autoencoders. In *IEEE International Conference on Computer Vision, ICCV*, pages 2551–2559. IEEE Computer Society.

Gong, P., Ye, J., and Zhang, C. (2012a). Multi-stage multi-task feature learning. In Bartlett, P. L., Pereira, F. C. N., Burges, C. J. C., Bottou, L., and Weinberger, K. Q., editors, *Advances in Neural Information Processing Systems 25: 26th Annual Conference on Neural Information Processing Systems 2012. Proceedings of a meeting held December 3-6, 2012, Lake Tahoe, Nevada, United States*, pages 1997–2005.

Gong, P., Ye, J., and Zhang, C. (2012b). Robust multi-task feature learning. In Yang, Q., Agarwal, D., and Pei, J., editors, *The 18th ACM SIGKDD International Conference on Knowledge Discovery and Data Mining, KDD '12, Beijing, China, August 12-16, 2012*, pages 895–903. ACM.

Han, L. and Zhang, Y. (2015). Learning tree structure in multi-task learning. In Cao, L., Zhang, C., Joachims, T., Webb, G. I., Margineantu, D. D., and Williams, G.,

editors, *Proceedings of the 21th ACM SIGKDD International Conference on Knowledge Discovery and Data Mining, Sydney, NSW, Australia, August 10-13, 2015*, pages 397–406. ACM.

Han, L. and Zhang, Y. (2016). Multi-stage multi-task learning with reduced rank. In Schuurmans, D. and Wellman, M. P., editors, *Proceedings of the Thirtieth AAAI Conference on Artificial Intelligence, February 12-17, 2016, Phoenix, Arizona, USA*, pages 1638–1644. AAAI Press.

Hein, M., Bousquet, O., Hein, M., and Bousquet, O. (2004). Kernels, associated structures and generalizations.

Hernández-Lobato, D. and Hernández-Lobato, J. M. (2013). Learning feature selection dependencies in multi-task learning. In Burges, C. J. C., Bottou, L., Ghahramani, Z., and Weinberger, K. Q., editors, *Advances in Neural Information Processing Systems 26: 27th Annual Conference on Neural Information Processing Systems 2013. Proceedings of a meeting held December 5-8, 2013, Lake Tahoe, Nevada, United States*, pages 746–754.

Hernández-Lobato, D., Hernández-Lobato, J. M., and Ghahramani, Z. (2015). A probabilistic model for dirty multi-task feature selection. In Bach, F. R. and Blei, D. M., editors, *Proceedings of the 32nd International Conference on Machine Learning, ICML 2015, Lille, France, 6-11 July 2015*, volume 37 of *JMLR Workshop and Conference Proceedings*, pages 1073–1082. JMLR.org.

III, H. D. (2007). Frustratingly easy domain adaptation. In Carroll, J. A., van den Bosch, A., and Zaenen, A., editors, *ACL 2007, Proceedings of the 45th Annual Meeting of the Association for Computational Linguistics, June 23-30, 2007, Prague, Czech Republic*. The Association for Computational Linguistics.

III, H. D. (2009). Bayesian multitask learning with latent hierarchies. In Bilmes, J. A. and Ng, A. Y., editors, *UAI 2009, Proceedings of the Twenty-Fifth Conference on Uncertainty in Artificial Intelligence, Montreal, QC, Canada, June 18-21, 2009*, pages 135–142. AUAI Press.

Jacob, L., Bach, F. R., and Vert, J. (2008). Clustered multi-task learning: A convex formulation. In Koller, D., Schuurmans, D., Bengio, Y., and Bottou, L., editors, *Advances in Neural Information Processing Systems 21, Proceedings of the Twenty-Second Annual Conference on Neural Information Processing Systems, Vancouver, British Columbia, Canada, December 8-11, 2008*, pages 745–752. Curran Associates, Inc.

Jaderberg, M., Simonyan, K., Zisserman, A., and Kavukcuoglu, K. (2015). Spatial transformer networks.

Jalali, A., Ravikumar, P., Sanghavi, S., and Ruan, C. (2010). A dirty model for multi-task learning. In Lafferty, J. D., Williams, C. K. I., Shawe-Taylor, J., Zemel, R. S., and Culotta, A., editors, *Advances in Neural Information Processing Systems 23: 24th Annual Conference on Neural Information Processing Systems 2010. Proceedings of a meeting held 6-9 December 2010, Vancouver, British Columbia, Canada*, pages 964–972. Curran Associates, Inc.

Jawanpuria, P. and Nath, J. S. (2012). A convex feature learning formulation for latent task structure discovery. In *Proceedings of the 29th International Conference on Machine Learning, ICML 2012, Edinburgh, Scotland, UK, June 26 - July 1, 2012*. icml.cc / Omnipress.

Jebara, T. (2004). Multi-task feature and kernel selection for svms. In Brodley, C. E., editor, *Machine Learning, Proceedings of the Twenty-first International Conference (ICML 2004), Banff, Alberta, Canada, July 4-8, 2004*, volume 69 of *ACM International Conference Proceeding Series*. ACM.

Jebara, T. (2011). Multitask sparsity via maximum entropy discrimination. *J. Mach. Learn. Res.*, 12:75–110.

Jeong, J. and Jun, C. (2018). Variable selection and task grouping for multi-task learning. In Guo, Y. and Farooq, F., editors, *Proceedings of the 24th ACM SIGKDD International Conference on Knowledge Discovery & Data Mining, KDD 2018, London, UK, August 19-23, 2018*, pages 1589–1598. ACM.

Kadri, H., Duflos, E., Preux, P., Canu, S., Rakotomamonjy, A., and Audiffren, J. (2016). Operator-valued kernels for learning from functional response data. *J. Mach. Learn. Res.*, 17:20:1–20:54.

Kang, Z., Grauman, K., and Sha, F. (2011). Learning with whom to share in multi-task feature learning. In Getoor, L. and Scheffer, T., editors, *Proceedings of the 28th International Conference on Machine Learning, ICML 2011, Bellevue, Washington, USA, June 28 - July 2, 2011*, pages 521–528. Omnipress.

Kumar, A. and III, H. D. (2012). Learning task grouping and overlap in multi-task learning. In *Proceedings of the 29th International Conference on Machine Learning, ICML 2012, Edinburgh, Scotland, UK, June 26 - July 1, 2012*. icml.cc / Omnipress.

Lawrence, N. D. and Platt, J. C. (2004). Learning to learn with the informative vector machine. In Brodley, C. E., editor, *Machine Learning, Proceedings of the Twenty-first International Conference (ICML 2004), Banff, Alberta, Canada, July 4-8, 2004*, volume 69 of *ACM International Conference Proceeding Series*. ACM.

LeCun, Y., Bottou, L., Bengio, Y., and Haffner, P. (1998). Gradient-based learning applied to document recognition. *Proc. IEEE*, 86(11):2278–2324.

Li, Y., Tian, X., Song, M., and Tao, D. (2015). Multi-task proximal support vector machine. *Pattern Recognit.*, 48(10):3249–3257.

Liang, L. and Cherkassky, V. (2008). Connection between SVM+ and multi-task learning. In *Proceedings of the International Joint Conference on Neural Networks, IJCNN 2008, part of the IEEE World Congress on Computational Intelligence, WCCI 2008, Hong Kong, China, June 1-6, 2008*, pages 2048–2054. IEEE.

Liu, H., Palatucci, M., and Zhang, J. (2009). Blockwise coordinate descent procedures for the multi-task lasso, with applications to neural semantic basis discovery. In Danyluk, A. P., Bottou, L., and Littman, M. L., editors, *Proceedings of the 26th Annual International Conference on Machine Learning, ICML 2009, Montreal, Quebec, Canada, June 14-18, 2009*, volume 382 of *ACM International Conference Proceeding Series*, pages 649–656. ACM.

Long, M. and Wang, J. (2015). Learning multiple tasks with deep relationship networks. *CoRR*, abs/1506.02117.

Loshchilov, I. and Hutter, F. (2019). Decoupled weight decay regularization. In *7th International Conference on Learning Representations, ICLR 2019, New Orleans, LA, USA, May 6-9, 2019*. OpenReview.net.

Lozano, A. C. and Swirszcz, G. (2012). Multi-level lasso for sparse multi-task regression. In *Proceedings of the 29th International Conference on Machine Learning, ICML 2012, Edinburgh, Scotland, UK, June 26 - July 1, 2012*. icml.cc / Omnipress.

Maurer, A. (2006a). Bounds for linear multi-task learning. *J. Mach. Learn. Res.*, 7:117–139.

Maurer, A. (2006b). The rademacher complexity of linear transformation classes. In Lugosi, G. and Simon, H. U., editors, *Learning Theory, 19th Annual Conference on Learning Theory, COLT 2006, Pittsburgh, PA, USA, June 22-25, 2006, Proceedings*, volume 4005 of *Lecture Notes in Computer Science*, pages 65–78. Springer.

Maurer, A. (2009). Transfer bounds for linear feature learning. *Mach. Learn.*, 75(3):327–350.

Maurer, A. and Pontil, M. (2010). K -dimensional coding schemes in hilbert spaces. *IEEE Trans. Inf. Theory*, 56(11):5839–5846.

Maurer, A., Pontil, M., and Romera-Paredes, B. (2013). Sparse coding for multitask and transfer learning. In *Proceedings of the 30th International Conference on Machine Learning, ICML 2013, Atlanta, GA, USA, 16-21 June 2013*, volume 28 of *JMLR Workshop and Conference Proceedings*, pages 343–351. JMLR.org.

Maurer, A., Pontil, M., and Romera-Paredes, B. (2016). The benefit of multitask representation learning. *J. Mach. Learn. Res.*, 17:81:1–81:32.

Micchelli, C. A. and Pontil, M. (2004). Kernels for multi–task learning. In *Advances in Neural Information Processing Systems 17 [Neural Information Processing Systems, NIPS 2004, December 13-18, 2004, Vancouver, British Columbia, Canada]*, pages 921–928.

Micchelli, C. A. and Pontil, M. (2005). On learning vector-valued functions. *Neural Comput.*, 17(1):177–204.

Misra, I., Shrivastava, A., Gupta, A., and Hebert, M. (2016). Cross-stitch networks for multi-task learning. In *2016 IEEE Conference on Computer Vision and Pattern Recognition, CVPR 2016, Las Vegas, NV, USA, June 27-30, 2016*, pages 3994–4003. IEEE Computer Society.

Obozinski, G., Taskar, B., and Jordan, M. (2006). Multi-task feature selection. *Statistics Department, UC Berkeley, Tech. Rep*, 2(2.2):2.

Parameswaran, S. and Weinberger, K. Q. (2010). Large margin multi-task metric learning. In Lafferty, J. D., Williams, C. K. I., Shawe-Taylor, J., Zemel, R. S., and Culotta, A., editors, *Advances in Neural Information Processing Systems 23: 24th Annual Conference on Neural Information Processing Systems 2010. Proceedings of a meeting held 6-9 December 2010, Vancouver, British Columbia, Canada*, pages 1867–1875. Curran Associates, Inc.

Paszke, A., Gross, S., Massa, F., Lerer, A., Bradbury, J., Chanan, G., Killeen, T., Lin, Z., Gimelshein, N., Antiga, L., Desmaison, A., Kopf, A., Yang, E., DeVito, Z., Raison, M., Tejani, A., Chilamkurthy, S., Steiner, B., Fang, L., Bai, J., and Chintala, S. (2019). Pytorch: An imperative style, high-performance deep learning library. In *Advances in Neural Information Processing Systems 32*, pages 8024–8035.

Pong, T. K., Tseng, P., Ji, S., and Ye, J. (2010). Trace norm regularization: Reformulations, algorithms, and multi-task learning. *SIAM J. Optim.*, 20(6):3465–3489.

Ruder, S. (2017). An overview of multi-task learning in deep neural networks. *CoRR*, abs/1706.05098.

Ruder, S., Bingel, J., Augenstein, I., and Søgaard, A. (2017). Sluice networks: Learning what to share between loosely related tasks. *CoRR*, abs/1705.08142.

Ruiz, C., Alaíz, C. M., and Dorronsoro, J. R. (2019). A convex formulation of svm-based multi-task learning. In *HAIS 2019*, volume 11734 of *Lecture Notes in Computer Science*, pages 404–415. Springer.

Ruiz, C., Alaíz, C. M., and Dorronsoro, J. R. (2021). Convex formulation for multi-task l1-, l2-, and ls-svms. *Neurocomputing*, 456:599–608.

Ruiz, C., Alaíz, C. M., and Dorronsoro, J. R. (2022). Convex mtl for neural networks. *Logic Journal of the IGPL*.

Schölkopf, B., Herbrich, R., and Smola, A. J. (2001). A generalized representer theorem. In Helmbold, D. P. and Williamson, R. C., editors, *Computational Learning Theory, 14th Annual Conference on Computational Learning Theory, COLT 2001 and 5th European Conference on Computational Learning Theory, EuroCOLT 2001, Amsterdam, The Netherlands, July 16-19, 2001, Proceedings*, volume 2111 of *Lecture Notes in Computer Science*, pages 416–426. Springer.

Sun, X., Panda, R., Feris, R., and Saenko, K. (2020). Adashare: Learning what to share for efficient deep multi-task learning. In Larochelle, H., Ranzato, M., Hadsell, R., Balcan, M., and Lin, H., editors, *Advances in Neural Information Processing Systems 33: Annual Conference on Neural Information Processing Systems 2020, NeurIPS 2020, December 6-12, 2020, virtual*.

Suykens, J. A. K. and Vandewalle, J. (1999). Least squares support vector machine classifiers. *Neural Process. Lett.*, 9(3):293–300.

Thrun, S. and O'Sullivan, J. (1996). Discovering structure in multiple learning tasks: The TC algorithm. In Saitta, L., editor, *Machine Learning, Proceedings of the Thirteenth International Conference (ICML '96), Bari, Italy, July 3-6, 1996*, pages 489–497. Morgan Kaufmann.

Vapnik, V. (1982). *Estimation of dependences based on empirical data*. Springer Science & Business Media.

Vapnik, V. (2000). *The Nature of Statistical Learning Theory*. Statistics for Engineering and Information Science. Springer.

Vapnik, V. and Izmailov, R. (2015). Learning using privileged information: similarity control and knowledge transfer. *J. Mach. Learn. Res.*, 16:2023–2049.

Vapnik, V. and Vashist, A. (2009). A new learning paradigm: Learning using privileged information. *Neural Networks*, 22(5-6):544–557.

Weinberger, K. Q. and Saul, L. K. (2009). Distance metric learning for large margin nearest neighbor classification. *J. Mach. Learn. Res.*, 10:207–244.

Xiao, H., Rasul, K., and Vollgraf, R. (2017). Fashion-mnist: a novel image dataset for benchmarking machine learning algorithms.

Xu, S., An, X., Qiao, X., and Zhu, L. (2014). Multi-task least-squares support vector machines. *Multim. Tools Appl.*, 71(2):699–715.

Xue, Y., Liao, X., Carin, L., and Krishnapuram, B. (2007). Multi-task learning for classification with dirichlet process priors. *J. Mach. Learn. Res.*, 8:35–63.

Yang, Y. and Hospedales, T. M. (2017a). Deep multi-task representation learning: A tensor factorisation approach. In *5th International Conference on Learning Representations, ICLR 2017, Toulon, France, April 24-26, 2017, Conference Track Proceedings*. OpenReview.net.

Yang, Y. and Hospedales, T. M. (2017b). Trace norm regularised deep multi-task learning. In *5th International Conference on Learning Representations, ICLR 2017, Toulon, France, April 24-26, 2017, Workshop Track Proceedings*. OpenReview.net.

Yu, K., Tresp, V., and Schwaighofer, A. (2005). Learning gaussian processes from multiple tasks. In Raedt, L. D. and Wrobel, S., editors, *Machine Learning, Proceedings of the Twenty-Second International Conference (ICML 2005), Bonn, Germany, August 7-11, 2005*, volume 119 of *ACM International Conference Proceeding Series*, pages 1012–1019. ACM.

Zhang, Y. and Yeung, D. (2010). A convex formulation for learning task relationships in multi-task learning. In Grünwald, P. and Spirtes, P., editors, *UAI 2010, Proceedings of the Twenty-Sixth Conference on Uncertainty in Artificial Intelligence, Catalina Island, CA, USA, July 8-11, 2010*, pages 733–442. AUAI Press.

Zhang, Y. and Yeung, D. (2013). A regularization approach to learning task relationships in multitask learning. *ACM Trans. Knowl. Discov. Data*, 8(3):12:1–12:31.

Zhang, Y., Yeung, D., and Xu, Q. (2010). Probabilistic multi-task feature selection. In Lafferty, J. D., Williams, C. K. I., Shawe-Taylor, J., Zemel, R. S., and Culotta, A., editors, *Advances in Neural Information Processing Systems 23: 24th Annual Conference on Neural Information Processing Systems 2010. Proceedings of a meeting held 6-9 December 2010, Vancouver, British Columbia, Canada*, pages 2559–2567. Curran Associates, Inc.

Zhou, J., Chen, J., and Ye, J. (2011). Clustered multi-task learning via alternating structure optimization. In Shawe-Taylor, J., Zemel, R. S., Bartlett, P. L., Pereira, F. C. N., and Weinberger, K. Q., editors, *Advances in Neural Information Processing Systems 24: 25th Annual Conference on Neural Information Processing Systems 2011. Proceedings of a meeting held 12-14 December 2011, Granada, Spain*, pages 702–710.

Zweig, A. and Weinshall, D. (2013). Hierarchical regularization cascade for joint learning. In *Proceedings of the 30th International Conference on Machine Learning, ICML 2013, Atlanta, GA, USA, 16-21 June 2013*, volume 28 of *JMLR Workshop and Conference Proceedings*, pages 37–45. JMLR.org.